
Climate and Hydrology Datasets for RMJOC Long-Term Planning Studies: Second Edition (RMJOC-II)

Part I: Hydroclimate Projections and Analyses

June 2018



**River Management Joint Operating Committee (RMJOC):
Bonneville Power Administration, United States Army Corps of Engineers,
United States Bureau of Reclamation**



**Climate and Hydrology Datasets for RMJOC
Long-Term Planning Studies:
Second Edition (RMJOC-II)**

Part I: Hydroclimate Projections and Analyses

RMJOC-II Project Sponsors and Chairs:

Rick Pendergrass, Bonneville Power Administration

Steven Barton, US Army Corp of Engineers, Northwestern Division

John Roache, Bureau of Reclamation

Lead Authors:

Erik Pytlak, Bonneville Power Administration, Portland, OR

Chris Frans, US Army Corps of Engineers Seattle District, Seattle, WA

Keith Duffy, US Army Corps of Engineers Portland District, Portland, OR

Jennifer Johnson, US Department of Interior, Bureau of Reclamation, Boise, ID

Bart Nijssen and Oriana Chegwidan, Department of Civil and Environmental Engineering, University of Washington

David Rupp, College of Earth, Ocean, and Atmospheric Sciences, Oregon State University

RMJOC Agency Contributors:

Bonneville Power Administration: Abdullah Dakhalla, Bruce Glabau, Kari Hay, Ann McManamon, Mariano Mezzatesta, Arun Mylvahanan, Eric Nielsen, Travis Roth, Nancy Stephan, and Rick van der Zweep

US Army Corps of Engineers: Pete Dickerson, Jeremy Giovando, Kristian Mickelson, and Jason Ward

Bureau of Reclamation: Jennifer Cuhacyian and Bob Lounsbury

Other Contributors:

Dan Hua, Northwest Power and Conservation Council

Shih-Chieh Kao, Oak Ridge National Laboratory

Editorial Assistance:

David Donnell and Stacey Williams, Bonneville Power Administration

Project Management:

Bonneville Power Administration, Office of Technology and Innovation:

James Bowen, Judith Estep, Terry Oliver, Justin Reel, and Erik Pytlak

Editorial comments provided by:

Columbia River Intertribal Fish Commission

Idaho Power Company

Northwest Power and Conservation Council

Cover photo: Tony Norris, BPA

Abbreviations and Acronyms

AR	Atmospheric River
AR5	Fifth Assessment Report from the Intergovernmental Panel of Climate Change
BCSD	Bias Corrected Spatial Disaggregation
BPA	Bonneville Power Administration
cfs	cubic feet per second
CMIP	Coupled Model Intercomparison Project
CO ₂	carbon dioxide
CRFG	Columbia River Forecasting Group
CRT	Columbia River Treaty
GCM	Global Climate Model (also known as General Circulation Models)
IPCC-5	Intergovernmental Panel on Climate Change, Fifth Assessment Report
kcfs	thousands of cubic feet per second
MACA	Multivariate Adaptive Constructed Analog
NCAR	National Centers for Atmospheric Research
NRNI	No Regulation-No Irrigation
ORNL	Oak Ridge National Laboratories
P	Precipitation
ppm	parts per million
PRISM	Parameter-elevation Regressions on Independent Slopes Model
PRMS	Precipitation Runoff Modeling System
RCM	Regional Climate Model
RCP	Resource Concentration Pathway
RMJOC	River Management Joint Operating Committee
RMJOC-I	First Edition: Climate and Hydrology Datasets for Long Range Planning (Published in 2010-11)
RMJOC-II	Second Edition: Climate and Hydrology Datasets for RMJOC Long-Term Planning Studies
SWE	Snow-Water Equivalent
T	Temperature
USACE	US Army Corps of Engineers
USBR	US Bureau of Reclamation
USGS	US Geological Survey
UW	University of Washington
UW-CIG	University of Washington Climate Impacts Group
VIC	Variable Infiltration Capacity model
WC2N	Western Canadian Cryosphere Network
WY	Water Year

Table of Contents

Second Climate and Hydrology Datasets for RMJOC Agencies' Long-Term Planning Studies (RMJOC-II)

Part I: Hydroclimate Projections and Analyses

List of Tables	v
List of Figures	v
Preface	1
Executive Summary.....	2
1.0 Introduction	3
1.1 Overview and Review of RMJOC-I Study (2009-2011).....	3
1.2 Literature Review.....	7
1.2.1 Climate Change Progression, and Expected Impacts on the Hydrologic Cycle.....	7
1.2.2 Hydroclimate Modeling Science	11
2.0 Project Design	13
2.1 BPA Opportunity for Proposals Research (2013) and RMJOC Commissioning.....	13
2.2 Project Statement of Work.....	13
2.3 Technical Stakeholder Feedback Process	15
3.0 No Irrigation-No Regulation Dataset Development	17
3.1 Background	17
3.2 Methodology.....	19
3.3 Daily NRNI Flow Development.....	21
3.3.1 Upper Columbia and Kootenay Basins.....	21
3.3.2 Pend Oreille and Spokane Basins.....	21
3.3.3 Upper Snake Basin, Yakima Basin, and Deschutes Basin.....	22
3.3.4 Lower Snake River Basin	22
3.3.5 Mid-Columbia Basin.....	23
3.3.6 Lower Columbia River and Oregon Closed Basin.....	23
3.3.7 Willamette Basin.....	24
3.4 Statistical Analyses of the NRNI Dataset.....	25
3.4.1 Nonstationarities	25
3.4.2 Monotonic Trend Analyses	30
3.5 Discussion	31
4.0 Hydroclimate Dataset Development	32
4.1 Introduction	32
4.1.1 Uncertainty and Ensemble Spread	33
4.1.2 Systematic Biases in Modeling Framework and Historical Datasets	33
4.2 Modeling Components	33

4.2.1	Representative Concentration Pathways (RCPs)	33
4.2.2	GCM Selection	34
4.2.3	Downscaling Methods and Characteristics	37
4.2.4	Hydrologic Models	39
4.2.5	Variable Infiltration Capacity Model (VIC)	41
4.2.6	Precipitation Runoff Modeling System (PRMS)	41
4.3	Historical Data Sources and Characteristics	42
4.4	Hydrologic Model Calibration	43
4.4.1	University of Washington Calibrations	43
4.4.2	VIC-ORNL Calibration	44
4.4.3	VIC-NCAR Calibration	45
4.4.4	Hydrologic Model Historical Performance	45
4.5	Streamflow Bias Correction	47
4.6	Streamflow Scenarios and Naming Convention	48
5.0	Downscaled Temperature and Precipitation Projections	51
5.1	Columbia Basin Summary	51
5.1.1	Temperature Trends	51
5.1.2	Precipitation Trends	58
5.2	Upper Columbia River Basin Summary	66
5.3	Snake River Basin Summary	67
5.4	Willamette River Basin Summary	68
5.5	Discussion	69
6.0	Cryosphere Projections	70
6.1	Basin Snowpack Projections	70
6.2	Upper Columbia Glacier Projections	71
7.0	Streamflow Projections	73
7.1	Modeling Chain Elements Influence on Projection Spread	73
7.1.1	Emissions Scenario	74
7.1.2	Global Climate Model	75
7.1.3	Downscaling Technique	76
7.1.4	Hydrological Model and Parameterizations	78
7.2	Streamflow Projections	81
7.2.1	Basinwide Projections	81
7.2.2	Upper Columbia, Kootenai, and Pend Oreille River Basins	85
7.2.3	Snake River Basin	89
7.2.4	Willamette River Basin	91
8.0	Dataset Selection for Hydroregulation Modeling	93
8.1	Introduction	93
8.2	Subset Selection for Hydropower Analyses	93
8.2.1	Impact-Relevant Streamflow Metrics	94
8.2.2	Objective Subset Selection Method	96
8.3	Selected Subset and Characteristics	98
9.0	Summary and Conclusions	104
	References	106

List of Tables

Table 1: Upper Columbia and Kootenay Basins NRNI daily flow sites.....	21
Table 2: Pend Oreille and Spokane Basins NRNI daily flow sites.....	21
Table 3: Mid-Columbia Basin NRNI daily flow sites.....	23
Table 4: Lower Columbia River and Oregon Closed Basin NRNI daily flow sites.....	23
Table 5: Willamette Basin NRNI daily flow sites.....	24
Table 6: Performance metrics used for initial GCM selection (from Rupp <i>et al.</i> , 2013). MMM = DJF (December - February) or JJA (June - August).....	35
Table 7: Global Climate Model (GCM) outputs used for RMJOC-II Study. All GCM data is from ensemble member r1i1p1 from each GCM dataset, except CCSM4, which is from ensemble member r6i1ip1:.....	36
Table 8: Overview of calibration techniques used in study.....	44
Table 9: Median, minimum and maximum (in parentheses) of Kling-Gupta Efficiency for weekly average flows WY 1961-2005, relative to the calibration period of WY 1992-2001.....	46
Table 10: Streamflow metrics and vulnerabilities identified in stakeholder outreach discussions.....	95
Table 11: Table of the 19 projections selected as a representative subset of the 80-member ensemble.....	99

List of Figures

Figure 1: Site map showing the Columbia River Basin with the sub-basins, large dams, and major tributaries (regions) noted.....	3
Figure 2: Monthly unregulated flow averages from six scenarios used for the RMJOC-I Study (RMJOC, 2011b) for the 2020s (2010-2039) at The Dalles, OR, relative to the long-term Modified Flows mean (1929-1998).....	5
Figure 3: Monthly flow averages from six scenarios used for the RMJOC-I Study (RMJOC, 2011b) for the 2040s (2030-2059) at The Dalles, OR, relative to the long-term Modified Flows mean (1929-1998).....	6
Figure 4: Projected changes in annual streamflow (%) for the Mica, BC basin. Comparisons between WC2N and PCIC projections (2012) and UW-CIG streamflow models (2010) for the 2040s. Note the greater increase in annual flows in the two BC Hydro study flows compared to UW-CIG, and greater range of potential outcomes. From Jost and Weber (2012).....	7
Figure 5: Average global temperature, relative to the long-term mean (°C). From NOAA National Centers for Environmental Information, 2018.....	8
Figure 6: Surface temperature change (in °F) for the period 1986-2015 relative to 1901-1960 from the NOAA National Centers for Environmental Information's (NCEI) surface temperature product. From USGCRP (2017).....	9
Figure 7: Summary matrix of observed and projected climate trends and literary consensus reported in USACE (2015).....	10

Figure 8: Project Deliverables, Timeline and Stage Gate Breakpoints. Stage Gates 5 and 6 were structured to this final flowchart in Year 3 of the project (2016).....	15
Figure 9: NRNI time series locations.	18
Figure 10: 2010 Level Modified Streamflow locations for the Columbia Basin (in BPA, 2011a).....	19
Figure 11: Nonstationarities detected in time series (WY 1929-2008) of annual maximum 1-day duration flows at NRNI locations (colored circles). NRNI locations where nonstationarities were not found are indicated with white squares.....	27
Figure 12: Nonstationarities detected in time series (WY 1929-2008) of annual maximum 30-day duration flows at NRNI locations (colored circles). NRNI locations where nonstationarities were not found are indicated with white squares.....	28
Figure 13: Nonstationarities detected in time series (WY 1929-2008) of annual minimum summer 7-day mean flows at NRNI locations (green-blue circles). NRNI locations where nonstationarities were not found are indicated with white squares.	29
Figure 14: Monotonic trends for 1929-2008 identified in time series of (a) annual maximum 1-day duration, (b) annual maximum 30-day duration, and (c) minimum 7-day mean summer flows at NRNI locations. Blue upward pointing triangles indicate positive trends and red downward facing triangles indicate negative trends. The marker size is scaled by the magnitude of the trend present (slope in %, relative to all locations). Statistical significance (p-value) was calculated using the Mann-Kendal statistic and magnitude by Sen’s slope estimator.	31
Figure 15: Hydroclimate modeling process flowchart.....	32
Figure 16: Emissions pathways used for the IPCC AR-5 climate modeling effort, and recent emissions trends through 2015. From Fuss et al, 2014.	34
Figure 17: Global Climate Model Performance Quilt, prepared using methodology from Rupp et al. (2013) for overall historical performance in the Pacific Northwest. Two initial selections (NorESM1-M and bcc-csm1-1-m, highlighted by the red outlining of the model names) were replaced by HadGEM2-CC and GFDL-ESM2M (green outlining) in the final selection (blue plus green outlining).....	36
Figure 18: Schematic comparing VIC and PRMS soil and runoff processes, from Mizukami et al. (2016).	40
Figure 19: Historical performance of each of the four calibrated hydrologic models. Performance was calculated using the weekly Kling-Gupta Efficiency upon the period WY 1961-2005, removing the calibration period of WY 1992-2001.	46
Figure 20: Comparison of modeled 10 th , 50 th (median), and 90 th percentile daily flows from the 4 hydrological models (VIC_P1=UW; VIC_P2=ORNL; VIC_P3=NCAR) and NRNI data for the period of 1950-2005. The modeled flows are raw (no bias correction was applied). Locations include Libby (LIB), Arrow Lakes (ARD), Grand Coulee (GCL), Brownlee (BRN), and The Dalles (TDA).	47
Figure 21: Raw streamflow locations. For bias-corrected flow locations, see Figure 9.	49
Figure 22: Streamflow scenarios sorted by GCM, downscaling technique, hydrologic mode, and model parameter set.	50

Figure 23: Average annual daily maximum temperatures, and 10th and 90th percentile temperatures, for the ten GCMs in this study for the Columbia River Basin and Pacific coastal drainages in Washington and Oregon. For RCP 4.5 and 8.5, from 1901-2100. The 20th century period (shown in black and gray) is the control period for each GCM and is used to evaluate performance. The GCM time series are also bias-corrected based upon the comparison of the latter half of the control simulation to a reference dataset.).....	51
Figure 24: Annual temperature change (in °F) between historical period (1970-1999) and the 2030s (2020-2059) for RCP4.5, for all ten GCMs used for this study.	53
Figure 25: Same as Figure 24, except for RCP8.5. The temperature projections available from the hybrid dynamical downscaling by ORNL are included.....	54
Figure 26: Temperature change (in °F) between historical period (1970-1999) and the 2070s (2060-2089) for RCP4.5.....	55
Figure 27: Same as Figure 26, except for RCP 8.5.....	56
Figure 28: Seasonal change in temperature (in °F) between historical period 1970-1999 and the 2030s (2020-2039) for the three RCP 8.5 GCMs having data for all three downscaling techniques. DJF: December-February (winter); MAM: March-May (spring); JJA: June-August (summer); and SON: September-November (fall).	57
Figure 29: Average annual and seasonal temperature change (in °F) and precipitation (in %) relative to the long-term mean (1970-1999) for the 2030s (2030-2059, left) and the 2070s (2060-2089, right) above The Dalles, OR, for RCP 4.5 and RCP8.5. The individual GCM averages are indicated by numbers 1-10, with the median of the 10 marked by the thin horizontal line.	58
Figure 30: Average annual precipitation, and 10th and 90th percentile precipitation, for the ten GCMs in this study for the Columbia River Basin and Pacific coastal drainages in Washington and Oregon. For RCP 4.5 and 8.5, from 1901-2100 (1901-2004 as the historical period). The 20th century period (shown in black and grey) is the control period for each GCM and is used to evaluate performance. The GCM time series are also bias-corrected based upon the comparison of the latter half of the control simulation to a reference dataset.	59
Figure 31: Annual precipitation change (in %) between historical period (1970-1999) and the 2030s (2020-2059) for RCP4.5, for all ten GCMs used for this study.	60
Figure 32: Same as Figure 31, except for RCP8.5.....	61
Figure 33: Annual precipitation change (in %) between historical period (1970-1999) and the 2030s (2020-2059) for RCP4.5.	62
Figure 34: Same as Figure 33, except RCP 8.5.	63
Figure 35: Seasonal change in precipitation (in %) between historical period 1970-1999 and the 2030s (2020-2039) for the three RCP 8.5 GCMs having data for all three downscaling techniques. DJF: December-February (winter); MAM: March-May (spring); JJA: June-August (summer); and SON: September-November (fall).	64
Figure 36: Change in annual temperature and precipitation between the historical period (1970-1999), the 2030s (2020-2049, left), and the 2070s (2060-2089, right) for each of the 10 GCMs used for this study, for RCP 4.5 and 8.5, above The Dalles, OR. The blue box denotes the 10 and 90 percentile changes in temperature and precipitation for all 20 scenarios. The blue lines in each box depict the median of all 20 scenarios.....	65

Figure 37: Comparison of annual temperature and precipitation trends between the historical period (1970-1999) and the 2040s (2030-2059) for RMJOC-I and RMJOC-II datasets. The blue box denotes the 10 and 90 percentile changes in temperature and precipitation for all GCMs available, including those not used for RMJOC studies. The gray box depicts the p10 and p90 changes in temperature (in °C) and percentage change in precipitation from CMIP-3 (2007) used for the RMJOC-I study, with the light blue box depicting p10 and p90 changes from CMIP-5 (2013) used for the RMJOC-II study. Red dots are scenarios used from the Hamlet et al. (2008) hydroclimate study for the first RMJOC study (2010). Black dots are scenarios generated for this study. The overlap between the two CMIP studies is in dark blue..... 66

Figure 38: Basin average changes in temperature and precipitation above Grand Coulee Dam, WA, from the historical period to the 2030s (left) and 2070s (right)..... 67

Figure 39: Same as Figure 38, except for above Lower Granite Dam, WA, for the Snake River Basin..... 68

Figure 40: Same as Figure 38, except for above Willamette Falls, OR for the Willamette Basin. 69

Figure 41: Columbia Basin Snow Water Equivalent (SWE) in the 1980s, and average SWE changes by the 2020s (2010-2039), 2050s (2040-2069), and 2080s (2070-2099) on April 1, for the 10 GCMs using RCP8.5 and downscaled via BCSD. Areas in tan historically have less than 10 mm of snow-water equivalent..... 70

Figure 42: Fractional changes in 20-year centered mean SWE (relative to 1950-2010 mean). The SWE fields represent spatial aggregates of the areas upstream of the Yakima River at Kiowa, WA (YAK), Brownlee Dam, ID (BRN), and Arrow Lakes, BC (ARD). Each trace indicates one of the 80 RCP8.5 projections. The colors indicate the GCM used for the individual projection..... 71

Figure 43: Comparison of observed versus modeled glacier presence in the Columbia Basin for the historical period (1976-2005). 72

Figure 44: Range of 10/50/90 percentile flows at The Dalles, OR (TDA, Lower Columbia Basin), for each day of the water year for the historical (1976-2005) and future periods. These ranges represent the 80 statistically downscaled RCP8.5 projections..... 73

Figure 45: Average monthly flows for each streamflow scenario derived from BCSD and MACA downscaling using all GCMs and all hydrologic models, aggregated by RCP 4.5 for the Control period (WY 1951-2005), the 2030s (WY 2020-2049), and 2070s (WY 2060-2089) at The Dalles, OR..... 74

Figure 46: Same as Figure 45, but for RCP 8.5 (in red). 74

Figure 47: Average monthly flows for each streamflow scenario (gray), aggregated by GCM CanESM-2 (in orange), derived from both RCP4.5 and RCP8.5, for BCSD and MACA downscaling, and all hydrologic models for the Control period (WY 1951-2005), the 2030s (WY 2020-2049), and 2070s (WY 2060-2089) at The Dalles, OR. 75

Figure 48: Same as Figure 47, but for GCM GFDL-ESM2M (in green). 75

Figure 49: Day-average streamflows (in kcfs), by climate model, for RCP 8.5, BCSD and MACA downscaling, for all four hydrologic model sets, at The Dalles, OR. Black line is the historical NRNI average (1976-2005). Left is for the 2030s (2020-2049). Right is for the 2070s (2060-2089). 76

Figure 50: Same as Figure 49, but for Lower Granite Dam, WA. Left is for the 2030s (2020-2049). Right is for the 2070s (2060-2089).	76
Figure 51: Average monthly flows for each streamflow scenario (gray), aggregated by the BCSD downscaling (in purple), derived from both RCP 4.5 and 8.5 for all GCMs, and all hydrologic models for the control period (WY 1951-2005), the 2030s (WY 2020-2049), and 2070s (WY 2060-2089) at The Dalles, OR.....	77
Figure 52: Same as Figure 51 but for MACA (in orange).	77
Figure 53: Day-average streamflows (in kcfs), by BCSD, MACA, and ORNL Dynamical-Hybrid downscaling, from CCSM4, GFDL-ESM2m, and MIROC5 GCMs, for RCP 8.5, at The Dalles, OR. Solid black line is the historical NRNI average (1976-2005). Left is for the historical period (1976-2005). Right is for the 2030s (2020-2049).	78
Figure 54: Average monthly flows for each streamflow scenario (gray), aggregated by the VIC calibration from UW (P1, in orange), derived from both RCP4.5 and RCP8.5, for BCSD and MACA downscaling, for the Control period (WY 1951-2005), the 2030s (WY 2020-2049), and 2070s (WY 2060-2089) at The Dalles, OR.	79
Figure 55: Same as Figure 54, expect for PRMS calibration from UW (P1, in green).	79
Figure 56: Same as Figure 54, expect for VIC calibration from ORNL (P2, in purple).....	79
Figure 57: Same as Figure 54, except for VIC calibration from NCAR (P3, in blue).	80
Figure 58: Day-averaged streamflows (in kcfs), by hydrologic model set, for all RCP 8.5 GCMs, BCSD and MACA downscaling, at The Dalles, OR. Black line is the historical NRNI average (1976-2005). Left is for the 2030s (2020-2049). Right is for the 2070s (2060-2089).....	80
Figure 59: Day-averaged streamflows (in kcfs) by hydrological model set, for all RCP8.5 GCMs, BCSD and MACA downscaling, at Mica Dam, BC. Black line is the historical NRNI average (1976-2005). Left are the averaged flows in the 1976-2005 historical period. Right is for the 2030s (2020-2049).....	81
Figure 60: Percent change in annual volume from the historical period (1976-2005) for the 2030s (2020-2049), averaged for the 10 RCP8.5 GCMs used for this study, and using BCSD and MACA downscaling. Each circle is an NRNI control point, with circle size denoting relative annual volumes in the historical (1976-2005) period.....	82
Figure 61: Generalized depiction of scenario agreement for annual volume changes from the historical period (1976-2005) and the 2030s (2020-2049), averaged for the 10 RCP8.5 GCMs used for this study, and using BCSD and MACA downscaling. Each circle is a NRNI control point, with circle size denoting relative annual volumes in the historical (WY 1970-1999) period.	82
Figure 62: Generalized depiction of scenario spread for annual volume changes from the historical period (1976-2005) and the 2030s (2020-2049), averaged for the 10 RCP8.5 GCMs used for this study, and using BCSD and MACA downscaling. Each circle is an NRNI control point, with circle size denoting relative annual volumes in the historical (1970-1999) period.....	83
Figure 63: Same as Figure 60, but by season (DJF: December-February/Winter; MAM: March-May/Spring;.....	84
Figure 64: Same as Figure 61, but by season (DJF: December-February/Winter; MAM: March-May/Spring; JJA: June-August/Summer; SON: September-November/Fall).	84

Figure 65: Same as Figure 62, but by season (DJF: December-February/Winter; MAM: March-May/Spring; JJA: June-August/Summer; SON: September-November/Fall).	85
Figure 66: Range of 10/50/90 percentile flows at Mica, BC (MCD, Upper Columbia Basin), for each day of the water year for the historical (1976-2005) and future periods 2030s (WY 2020-2049) and 2070s (WY 2060-2089). These ranges represent the 80 statistically downscaled RCP8.5 projections.	86
Figure 67: Same as Figure 66, except at Arrow Lakes, BC (ARD, Upper Columbia Basin).	86
Figure 68: Same as Figure 66, except for Corra Linn, BC (COR, Kootenay Basin).	87
Figure 69: Same as Figure 66, except at Hungry Horse Dam, MT (HGH, Flathead Basin).	88
Figure 70: Same as Figure 66, except at Albeni Falls Dam, ID (ALB, Pend Oreille Basin).	88
Figure 71: Same as Figure 61, except for Grand Coulee Dam, WA (GCL, mid-Columbia Basin).....	89
Figure 72: Same as Figure 66, except at Brownlee Dam, ID (BRN, Upper Snake Basin).	90
Figure 73: Same as Figure 66, except at Dworshak Dam, ID (DWR, Clearwater Basin).....	90
Figure 74: Same as Figure 66, except at Ice Harbor Dam, WA (IHR, Lower Snake Basin).	91
Figure 75: Same as Figure 66, except at Willamette Falls, OR (Willamette Basin).....	92
Figure 76: Locations (circled, labeled with boxes) in the Columbia River Basin used to define subset selection criteria.	95
Figure 77: Example distribution of changes in streamflow metric (Half Volume Day) for the 2030 epoch (2030s) at The Dalles, OR (TDA). Model count indicates the number of the 80 projections that fall within in each range of changes in the metric. The yellow arrows indicate the ranges included to define each 10, 50, and 90 percentile targets.	97
Figure 78: Schematic demonstrating the iterative technique for selecting a representative subset based on constraints derived from distributions of changes in streamflow.	98
Figure 79: Comparisons of the spread of the 80-member ensemble and the spread of the 19-member subset using daily summary statistics (5%, 50%, and 95%) for locations not included in the selection method (Revelstoke, RVC; Waneta, WAT; Lower Granite, LWG; McNary, MCN).....	100
Figure 80: Average annual volumes at The Dalles, OR, for the 2030s (WY 2020-2049) for each of the 80 scenarios using RCP8.5, the 10 GCMs used for this study, and statistical downscaling (BCSD and MACA). Red scenarios are the nineteen selected using the iterative technique described in Section 9.2.2.	101
Figure 81: Same as Figure 80, except for the 2070s (WY 2060-2089).....	101
Figure 82: Same as Figure 80, except for Grand Coulee, WA, for the 2030s (WY 2020-2049).....	102
Figure 83: Same as Figure 82, except for the 2070s (WY 2060-2089).....	102
Figure 84: Same as Figure 80, except for Lower Granite for the 2030s (WY 2020-2049).	102
Figure 85: Same as Figure 84, except for the 2070s (WY 2060-2089).....	103

Preface

The overarching objective of the Bonneville Power Administration (BPA), US Army Corps of Engineers (USACE), and the US Bureau of Reclamation (USBR), which comprise the River Management Joint Operating Committee (RMJOC), is to continuously evaluate and anticipate vulnerabilities, risk, and resiliency of the Federal Columbia River Power System (FCRPS). Assessments include potential future changes to hydropower generation and reliability, flood risk management, water supply, recreation, cultural resources, fisheries, navigation, and functioning of the ecological system. The purposes served by the Columbia River reservoir system can be challenged by changes in future conditions, including changes to the regional hydro-climatology. The priority of these agencies is to identify and anticipate the impacts of these changes in regional hydro-climatology to infrastructure and system objectives, irrespective of what is driving the changes.

This objective motivated the RMJOC to work with the research community to update and improve the first climate change study completed in 2009-2011. The Bonneville Power Administration, through its Office of Technology and Innovation, provided project management expertise and almost half of the research funding to this renewed effort. In addition, USACE and USBR also contributed funding. More than a dozen technical experts from the RMJOC agencies provided subject matter expertise throughout the four year research effort, and worked closely with the research teams and regional stakeholders to develop this updated and improved regional climate change dataset.

The RMJOC is particularly grateful to the research teams at the University of Washington and Oregon State University. Both teams were instrumental in not only producing this important and scientifically sound dataset for the region, but as active participants in the considerable stakeholder outreach and collaboration throughout the length of the project.

This is the first report on projected climate change impacts in the Columbia and Willamette River Basins. The report focuses on the temperature, precipitation, snowpack, and streamflow changes that are projected to occur as the regional climate changes through the rest of the 21st century. Subsequent impact reports from the RMJOC, academic papers published from the research teams, and studies associated with regional stakeholder processes like the Columbia River System Operations (CRSO) and Columbia River Treaty (CRT) will be forthcoming. However, the new dataset from this project, and information contained in this report, will be used to identify potential vulnerabilities, and the resilience of the many purposes that the FCRPS serves.

Executive Summary

In 2013, the River Management Joint Operating Committee (RMJOC) commissioned a new climate change study using a new set of naturalized streamflow datasets derived from the CMIP-5 Global Climate Model projections. The RMJOC, through the BPA Technology and Innovation Office, commissioned a research team from the University of Washington and Oregon State University to complete the work, with support from technical teams from the RMJOC agencies and regional stakeholders.

This renewed effort sought to better account for the range of climate change outcomes, and for the additional spread introduced by the methodological choices made in the hydrologic modeling chain. As the project proceeded, other research opportunities emerged, including the evaluation of how different sets of calibration parameters can lead to different streamflow outcomes, the incorporation of an improved streamflow bias correction technique, and the use of inverse routing, which allows for faster model recalibrations.

Based on the results detailed in the temperature, precipitation, snowpack, and streamflow scenarios prepared for this study:

- Temperatures have already warmed about 1.5°F in the region since the 1970s. They are expected to warm another 1 to 4°F by the 2030s.
- Temperatures are likely to warm 3 to 6°F over what is currently observed in the basin by the 2070s if RCP4.5 emissions pathways are attained. If current trajectory RCP8.5 emissions pathways are realized, though, 4 to 10°F of warming above what is currently observed will be likely by the 2070s.
- Warming is likely to be greatest in the interior, with a greater range of possible outcomes, with less pronounced warming near the coast.
- Future precipitation trends are more uncertain, but a general upward trend is likely for the rest of the 21st century, particularly in the winter months. Already dry summer months could become drier.
- Average winter snowpacks are very likely to decline over time as more winter precipitation falls as rain instead of snow, especially in the US side of the Columbia Basin.
- By the 2030s, higher average fall and winter flows, earlier peak spring runoff, and longer periods of low summer flows are very likely. The earliest and greatest streamflow changes are likely to occur in the Snake River Basin, although that is also the basin with the greatest modeling and forecast uncertainty.
- In the Willamette Basin, fall and winter flows are likely to increase. A slight decrease in spring flows is possible, with a longer period of low summer flows more likely than not.
- To support subsequent RMJOC-II efforts, an objective method of selecting subsets of scenarios was developed. This method found a 19-member subset of 80 statistically downscaled RCP8.5 projections to be representative of projected changes in stakeholder-identified natural streamflow metrics for the 2030s.

1.0 Introduction

1.1 Overview and Review of RMJOC-I Study (2009-2011)

For more than a decade, BPA, USACE, and USBR have monitored and anticipated regional warming and streamflow changes in the Columbia River Basin induced by anthropogenic greenhouse gas emissions into the atmosphere. Since 2008, the three agencies have collaborated to facilitate the development of state-of-the-science climate change and hydrology datasets, and use the datasets in long-term planning activities for the Columbia River Basin (Figure 1).



Figure 1: Site map showing the Columbia River Basin with the sub-basins, large dams, and major tributaries (regions) noted.

The three agencies coordinate climate change research and planning activities through the River Management Joint Operating Committee (RMJOC). The RMJOC is charged to review river management and operations practices, procedures, and processes, and to identify changes that could improve the overall effectiveness of the operation and management of the Federal Columbia River Power System (FCRPS). In addition to using the latest and best-available climate change information and datasets, the RMJOC agencies worked together to adopt a set of methods for incorporating these data into those longer-term planning activities.

In 2009-2011, the RMJOC commissioned a comprehensive study of potential climate change impacts in the Columbia River Basin (RMJOC, 2010, RMJOC, 2011a, RMJOC, 2011b, RMJOC, 2011c). That study used a subset of the temperature, precipitation, and streamflow datasets developed by the University of Washington Climate Impacts Group for the Columbia River and other parts of western Oregon and Washington, as documented in Hamlet *et al.* (2008), and UW-CIG (2010).

At that time, the data and subsequent analyses incorporated the latest state of climate change science. The UW-CIG dataset was developed using temperature and precipitation information from ten Global Climate Models (GCMs) from the Third Coupled Model Intercomparison Project (CMIP-3), which provided the data support for the Fourth Intergovernmental Panel on Climate Change (IPCC-4, 2007). The coarse resolution climate model data was then downscaled using two different statistical methods: the Bias-Correction Spatial-Disaggregation (BCSD) technique developed by Wood *et al.* (2002) and the hybrid delta technique developed by Hamlet *et al.* (2008). The downscaled meteorological forcings were then used in the Variable Infiltration Capacity (VIC) hydrological model (Liang *et al.*, 1994; Liang *et al.*, 1996; Nijssen *et al.*, 1997), which was calibrated to the 2000 Modified Flows historical dataset (BPA, 2004). The resulting raw streamflows were then post-processed on monthly time steps applying the probability mapping technique from Snover *et al.* (2003) using the 2000 Modified Flows dataset. Finally, a subset of nineteen streamflow scenarios was chosen by the RMJOC, with input from external stakeholders, for hydroregulation studies across the Columbia Basin.

Key conclusions from this initial study on future regional hydroclimate in BPA (2011) were that:

- Air temperatures were expected to increase by 1 to 3 degrees Fahrenheit (approximately 0.5 to less than 2 degrees Celsius) from 2010 to 2039 and by 2 to 5 degrees Fahrenheit (approximately 1 to less than 3 degrees Celsius) from 2030 to 2059.
- Overall annual precipitation changes in the study were minimal. However, some global climate models showed large seasonal changes, including more extreme wet and dry periods, some showed wetter fall and winter periods, and some showed drier summers.
- More winter precipitation would fall as rain instead of snow, producing more runoff in the winter, earlier runoff in the spring, and lower flows in the summer (**Figures 2 and 3**).
- In the Yakima, Deschutes, and Snake River Basins, season-specific impacts on water supply were likely. Reservoir system inflow would increase during the cool season (November through March) and decrease during the warm season (April through September). Peak inflows were likely to occur one to two months earlier than historical timing.
- Flood risk management procedures of the future would need to anticipate that runoff might come weeks earlier, shifting the peak runoff from June to May. Earlier releases of

water from reservoirs at the flood risk management projects may be needed to capture the earlier runoff.

- Impacts to the timing of Federal hydro system operations could also impact other spring and summer objectives such as flows for biological support.
- Higher temperatures in the summer would result in more energy use to cool homes and businesses. Warmer temperatures in the winter would reduce energy use for heating. Changes in energy consumption from 2010 to 2039 would increase from 1 to 3 percent in July and decrease from 3 to 4 percent in December, but with considerable uncertainty.
- The increase in the January through April flows would result in higher generation and increased spill at most dams. Reduced flows during July and August may impact the ability to meet Biological Opinion (BiOp) objectives, including flow management.

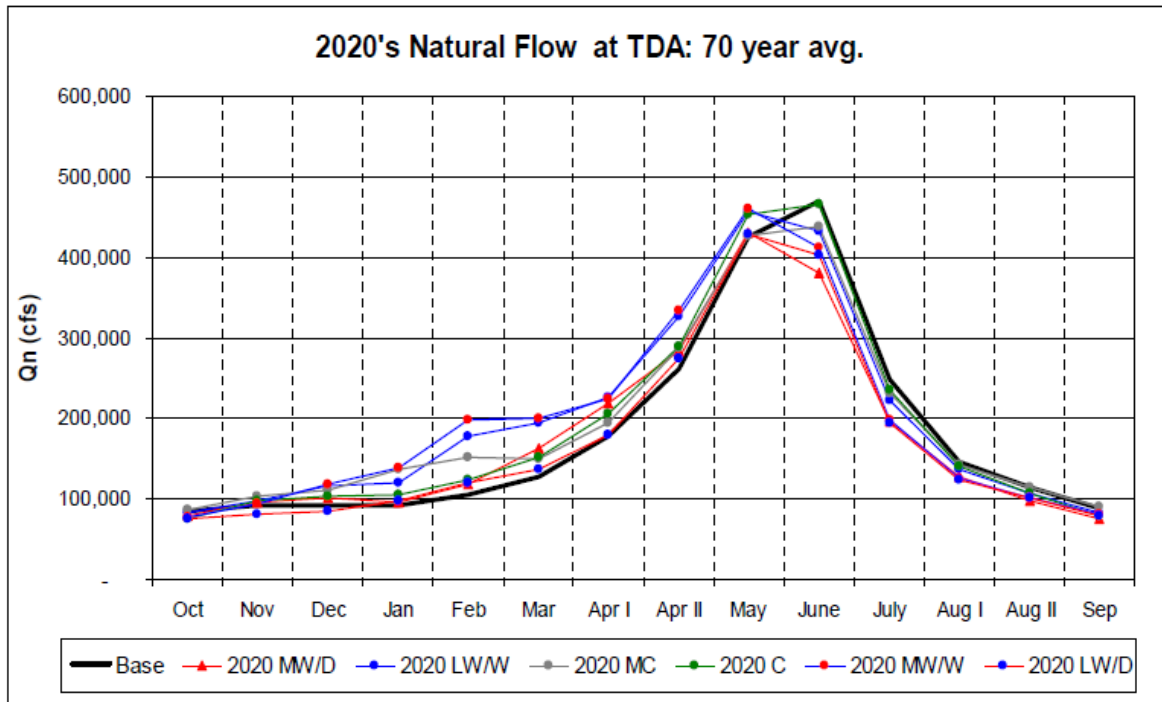


Figure 2: Monthly unregulated flow averages from six scenarios used for the RMJOC-I Study (RMJOC, 2011b) for the 2020s (2010-2039) at The Dalles, OR, relative to the long-term Modified Flows mean (1929-1998).

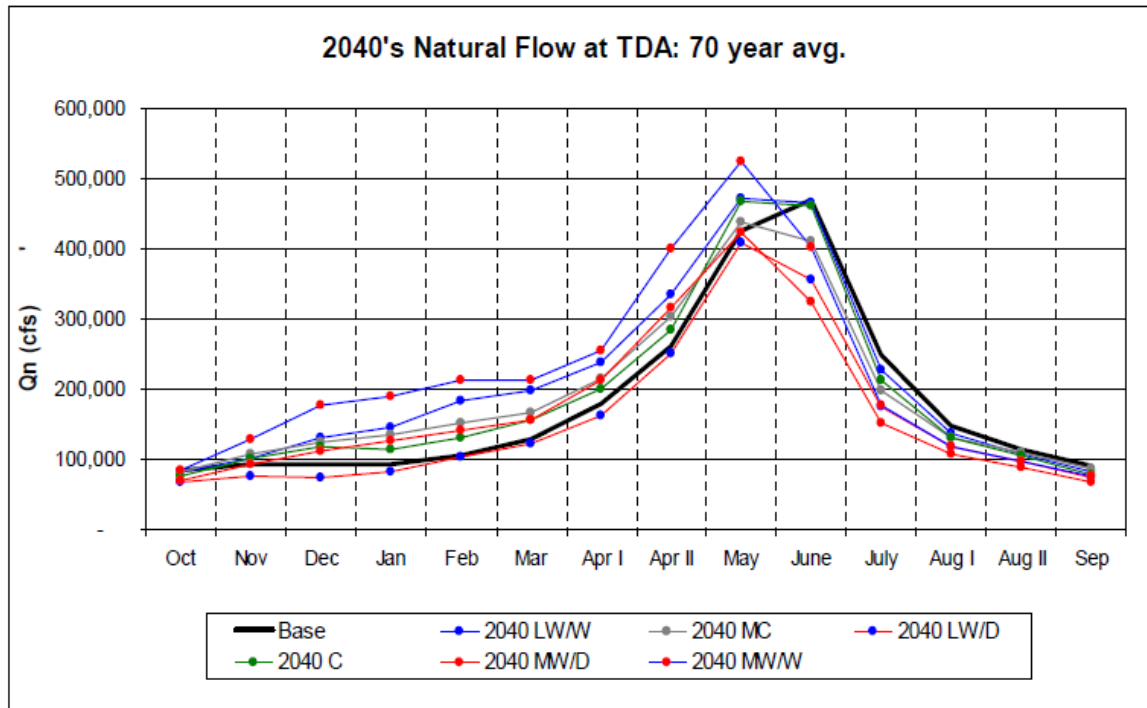


Figure 3: Monthly flow averages from six scenarios used for the RMJOC-I Study (RMJOC, 2011b) for the 2040s (2030-2059) at The Dalles, OR, relative to the long-term Modified Flows mean (1929-1998).

In addition to highlighting the conclusions above, the 2011 study cited several climate and modeling uncertainties (RMJOC, 2011c) which needed to be considered when using the results for planning purposes, and could be used to guide future hydroclimate research. These stated uncertainties, along with concerns expressed during peer review of RMJOC-I and subsequent regional change studies, helped to inform the project design for this research effort (Section 2). Broadly, the study suggested that future efforts should account not only for the uncertainties in future climate and climate modeling, but also for the uncertainties introduced in the downscaling and hydrologic modeling processes applied to make the outputs from the GCM models more relevant in terms of time scale, spatial resolution and data type to water resources planning.

In 2012, BC Hydro (Jost and Weber, 2012) conducted a key hydroclimate study concurrent to the 2011 RMJOC assessment. The BC Hydro analysis was produced using the same CMIP-3/IPCC-4 datasets used for RMJOC-I and discusses the uncertainties associated with projected climate-changed hydrology introduced by the hydroclimate modeling chain. BC Hydro, which is the largest electric utility in British Columbia and the official Canadian representative for the Columbia River Treaty, conducted its study with the Pacific Northwest Climate Impacts Consortium (PCIC). Unlike UW-CIG/RMJOC-I, the BC Hydro study utilized a hybrid downscaling technique, which included the use of the Canadian Regional Climate Model to downscale ten GCM temperature and precipitation fields to a resolution of 25km, with the outputs then statistically downscaled to 1-4km grid resolution for hydrologic modeling. The team also used the same hydrologic model used by the University of Washington, but used a different parameter set developed by PCIC. In addition, the project team from the Western Canadian Cryosphere Network (WC2N) utilized a different hydrologic model – the Hydrologiska Byråns

Vattenbalansavdelning Model from Scandinavia, which is well suited for glaciated catchments and parameterized by Environment Canada (HBV-EC) (Schnorbus and Rodenhuis, 2010).

While the BC Hydro study noted that streamflow trends were similar to what was found in the UW-CIG/RMJOC-I study, the BC Hydro projections indicated a greater overall increase in upper Canadian Basin precipitation, which resulted in more sustained annual flow and volume increases. The study also showed that outputs using different downscaling techniques and hydrologic models can yield a greater range of possible streamflow outcomes than RMJOC-I. Furthermore, the UW-CIG flows were generated with only one hydrologic model (VIC) and one calibration parameter set. Due to the above differences, it appeared that RMJOC-I had notably underestimated the range of uncertainty in possible future streamflow outcomes (**Figure 4**).

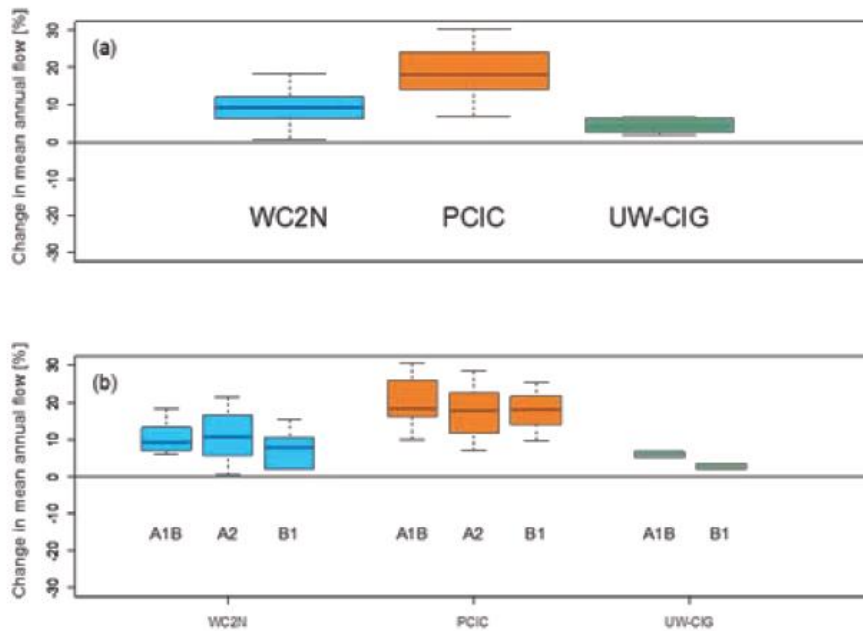


Figure 4: Projected changes in annual streamflow (%) for the Mica, BC basin. Comparisons between WC2N and PCIC projections (2012) and UW-CIG streamflow models (2010) for the 2040s. Note the greater increase in annual flows in the two BC Hydro study flows compared to UW-CIG, and greater range of potential outcomes. From Jost and Weber (2012).

1.2 Literature Review

1.2.1 Climate Change Progression, and Expected Impacts on the Hydrologic Cycle

Since the RMJOC-I study was completed in 2011, evidence has continued to mount that anthropogenic climate warming has begun over most of the planet, as expected, and that continued warming will almost certainly have increasing effects and impacts on global and regional climate well into the 21st century. This is most clearly articulated in the Fifth Intergovernmental Report on Climate Change: The Physical Science Basis (IPCC, 2013) and subsequent IPCC reports, including its Climate Change 2014 Synthesis Report (IPCC, 2014). Based on numerous studies cited in the report, “Warming of the climate system is unequivocal, and since the 1950s, many of the observed changes are unprecedented over decades to millennia. The atmosphere and ocean have warmed, the amounts of snow and ice have diminished, and sea level has risen.” Furthermore, “Surface temperature is projected to rise over the 21st century under all assessed emission scenarios. It is very likely that heat waves will

occur more often and last longer, and that extreme precipitation events will become more intense and frequent in many regions.” (IPCC, 2014).

Since the 2014 IPCC report was published, observed temperature records demonstrate that global warming is continuing to occur. In 2018, NOAA’s National Centers for Environmental Information reported that 2016 was the warmest year globally since reliable surface-based records have been kept (since 1883), with all four of the warmest years on record occurring in the 2014-2017 period (**Figure 5**).

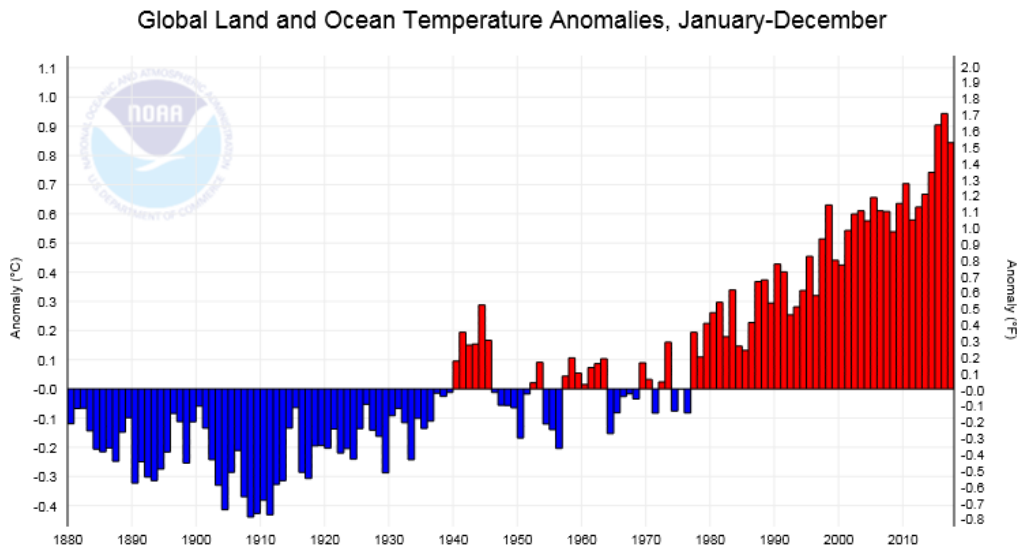


Figure 5: Average global temperature, relative to the long-term mean (°C). From NOAA National Centers for Environmental Information, 2018.

In the United States, the Fourth National Climate Assessment was published (USGCRP, 2017), which reconfirmed that unprecedented warming trends were also occurring across much of the earth, including North America and the Columbia River Basin (**Figure 6**). Its summary statements were particularly conclusive and relevant for long-range hydroclimate trends:

“Global annually averaged surface air temperature has increased by about 1.8°F (1.0°C) over the last 115 years (1901-2016). This period is now the warmest in the history of modern civilization, and the last three years have been the warmest years on record for the globe. These trends are expected to continue over climate timescales.

[Based] on extensive evidence, (...) it is extremely likely that human activities, especially emissions of greenhouse gases, are the dominant cause of the observed warming since the mid-20th century. For the warming over the last century, there is no convincing alternative explanation supported by the extent of the observational evidence.

In addition to warming, many other aspects of global climate are changing, primarily in response to human activities. Thousands of studies conducted by researchers around the world have documented changes in surface, atmospheric, and oceanic temperatures; melting glaciers; diminishing snow cover; shrinking sea ice; rising sea levels; ocean acidification; and increasing atmospheric water vapor . . . [and,]

Annual trends toward earlier spring melt and reduced snowpack are already affecting water resources in the western United States and these trends are expected to continue. Under higher scenarios, and assuming no change to current water resources management, chronic, long-duration hydrological drought is increasingly possible before the end of this century (USGCRP, 2017).”

Surface Temperature Change

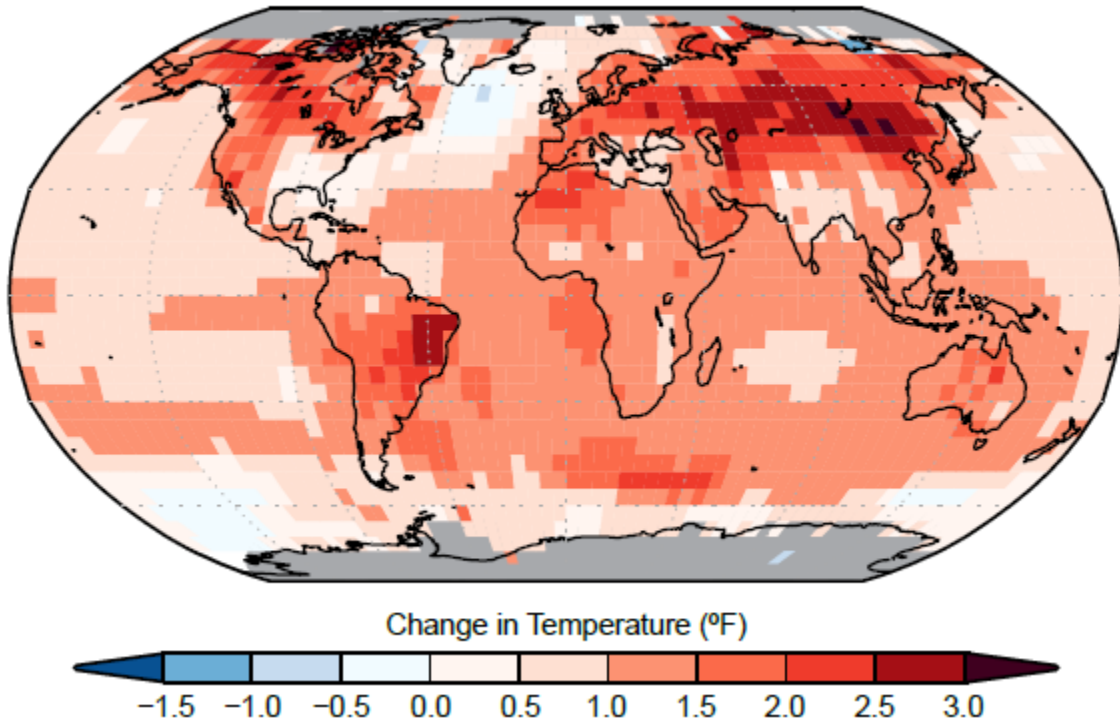


Figure 6: Surface temperature change (in °F) for the period 1986-2015 relative to 1901-1960 from the NOAA National Centers for Environmental Information’s (NCEI) surface temperature product. From USGCRP (2017).

In addition to these recent, well sourced, and cross-confirming peer-reviewed studies, regional climate experts have studied more specific climate change impacts to the Columbia River Basin, and the possible impacts on the hydroclimate system, for well over a decade. Numerous studies (e.g., Hamlet and Lettenmaier, 1999; Mote and Salathé, 2008; Hildalgo *et al.* 2009; Mantua *et al.*, 2009; Elsner *et al.*, 2010) have projected that as warming continues, Columbia River Basin snowpack is likely to decline, winter streamflows will tend to increase, peak seasonal snowmelt season (freshet) will tend to occur earlier in the spring, and summer flows will likely decrease.

More recently, in climate assessments mandated by the US Congress under the SECURE Water Act of 2009, both USBR (2016) and Department of Energy (2017) reached similar conclusions for Columbia River Basin hydroclimate using the most recent data from CMIP5/IPCC-5. While both reports were national in scope, and the underlying model outputs were rather coarse temporal and spatial resolutions for the Columbia Basin, they agreed that temperatures in the Columbia River Basin will almost certainly continue to rise over the next several decades, which will impact snowpack and subsequent seasonal runoff. Both reports also indicated that a signal may be emerging in the temperature and precipitation datasets produced by the GCMs and their

downscaled counterparts that wetter falls and winters may develop over time in the Columbia Basin, which would correspond to higher annual precipitation despite a possible, partially offsetting emerging trend for already dry summers to turn drier in parts of the basin. These findings are further supported by the region-specific USACE Climate Change Assessment for Water resources literature synthesis for the Pacific Northwest (USACE, 2015). For the region, there is strong consensus among studies that maximum temperature and precipitation extremes are projected to increase (Figure 7).

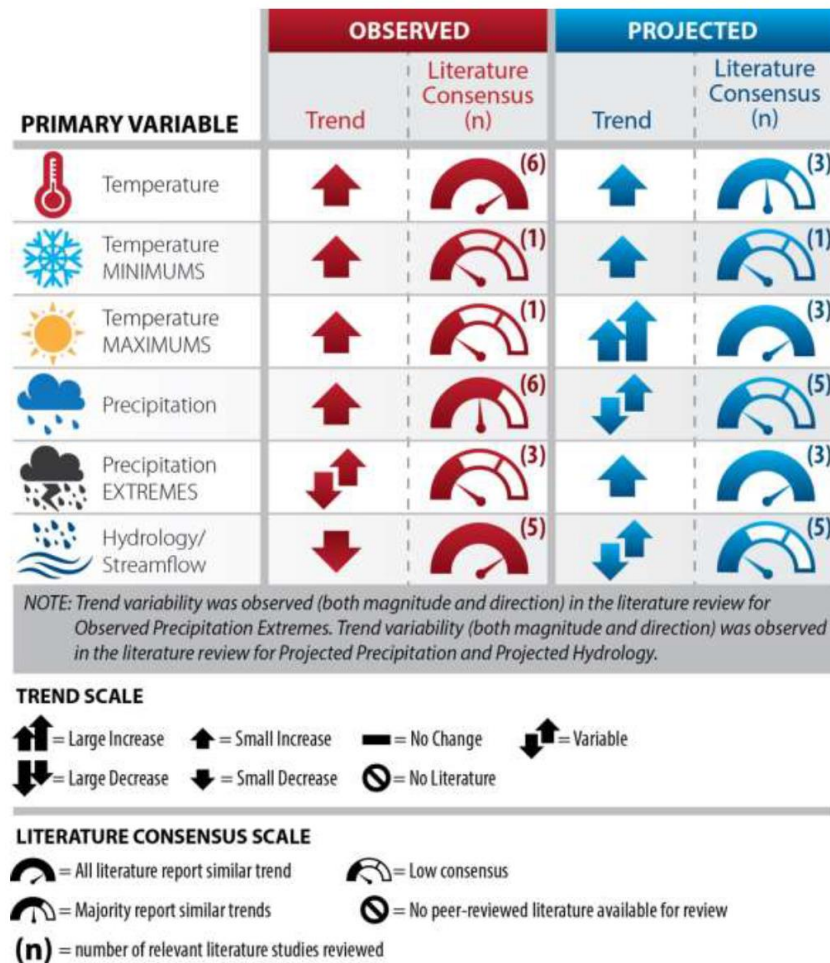


Figure 7: Summary matrix of observed and projected climate trends and literary consensus reported in USACE (2015).

Building on the potential for increasing Columbia River Basin precipitation, researchers have looked to intensification of Atmospheric Rivers (AR) as a potential cause for increasing cool season mean and extreme precipitation. The US West Coast receives the majority of its precipitation during the winter months (Neiman *et al.*, 2008). More recent climate model projections show increases in cool season precipitation mean (Salathé *et al.*, 2014; Tohver *et al.*, 2014; Rupp *et al.*, 2017) and variability (Rupp *et al.*, 2017), most likely due to increased moisture transport into the region. Warner *et al.* (2012) indicates that based on CMIP-5 GCM projections, winter mean precipitation along the US West Coast is likely to increase by 11% to 18% by late 21st century, while extreme precipitation days associated with atmospheric rivers are likely to increase 15% to 39%. Warner and Mass (2017) go further, using dynamically downscaled GCM data to show that while AR frequency and seasonality may only change slightly through the rest

of the 21st century in the northeast Pacific Ocean, the amount of moisture and precipitation each future AR event will bring to the coast is likely to increase. There is a growing body of work that implicates the intensification of ARs as a physical basis for the potential of increasing Columbia River Basin precipitation during the fall and winter months. Such precipitation increases, along with a warming climate, could have profound implications on both the magnitude and seasonality of future streamflows for hydroregulation operations and planning.

1.2.2 Hydroclimate Modeling Science

In addition to continued advances in climate change science since the last RMJOC study, the science of hydrologic modeling has also advanced. There is growing interest in uncertainties within the hydrological modeling process and impacts of different methodological decisions on those uncertainties (Poulin *et al.*, 2011; Mizukami *et al.*, 2016). Properly accounting for the spread or range of uncertainty down the modeling chain, from GCM to downscaling method, to hydrology model, and to hydrology model calibration and parameter set, is a complex and new effort in climate change hydrology (Clark *et al.*, 2016). In some applications (Wilby and Harris, 2006; Teng *et al.*, 2011) the largest part of the total uncertainty appeared to have come from emissions profiles and GCM spread. Other applications (Mendoza *et al.*, 2015) have shown the wide spread produced using different hydrology models including versions of VIC and PRMS used in this study, a spread across hydrology models larger than the climate change signal itself for Colorado River headwaters basins. At present, no consensus exists for a general statement on where in the modeling chain the majority of the uncertainty arises, and this study did not answer that question for the Columbia River basin.

This idea has been embraced in this particular climate change study, which sought to explicitly characterize and address these uncertainties throughout the hydroclimate modeling process: emission scenarios, global climate models, hydrological model, and hydrological model parameters. However, there are yet more uncertainties in the modeling chain, beyond what is addressed in this project, which must be considered in certain situations. For example, uncertainties in historical climate and hydrology records are often ignored, yet vary over space and time (Tripathi and Govindaraju, 2008). Kotlarski *et al.* (2017) showed how uncertainty in gridded observational datasets, while usually small in the context of climate change, can be pronounced in some situations. These can be further amplified where impacts are linked to defined thresholds (*e.g.*, snowmelt processes, forest fires). Eum *et al.* (2014) showed that temperature and precipitation in two gridded climate records can be quite different, especially in data-sparse areas, which can lead to significant differences in downscaling results.

One other consideration during this project involved how hydrological model streamflow outputs are post-processed to adjust flows to a historical dataset to remove any biases that arise from the hydroclimate modeling process. Streamflow simulations commonly exhibit biases relative to a historical period, despite intensive efforts to calibrate and bias-correct the temperature and precipitation forcings, and to carefully calibrate streamflow models. It is common to mitigate these issues by using an additional post-processing step relative to the historical period (Snover *et al.*, 2003). This “streamflow bias correction” process is particularly important for hydroregulation modeling and other streamflow or volume rules-based operations—many of which are based on historical flows. However, the most commonly used bias correction methods can have the unintended effect of artificially masking or even eliminating important climate change signals since the methods are based on quasi-stationary

historical trends, which are becoming non-stationary in a changing climate (Cannon *et al.*, 2015). While this issue is partially addressed in this particular study (see Section 4.5), bias-correcting both the meteorological forcings and hydrological outputs is an emerging, fertile area of research and it is likely that the recommended methodology adopted for this study will evolve or be replaced in time.

2.0 Project Design

2.1 BPA Opportunity for Proposals Research (2013) and RMJOC Commissioning

In March 2013, as Global Climate Model (GCM) results from the Fifth Coupled Modeling Intercomparison Project (CMIP-5) were becoming available, the Bonneville Power Administration issued a research Opportunity Announcement through its Office of Technology and Innovation (BPA, 2013a). In it, BPA cited climate change as a key focus area in need of outside research assistance as part of its overall and ongoing risk management assessment of its hydroelectric fuel supply (BPA, 2013b).

More specifically, the Opportunity for Proposals envisioned “development of a new set of temperature, precipitation, snowpack, and streamflow forecast projections for the entire Columbia River System, based on the new Global Climate Model datasets . . . published in conjunction with IPCC-5. For BPA and its Federal partners to use these datasets in hydroregulation and flood control studies, these projections should:

- Be available in daily time steps;
- Extend in time from the years 1950 through 2100;
- Take into account at least two Representative Concentration Pathways (RCPs) that are estimates of future carbon dioxide emissions;
- Take into account climate change-induced glacial melt, particularly in the Canadian portion of the Columbia River Basin;
- Use at least two different downscaling techniques;
- Use at least two different hydrologic models to generate unregulated (natural) flows;
- Provide streamflow projections that are unbiased in the 1950-2010 (historic) period relative to best-available, estimated natural streamflows during that time; and
- Be provided in a format usable by all three RMJOC members to run hydroregulation studies (BPA, 2013b).”

Simultaneous with the BPA Opportunity of Proposals, the RMJOC agencies signed a four-year Memorandum of Understanding to collaborate on the project, provide the research entities a nearly naturalized, historical streamflow dataset, provide technical assistance to the research teams, and coordinate how the new set of streamflows would be used to update long-range hydroregulation planning studies. The RMJOC also agreed that a subset of the studies would be used in common for its coordinated planning activities, and that whichever scenarios were selected would “make reasonable scientific attempts to capture the most reasonable range of possible streamflow scenarios as climate change takes hold over the Columbia River Basin (RMJOC, 2014).”

2.2 Project Statement of Work

Ultimately, a collaboration team from the University of Washington and Oregon State University completed the research documented in this report. The proposal, which was almost entirely executed as intended, not only met the key Opportunity of Proposals requirements, but in three

key areas also expanded the research scope as new opportunities and scientific advances arose during the four-year effort.

The University of Washington and Oregon State University research improved upon the 2011 RMJOC-I projected, climate changed streamflow dataset by fulfilling all nine of the Opportunity for Proposals requirements by specifically:

- Using the latest CMIP-5 climate change scenarios (IPCC, 2013), as well as recent regional downscaled climate modeling, if available;
- Using temperature and precipitation outputs from at least two downscaling methods;
- Developing a methodology to rapidly evaluate a large number of climate change projections to estimate changes in seasonal streamflow, with the methodology adaptable enough to be used after the end of the project to update seasonal streamflow projections as more climate change simulations became available; and
- Using at least two different hydrological models, one of which would include an explicit subroutine to model glacier melt and depletion in the upper Columbia Basin.

The proposal went further by utilizing a new objective technique to select the best-performing Global Climate Models in the Columbia Basin relative to historical conditions, and included an option to use dynamically downscaled temperature and precipitation data from Regional Climate Models (RCMs), if such data became available during the life of the project.

More broadly, the project proposal had two main objectives: to better account for the range of climate change outcomes; and to better account for the additional spread introduced by the methodological choices made in the hydrologic modeling chain. However, as the project proceeded, several other research opportunities emerged, which were incorporated in updates to the Statement of Work, including:

- The evaluation of how different sets of calibration parameters for the same hydrologic model can lead to different streamflow outcomes, even when using the same downscaled temperature and precipitation inputs;
- The incorporation of a different streamflow bias correction technique, which allowed climate change streamflow to adjust seasonally with climate change signals, and not be forced into previously observed climate; and
- Expanding on a recently devised inverse routing calibration technique, which allowed for rapid model recalibrations as new historical data became available or was corrected.

Consistent with BPA Technology and Innovation project requirements, the Statement of Work included a series of Go/No Go stage gates to monitor and evaluate project progress, and adjust timelines as needed (**Figure 8**). At each stage gate, the RMJOC technical teams, BPA's Technology and Innovation Office, and the University of Washington/Oregon State University research team, formally reviewed project scope, schedule and budget, and project deliverables for scientific validity. As the project proceeded, stage gate timing and scope was adjusted to account for new discoveries and information, which allowed the research team to incorporate new state-of-the-science techniques as they emerged in the broader research community.

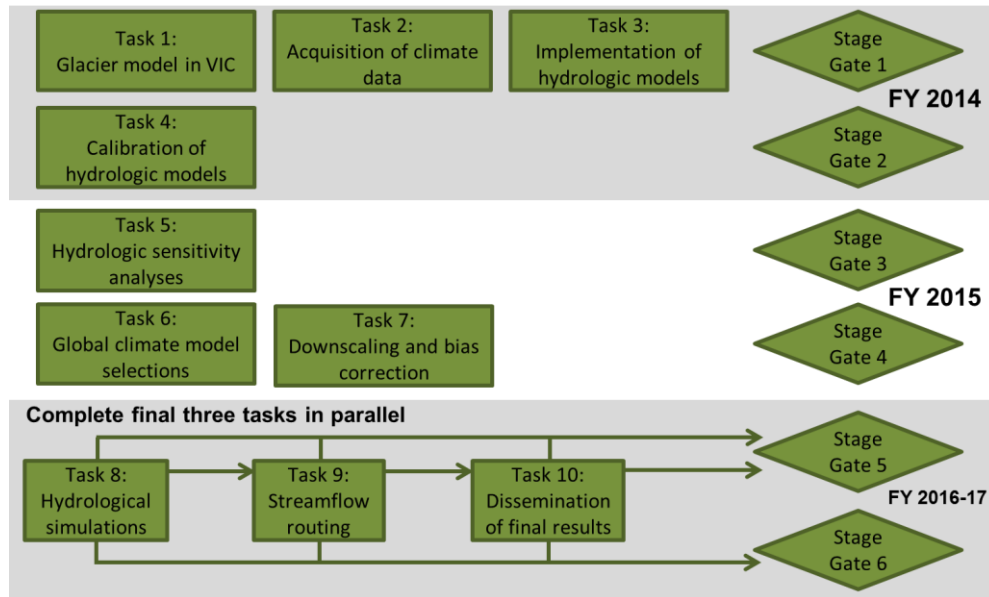


Figure 8: Project Deliverables, Timeline and Stage Gate Breakpoints. Stage Gates 5 and 6 were structured to this final flowchart in Year 3 of the project (2016).

The project structure gave the research teams the flexibility to incorporate new science or datasets as the project proceeded. For example, in 2015, when the project team was informed of a new, hybrid dynamical-statistical downscaled dataset from Oak Ridge National Laboratory as part of the 2017 9505 assessment (DOE, 2017), the scope for Task 7 was expanded to include this new option. In 2016, when provisional datasets became available, the Statement of Work for Tasks 8-10 was revised to allow for parallel quality control and data evaluation as sets of flows were generated. This allowed RMJOC technical teams to review each set of provisional data as it became available rather than wait for the entire dataset to be published at once at the end of the project.

2.3 Technical Stakeholder Feedback Process

One of the strengths of RMJOC-II was the stakeholder and feedback process that was established as the project began in 2013. Three layers of interaction were established, with different levels of interaction and detail throughout the modeling process.

At the highest level of review, several one or two-day Transboundary Workshops were held every three to nine months to brief over 100 technical regional stakeholders in the Columbia River Basin, including US and Canadian government scientists, Tribal and State representatives, and regional public and investor-owned hydropower utilities. The workshops served as the formal venue to brief stakeholders on project progress, to solicit feedback, and to share results as they became available, even if the results were preliminary and later revised. Three of these workshops were held in conjunction with annual BPA Technology and Innovation portfolio reviews. These allowed the research scientists to brief the principal project funders on progress, and for the RMJOC teams to brief the funders on how the resulting datasets would be used.

Second, the Columbia River Forecasting Group (CRFG) was used as a more advanced technical review body. The CRFG includes regional weather and streamflow forecasting experts from Federal agencies, states and tribes that forecast inter-annual water supply and streamflow

conditions across the basin, and also monitor the latest state-of-the-science in hydrologic forecasting, including advances in climate change research. The group met quarterly each year, which allowed the project teams to interact with stakeholders on more technical aspects of the research and dataset development, allowed the project team to educate CRFG members on climate change science on a fairly regular basis, and gave CRFG members direct access to the research leads to answer specific questions and maintain transparency during the modeling process.

Finally, the RMJOC technical leads, BPA project manager, and the University of Washington research team met monthly to brief each other on project progress. More frequent project check-ins were held as key stage gates were approached, or draft dataset outputs were reviewed. This allowed the teams to adjust resources as needs changed throughout the effort, and manage expectations on dataset deliveries and quality.

This highly interactive and somewhat unusual interaction structure paid unintended benefits throughout the effort (Chegwidden *et al.*, 2016). Not only did the project team receive ongoing and timely feedback as each step in the hydroclimate modeling chain was executed, but timelines were easily adjusted, particularly in the final project stage. This allowed for more in-depth peer reviews of provisional streamflow datasets before official publication. This restructuring facilitated improvement in the modeling process throughout the project, and led to better reproducibility of the streamflows not only for this study, but for future hydroclimate studies.

3.0 No Irrigation-No Regulation Dataset Development

3.1 Background

The No Regulation-No Irrigation (NRNI) dataset was developed to best represent streamflows unaffected by human activity in the Columbia River Basin, and other basins west of the Cascades, including the Willamette Basin, prior to any water resources development for the period of 1929-2008. The challenge with creating the NRNI dataset for the entire Columbia River basin is that available streamflow gauge observations include dam construction and operations, irrigation withdrawals and returns, and other development which changed the natural flow regime. In addition, the development of this infrastructure occurred throughout the 20th century, which makes adjustments to the observed streamflows spatially and temporally variable. The current practice by BPA, USACE, and USBR, as required for a variety of planning and operational purposes in the Columbia Basin, is to first create a homogeneous dataset of streamflows that reflect the current level development. This retroactive adjustment to regulation and irrigation to the systematic record is termed Modified Flows. The Modified Flows are then used to create the NRNI dataset.

One part of the NRNI dataset was developed by USBR for the Yakima River, the Deschutes River Basin, and the Snake River Basin above Brownlee Dam. These flows were “calculated from measured data using variations on mass balance equations that assume that water can neither be created nor destroyed in a system (USBR 2017).” USACE developed the NRNI dataset for the remainder of the Columbia River Basin, the Willamette Basin, and smaller basins in western Oregon and Washington that flow directly to the Pacific Coast. BPA provided technical guidance and quality control assistance throughout the process of generating the combined NRNI dataset.

NRNI flows were first used in 2012-13 to create the synthetic streamflows used by the USACE to assess flood risk impacts for the Columbia River Treaty (CRT). Since the intent of NRNI is to represent flows devoid of most historical human influences, the dataset allows for more accurate calibration of hydrology models to historical naturalized flows. For RMJOC-II these NRNI flows also served as the basis for bias-correcting the hydrology models. The dataset is available for download on the BPA historical streamflow website:

<https://www.bpa.gov/p/Power-Products/Historical-Streamflow-Data/Pages/Historical-Streamflow-Data.aspx>. Locations where NRNI data was generated are shown in **Figure 9**.

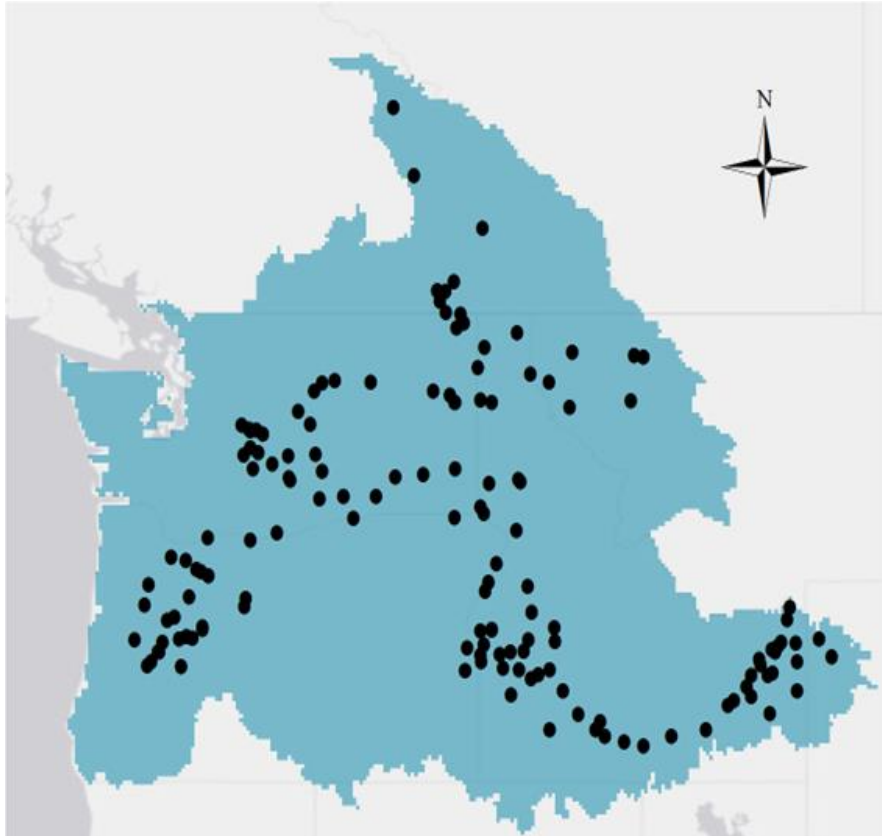


Figure 9: NRNI time series locations.

As the starting point for NRNI calculation, data from the 2010 Modified Streamflows dataset was used (BPA, 2011a). The dataset contains daily streamflow information for the Columbia River basin including:

- Upper Columbia and Kootenay Basins
- Pend Oreille and Spokane Basins
- Mid-Columbia Basin
- Snake Basins – Upper, Central and Lower Snake River Basin
- Lower Columbia Basin and Oregon Closed Basin
- Willamette Basin

Modified flows are defined as:

“ . . . The historical streamflows that would have been observed if current irrigation and depletions (as of year 2008) existed in the past and if the effects of river regulation were removed (except for the upper Snake, Deschutes and the Yakima basins where current upstream reservoir regulation practices are included) . . . the historical streamflows have been adjusted to account for current levels of irrigation depletions. The 2010 Modified Flows study includes 80 years of flows (1929-2008) adjusted to 2010 irrigation depletions (BPA, 2011a).”

Most of the 2010 Modified Streamflows computation points are at dams within the basin, but a few additional points corresponded to US Geological Survey (USGS) gaging stations and other

historically significant locations. The purpose of developing this standardized dataset is to provide consistent input hydrology for all operating agencies in the Columbia River basin. Modified Flows data locations are shown for point locations in **Figure 10**.

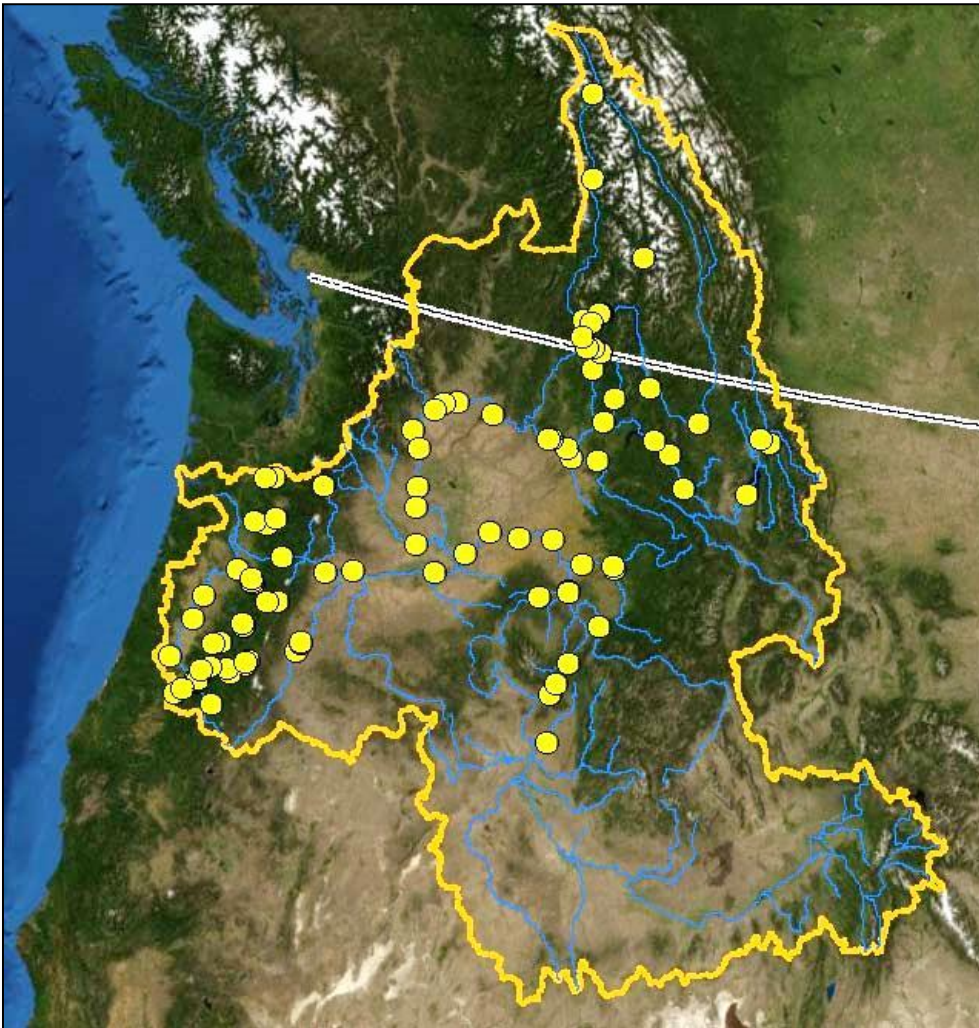


Figure 10: 2010 Level Modified Streamflow locations for the Columbia Basin (in BPA, 2011a).

3.2 Methodology

The daily NRNI flows were developed in two steps. The USBR initially developed streamflows for the three sub-basins in the Columbia River watershed: the Yakima, Deschutes, and Upper Snake Rivers (for flows into and above Brownlee Reservoir). Next, these data were assimilated with flows throughout the remainder of the Columbia basin to create the integrated basin-wide NRNI product.

The process for developing the NRNI dataset includes calculating either observed or adjusted observed streamflows (removing reservoir regulation effects), and then adding or subtracting volumes where irrigation activities have influenced the observations (*e.g.*, irrigation withdrawals or irrigation flow returns). The impacts of differences in evaporation from reservoirs' surface areas (as compared to pre-dam natural river reach area and vegetated land surfaces) are also

included in the adjustments to the observed streamflows. The following paragraphs further describe the detailed steps and data required to calculate NRNI flows.

The NRNI daily flows consist of a systematic record of observed streamflows which have the effects of man-made storage and regulation removed (A and ARF in cfs), along with the impacts of historic level depletions for irrigation (D and DD in cfs) and reservoir surface evaporation (E and EE in cfs). The single letter refers to incremental flow (local inflow between modified flow points), and the multiple letter acronym to cumulative flow at a site. The A and ARF flows are termed “unregulated” streamflow. The D and DD sub-types represent the irrigation that would have been observed during a given year. In NRNI, this D and DD volume increases the NRNI flow rates above the unregulated rates (A and ARF). The D and DD datasets were calculated from separate studies which analyze agricultural information for the United States Department of Agriculture (USDA). The E and EE volumes were calculated from previous evaporation studies during or shortly after dam constructions. The NRNI E or EE sub-type represents the evaporation without dams.

NRNI total flows (N) are defined with an equation that identifies the constituent components making up the NRNI daily time series. NRNI uses the historical project inflows and routed streamflows (A and ARF) developed in the 2010 Modified Streamflows study and replaces the D/DD and E/EE data with the converted NRNI version of the time series. The form of the NRNI equation at an NRNI computation point is:

$$\begin{aligned} \text{NRNI} &= \text{ARF} + \text{EE} - \text{DD (cumulative flow)} \\ \text{NRNI} &= \text{A} + \text{E} - \text{D (incremental flow)} \end{aligned}$$

Historical irrigation (D and DD) withdrawals and return flows were derived using individual state and Federal diversion reports along with streamflow gauge records from the US Geological Survey and other available sources. The irrigation withdrawals were calculated using USDA sprinkler and gravity depletions and monthly rates of depletion and returns, and then applied on a daily time step for each month. Calculations were performed to add back in the net loss volumes from estimates of historical daily depletions and return flows. Canadian site depletions were developed in a similar manner.

NRNI flow evaporation adjustments (E and EE) are made to the historical streamflow to reflect without-dam conditions. For Modified Streamflows development, E and EE values are zero after dam construction because the evaporation was accounted for in the observed data, but prior to the dam construction the values are negative to remove the water that would have been lost to evaporation if the dam had been in place. This adjustment is only applicable to the Modified flows application to reflect the conditions of the base year 2008. For the development of NRNI, the E and EE files are zero prior to dam construction so as to reflect the pre-dam conditions, but after dam construction they add back in the water that would have been lost each year to evaporation. Pre-dam observed streamflow records used for NRNI already incorporate losses due to evaporation from natural lakes. In both Modified Streamflows and NRNI, the absolute non-zero monthly values are the same in magnitude.

The evaporation/transpiration time series used to adjust the observed record reflects the natural stream system for water years 1928 through 2008. This time series accounts for differing vegetative cover before and after dam construction. In most cases, construction of a dam

increases evaporation from the reservoir area through evaporation from the water surface. However, in some cases at northern latitudes where reservoirs replaced dense forests, evaporation from reservoir surfaces is less than evapotranspiration of the natural forested pre-dam surface condition. In these cases dam construction led to gains in water through changes in evaporation and transpiration.

3.3 Daily NRNI Flow Development

3.3.1 Upper Columbia and Kootenay Basins

NRNI daily flows were generated for 13 sites in this part of the Columbia River basin (**Table 1**).

Table 1: Upper Columbia and Kootenay Basins NRNI daily flow sites

Site	Name	NRNI Equation
MCD	Mica	$MCD5N = MCD5A - MCD5DD + MCD5E$
RVC	Revelstoke	$RVC5N = RVC5ARF - RVC5DD + RVC5EE$
ARD	Arrow - Hugh Keenleyside	$ARD5N = ARD5ARF - ARD5DD + ARD5EE$
LIB	Libby	$LIB5N = LIB5A - LIB5DD + LIB5E$
BFE	Bonnors Ferry	$BFE5N = BFE5ARF + LIB5E - KMT5D + EKO5D$
DCD	Duncan	$DCD5N = DCD5A + DCD5E$
COR	Cora Linn	$COR5N = COR5ARF - COR5DD + COR5EE$
CAN	Kootenay Canal	$CAN5N = COR5N$
UBN	Upper Bonnington	$UBN5N = COR5N$
LBN	Lower Bonnington	$LBN5N = COR5N$
SLO	Slocan	$SLO5N = COR5N$
BRI	Brilliant	$BRI5N = BRI5ARF - BRI5DD + COR5EE$
MUC	Murphy Creek	$MUC5N = MUC5ARF - MUC5DD + MUC5EE$

The Upper Columbia and Kootenay basin sites were developed by the methodology described in Section 3.0. The 2010 Modified Flows time series were used for the NRNI flows, while the 2010 depletion (D and DD) and evaporation (E and EE) files from the Modified Flows process were replaced with historic-level time series.

3.3.2 Pend Oreille and Spokane Basins

NRNI daily flows at the Pend Oreille and Spokane Basin sites were developed using the methodology described in Section 3.2. Total NRNI daily flows were generated for 20 sites in these basins (**Table 2**).

Table 2: Pend Oreille and Spokane Basins NRNI daily flow sites

Site	Name	NRNI Equation
HGH	Hungry Horse	$HGH5N = HGH5A + HGH5E$
CFM	Columbia Falls	$CFM5N = CFM5ARF + HGH5E$
KER	Kerr	$KER5N = KER5ARF - KER5DD + HGH5E$
TOM	Thompson Falls	$TOM5N = TOM5ARF - TOM5DD + HGH5E$
NOX	Noxon Rapids	$NOX5N = NOX5ARF - NOX5DD + NOX5EE$
CAB	Cabinet	$CAB5N = CAB5ARF - CAB5DD + NOX5EE$

PSL	Priest Lake	PSL5N = PSL5A
ALF	Albeni Falls	ALF5N = ALF5ARF - ALF5DD + NOX5EE
BOX	Box	BOX5N = BOX5ARF - BOX5DD + NOX5EE
SUV	Sullivan Lake	SUV5N = SUV5A
BDY	Boundary	BDY5N = BDY5ARF - BDY5DD + NOX5EE
SEV	Seven Mile	SEV5N = SEV5ARF - SEV5DD + NOX5EE
WAT	Waneta	WAT5N = WAT5ARF - SEV5DD + NOX5EE
COE	Coeur D'Alene	COE5N = COE5A - COE5DD
PFL	Post Falls	PFL5N = COE5N
UPF	Upper Falls	UPF5N = UPF5ARF - UPF5DD
MON	Monroe Street	MON5N = UPF5N
NIN	Nine Mile	NIN5N = NIN5ARF - UPF5DD
LLK	Long Lake	LLK5N = LLK5ARF - UPF5DD
LFL	Little Falls	LFL5N = LLK5N

3.3.3 Upper Snake Basin, Yakima Basin, and Deschutes Basin

By and large, calculation of the NRNI flows was similar to how USBR calculated flows for the 2010 Modified Flows dataset (BPA, 2011a). A different calculation process is used to develop the NRNI flows for these three particular basins, because for long-range and annual hydroregulation planning purposes, USACE and BPA do not attempt to disaggregate natural flows with multi-year USBR irrigation facilities and projects. For this particular application, though, a record of relatively naturalized flows was required for hydrologic model calibration and bias correction.

For the Upper Snake and Deschutes sub-basins, USBR used the MODSIM reservoir simulation model to create simulated natural, historical daily flows and volumes. These flows attempt to simulate the natural condition by removing reservoir operations along with irrigation diversions and return flows. In places where daily diversion data was not available, monthly diversions were subsequently disaggregated by USBR to a daily time series using the simple method developed by Acharya and Ryu (2013). A similar calculation was used for the Yakima using spreadsheets. These data were provided to the USACE for use downstream of Brownlee Reservoir (upper Snake Basin), Kiona, WA (Yakima Basin), and Pelton/Round Butte, OR (Deschutes Basin).

3.3.4 Lower Snake River Basin

NRNI streamflows for the Snake River downstream of Brownlee dam were calculated by directly combining the daily Brownlee inflow time series generated by the USBR with local inflow time series, evaporation records, and depletion time series impacting each river reach between Brownlee Dam and points of hydrological significance (*e.g.*, tributary confluences, regulation control points). The method applied for the Lower Snake River Basin differs from the methodology described in Section 3.2 because the calculations described in Section 3.2 are based on mainstem unregulated flows that have been hydrologically routed (ARF). For the Lower Snake River Basin, hydraulic or hydrologic routing of the total upstream inflow and local inflow within each river reach was not represented, and thus flood wave timing and attenuation was not taken into account. However, tributary inflow timing and magnitudes inherited routing from when they were computed as part of the development of the Modified Flows dataset.

The influence of flood wave attenuation and timing on the ability to approximate Lower Snake River Basin flows was evaluated using the 2010 Modified Flows Dataset. Local inflow was hydrologically routed in the generation of the 2010 Modified Flows dataset using the Streamflow Synthesis and Reservoir Regulation (SSARR) model. For evaluation purposes, these flows were compared to the direct summation method described above to identify the relative influence of routing through the mainstem of the Lower Snake River. Comparing the summation method with the hydrologic routing method revealed some differences in streamflow timing at the daily timescale and little impact on magnitude. For example, some peak flows on the mainstem using the hydrological method could be lagged (1 to 3 days) behind flows using the summation method. At the monthly time scale, the differences in volumes were negligible except for cases where lagged peaks occurred at the beginning or end of month boundaries. These timing and volume differences were not deemed significant enough to adversely affect the intended usage for hydrological model calibration at the weekly time scale and streamflow bias-correction. Therefore, the simplified method for calculating total streamflow along the Lower Snake River was determined to be appropriate for the purposes of the project.

3.3.5 Mid-Columbia Basin

NRNI daily total flows were generated for eight Middle Columbia Basin computation points using the methodology described in Section 3.2. (**Table 3**).

Table 3: Mid-Columbia Basin NRNI daily flow sites

Site	Name	NRNI Equation
GCL	Grand Coulee	$GCL5N = GCL5ARF - GCL5DD + GCL5EE$
CHJ	Chief Joseph	$CHJ5N = CHJ5ARF - GCL5DD + CHJ5EE$
WEL	Wells	$WEL5N = WEL5ARF - WEL5DD + WEL5EE$
CHL	Chelan	$CHL5N = CHL5A$
RRH	Rocky Reach	$RRH5N = RRH5ARF - RRH5DD + RRH5EE$
RIS	Rock Island	$RIS5N = RIS5ARF - RIS5DD + RRH5EE$
WAN	Wanapum	$WAN5N = WAN5ARF - WAN5DD + WAN5EE$
PRD	Priest Rapids	$PRD5N = PRD5ARF - PRD5DD + PRD5EE$

The Yakima basin is also a part of the Mid-Columbia Basin, but the NRNI was generated using daily naturalized streamflows from USBR. The daily flow values for the Yakima River were provided from USBR’s RiverWare model. The values were not changed or combined with any other records.

3.3.6 Lower Columbia River and Oregon Closed Basin

The NRNI flows in the Lower Columbia River were developed using the methodology described in section 3.2. There were seven computation points where daily NRNI flows were generated (**Table 4**).

Table 4: Lower Columbia River and Oregon Closed Basin NRNI daily flow sites

Site	Name	NRNI Equation
MCN	McNary	$MCN5N = MCN5ARF - MCN5DD + MCN5EE$
JDA	John Day	$JDA5N = JDA5ARF - JDA5DD + JDA5EE$
*ROU	Round Butte	N/A
*PEL	Pelton	N/A
*RER	Pelton REREG	N/A
TDA	The Dalles	$TDA5N = TDA5ARF - TDA5DD + TDA5EE$
BON	Bonneville	$BON5N = BON5ARF - BON5DD + TDA5EE$

The Deschutes River Basin is part of the Lower Columbia and Closed basins. Similar to the Upper Snake River flows, the monthly volumes were provided by USBR. For this study, the flows at Madras, OR were disaggregated and combined with the flows at The Dalles.

3.3.7 Willamette Basin

The Willamette Basin sites were developed by the methodology described in Section 3.2. Total NRNI daily flows were generated for 27 sites in this basin (**Table 5**).

Table 5: Willamette Basin NRNI daily flow sites

Site	Names	NRNI Equation
HCR	Hills Creek	$HCR5N = HCR5A$
LOP	Lookout Point	$LOP5N = LOP5ARF + LOP5E$
DEX	Dexter	$DEX5N = LOP5N$
FAL	Falls Creek	$FAL5N = FAL5A$
DOR	Dorena	$DOR5N = DOR5A$
COT	Cottage Grove	$COT5N = COT5A$
CAR	Carmen Diversion	$CAR5N = CAR5H$
SMH	Smith R Reservoir	$SMH5N = SMH5A$
C_S	Carmen-Smith PP Inflow	$C_S5N = C_S5A$
TRB	Trail Bridge	$TRB5N = TRB5ARF$
CGR	Cougar	$CGR5N = CGR5A$
BLU	Blue River	$BLU5N = BLU5A$
LEA	Leaburg	$LEA5N = LEA5ARF$
WAV	Walterville	$WAV5N = WAV5ARF$
FRN	Fern Ridge	$FRN5N = FRN5A - FRN5D + FRN5E$
ALB	Albany	$ALB5N = ALB5ARF - ALB5DD + SVN5EE$
DET	Detroit	$DET5N = DET5A$
BCL	Big Cliff	$BCL5N = DET5A$
GPR	Green Peter	$GPR5N = GPR5A$
FOS	Foster	$FOS5N = FOS5ARF$
SLM	Salem	$SLM5N = SLM5ARF - SLM5DD + SVN5EE$
SVN	TW Sullivan	$SVN5N = SVN5ARF - SVN5DD + SVN5EE$
TMY	Timothy Meadows	$TMY5N = TMY5A$
OAK	Oak Grove	$OAK5N = OAK5A$
NFK	North Fork	$NFK5N = NFK5A$
FAR	Faraday	$FAR5N = NFK5A$

3.4 Statistical Analyses of the NRNI Dataset

3.4.1 Nonstationarities

The assumption of stationarity (statistical characteristics of hydrological time series are constant through time) has been a pillar of water management (Milly *et al.*, 2008). This assumption has enabled the use of well-accepted statistical methods in water resources planning and design that rely primarily on the observed record. Climate change has the potential to undermine this assumption. Recent issuance of USACE civil works policy guidance includes methodologies for the detection of nonstationarities in streamflow in support of USACE project planning, design, construction, operations, and maintenance (ECB 2016-25, USACE, 2016; ETL 1100-2-3, USACE, 2017).

Changes in hydrological processes can be abrupt or gradual. There are statistical techniques to detect abrupt and slow changes in mean, variance, and distribution of time series data. USACE (2017) identifies ten statistical techniques to detect these nonstationarities:

Mean-Based Tests detect a nonstationarity where there has been a significant change in the average value of the data:

1. Lombard Wilcoxon: Nonparametric test that nests the Wilcoxon score function within the Lombard test statistic to detect both smooth and abrupt shifts in mean by time.
2. Pettitt: Nonparametric test that identifies changepoints in the mean by testing whether two samples come from the same population.
3. Mann-Whitney: Nonparametric test on mean shift, that tests if a randomly selected value from one sample is greater than or less than a randomly selected value from the comparison sample (seen as the nonparametric counterpart to the t-test).
4. Bayesian CPD: Parametric (Gaussian) test that uses product partitions to identify change points within a sequence using MCMC sampling by assuming a sequence can be broken into partitions with a constant mean, where changes in the mean between partitions are change points.

Variance-Based Tests detect a nonstationarity where there has been a significant change in the variance of the data:

5. Mood: A nonparametric case of a Pearson's Chi-test that evaluates change points based on volatility in medians between defined samples.
6. Lombard Mood: Nests the Mood score function within the Lombard test statistic to detect both smooth and abrupt shifts in variance by time.

Distribution-Based Tests detect a nonstationarity where there has been a significant change in the underlying distribution of the data, which can be caused by a change in the parameters of the same distribution or from one distribution type to another (test shape, location, and modality):

7. Cramer-Von-Mises: Nonparametric goodness-of-fit test that compares two empirical distributions by evaluating a test statistic of distributional distance.
8. Kolmogorov-Smirnov: Nonparametric test that compares two empirical distributions by evaluating a test statistic of distributional distance.
9. LePage: Nonparametric test which simultaneously tests the equality of both the location and scale parameters, where inequality in one suggests distributional shift.
10. Energy Divisive: Nonparametric test based on hierarchical clustering, where change points are iteratively identified and can be diagrammed as a binary tree. The statistical significance is examined by means of a permutation test that combines bisection and multivariate divergence measures.

These statistical tests were applied to identify nonstationarities in time series of annual maximum annual flows at the 1 and 30-day durations and annual minimum summer 7-day mean flow for each NRNI location for the period of 1929-2008. These metrics were selected to represent flashy rain driven peaks, longer duration peaks associated with snowmelt, and low flows. The number of detections were summed for each statistical type (mean, variance, and distribution), for each location as an indicator of the relative strength of the nonstationarity detected within the time series at each location. Robust detection of nonstationarity is considered when sites show nonstationarities in multiple statistical properties.

Nonstationarities were detected in 65%, 52%, and 79% of the NRNI sites' time series of annual daily maximum flows for the mean, variance, and distributions, respectively (**Figure 11**). Slightly more nonstationarities were found in coarser duration peak flows. Nonstationarities were detected in 72%, 52%, and 87% of the NRNI sites' time series of annual daily maximum 30-day duration flows for the mean, variance, and distributions, respectively (**Figures 12**). With respect to low flows, nonstationarities were detected in 78%, 50%, and 88% of the NRNI sites' time series of annual minimum summer 7-day mean flows for the mean, variance, and distributions, respectively (**Figure 13**). For all annual metrics, the lowest amounts of nonstationarities were found for variance, and highest for distributional changes.

The spatial distribution of identified nonstationarities in annual maximum flows follows the hydroclimatology of the basin: more nonstationarities are found where annual flood peaks are attributed to spring snowmelt (Snake River, Columbia Mainstem). Areas where annual 1-day duration flood peaks are derived from rain events have lower detections of nonstationarities (Western Cascades, Willamette Basin). In these areas 30-day duration annual maxima display more nonstationarities, owing to the spring snowmelt season, which has lower daily peaks than the rainy season, but higher flows for longer durations during snowmelt. Snowmelt flooding is more sensitive to warming temperatures, particularly in regions where average winter temperature is close to freezing (32°F/0°C) and at lower latitudes that warm faster in the spring.

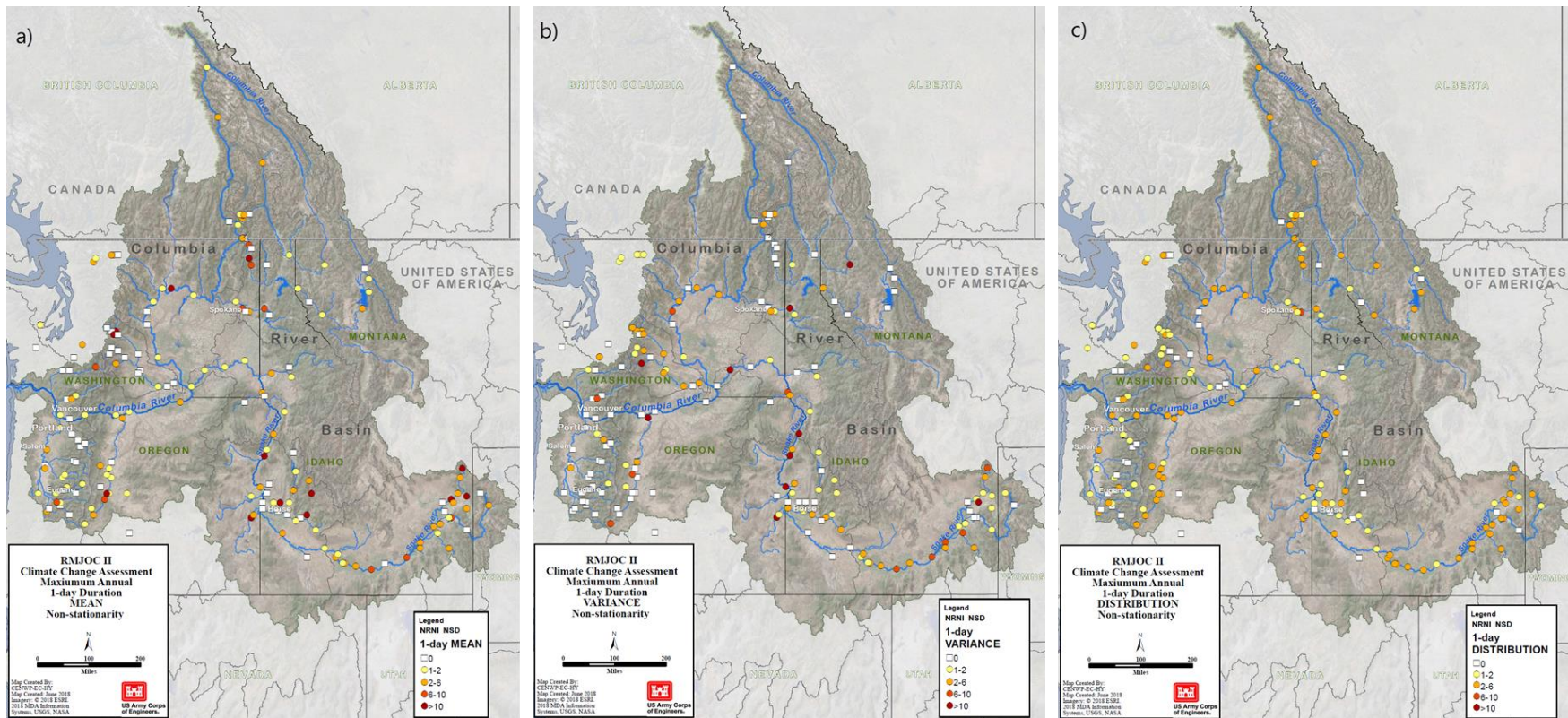


Figure 11: Nonstationarities detected in time series (WY 1929-2008) of annual maximum 1-day duration flows at NRNI locations (colored circles). NRNI locations where nonstationarities were not found are indicated with white squares.

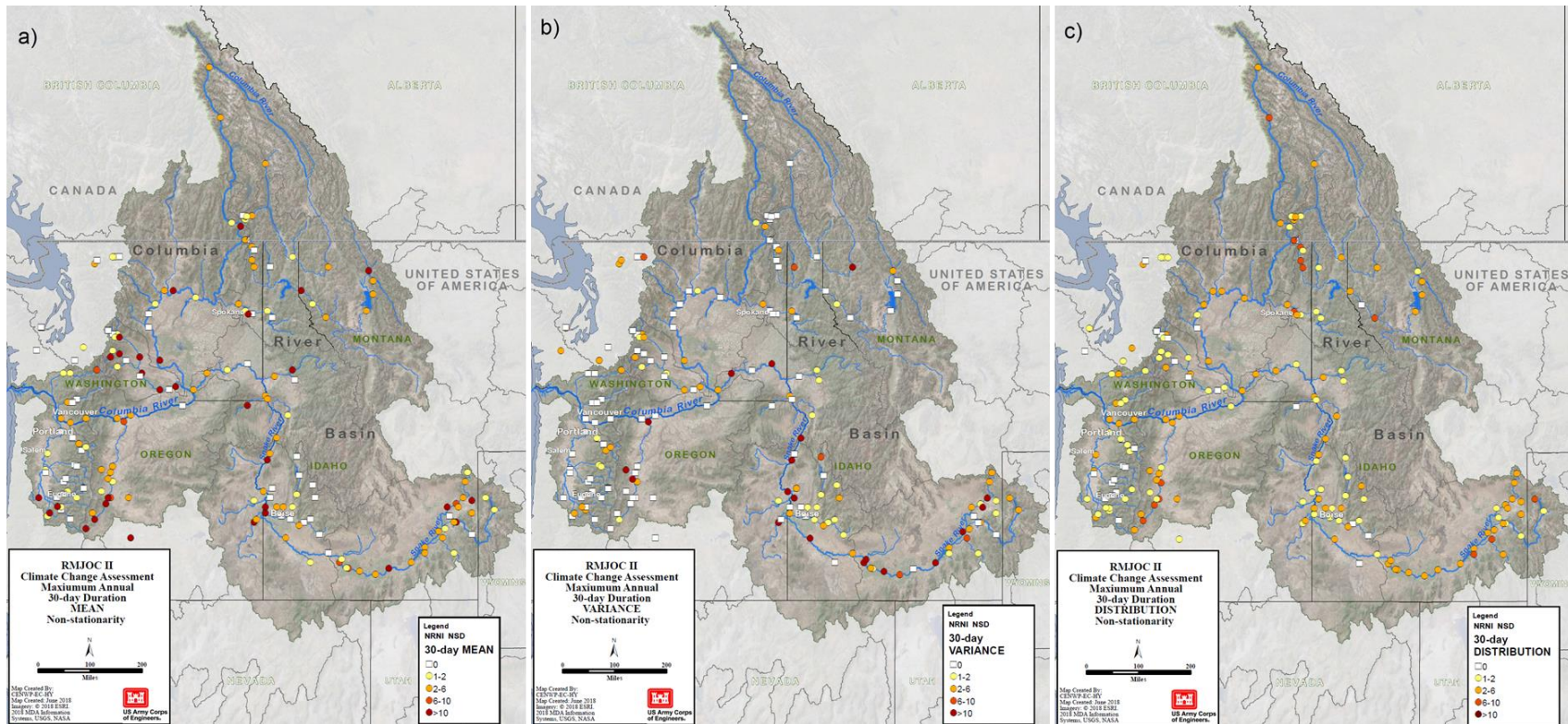


Figure 12: Nonstationarities detected in time series (WY 1929-2008) of annual maximum 30-day duration flows at NRNI locations (colored circles). NRNI locations where nonstationarities were not found are indicated with white squares.

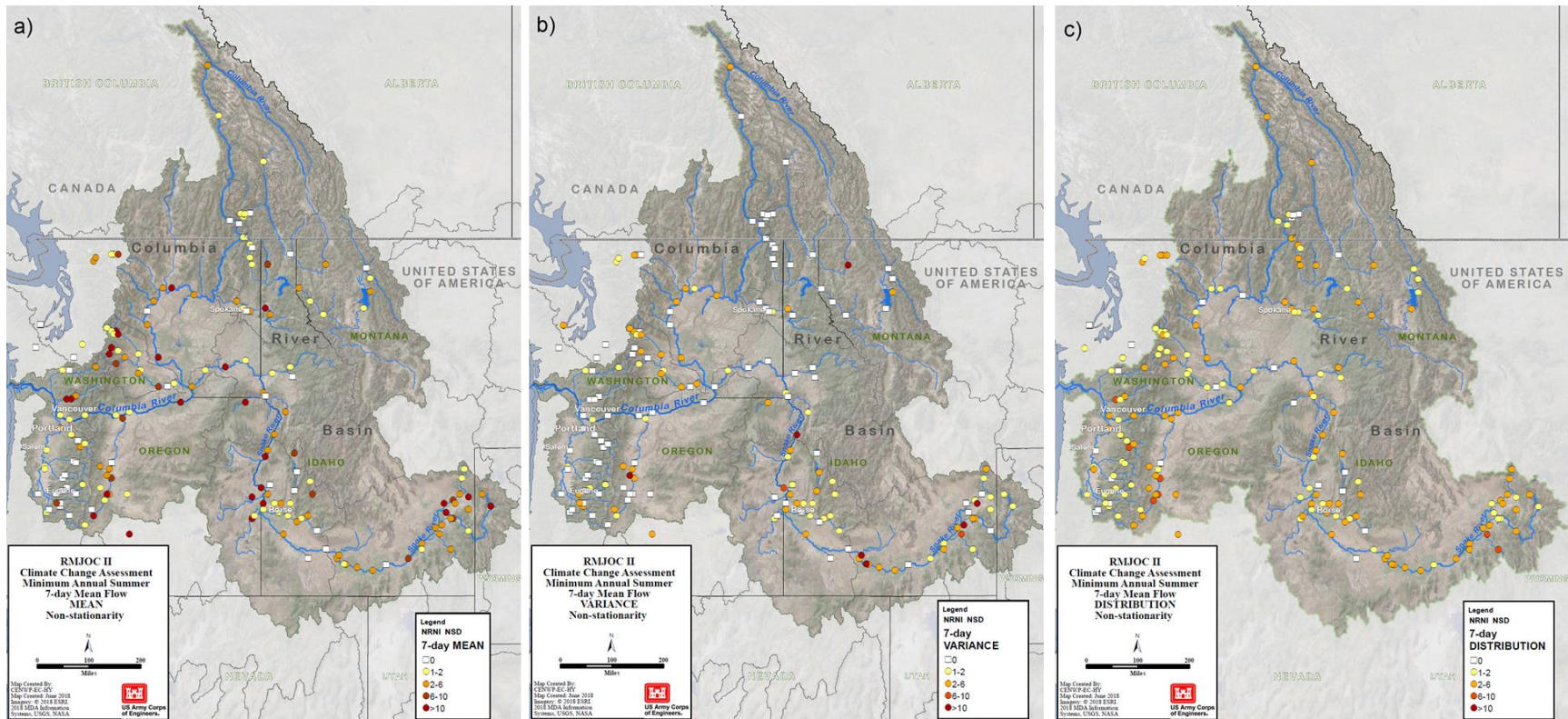


Figure 13: Nonstationarities detected in time series (WY 1929-2008) of annual minimum summer 7-day mean flows at NRNI locations (green-blue circles). NRNI locations where nonstationarities were not found are indicated with white squares.

Larger numbers of nonstationarities were detected in annual minimum 7-day mean summer flows (**Figure 13**). The geographic distribution of nonstationarities follows anticipated patterns consistent with topography and the relative snowmelt signature. In the majority of the basin the summer flows are linked with seasonal snowpack; snowmelt redistributes winter precipitation to the driest part of the year. The number of nonstationarities being detected decreases with increasing latitude. The northern portion of the basin is colder due to higher elevation and latitudinal position. Thus, the snowpack in the northern part of the basin is likely to be less sensitive to initial increases in air temperature.

The combination of the NRNI data and statistical tests facilitates the detection of changes to hydrological processes within the Columbia River Basin. Because the effects of man-made structures and changes in irrigation practices have been removed from the NRNI dataset, the detected nonstationarities are more likely to be caused by anthropogenic climate change that is already occurring with warming. However, other drivers of changes in streamflow could also contribute to nonstationarities (*e.g.*, land cover change). The spatial distribution of nonstationarities detected follow known sensitivities within the basin with respect to increasing temperature and snowmelt. The statistical detection tests indicate pervasive robust nonstationarities in flows within all the snowmelt-dominated areas in the basin with the exception of the northern, high-elevation basin. This further supports the attribution of nonstationarities to anthropogenic climate change.

However, it should be noted that the method for developing the NRNI data also has the potential to artificially introduce nonstationarities into the dataset. In areas where there is a large amount of irrigation (*e.g.*, Upper Snake River), the NRNI time series are more uncertain due to the assumptions made to estimate the unimpaired flow. The highest amounts of nonstationarities were found in these locations. Additionally, the records of some gauge sites were extended back in time or missing data were filled in using relationships with nearby gauges. These methodological limitations of the time series provide some confounding impacts on the nonstationarity results. Never the less, nonstationarities detected in the dataset do follow physical reasoning and extend to regions with less uncertainty in the NRNI data.

3.4.2 Monotonic Trend Analyses

The time series records at each NRNI location were tested for monotonic patterns in maximum annual 1 and 30-day duration flows and minimum annual summer 7-day mean flow. The entire period of record (WY 1929-2008) was used for trend analysis. The data were not adjusted for the potential presence of autocorrelation. The Mann-Kendall tau (Mann, 1945; Kendall, 1975) statistical test was applied to identify trend direction and statistical significance. A p-value of less than 0.05 (α) was used as the threshold to determine statistical significance. The nonparametric Sen's slope estimator (Sen, 1968) was used to determine trend magnitude.

Statistically significant increasing trends were identified in maximum annual 1-day flow time series for locations in the Snake River Basin and SW Washington Cascades (**Figure 14a**). The analyses of long-term trends resulted in fewer statistically significant changes in mean than were identified using the suite on nonstationarity statistics (Section 3.4.1); however, the trend patterns do overlap with the areas where the most nonstationarities were detected (**Figure 9**). Fewer statistically significant trends were found in 30-day duration annual maximum flows (**Figure 14b**). Similarly, the statistically significant trends in the annual minimum summer 7-day mean flow are sparse (**Figure 14c**). However, some positive trends are found clustered in the

Upper Snake Basin. More general patterns are found in the direction of all trends throughout the basin, albeit most were not found to be statistically significant. There are pervasive negative trends in summer minimum 7-day mean flows in the southern Cascade Range, while the upper Columbia, Columbia mainstem and Snake River are dominated by positive trends.

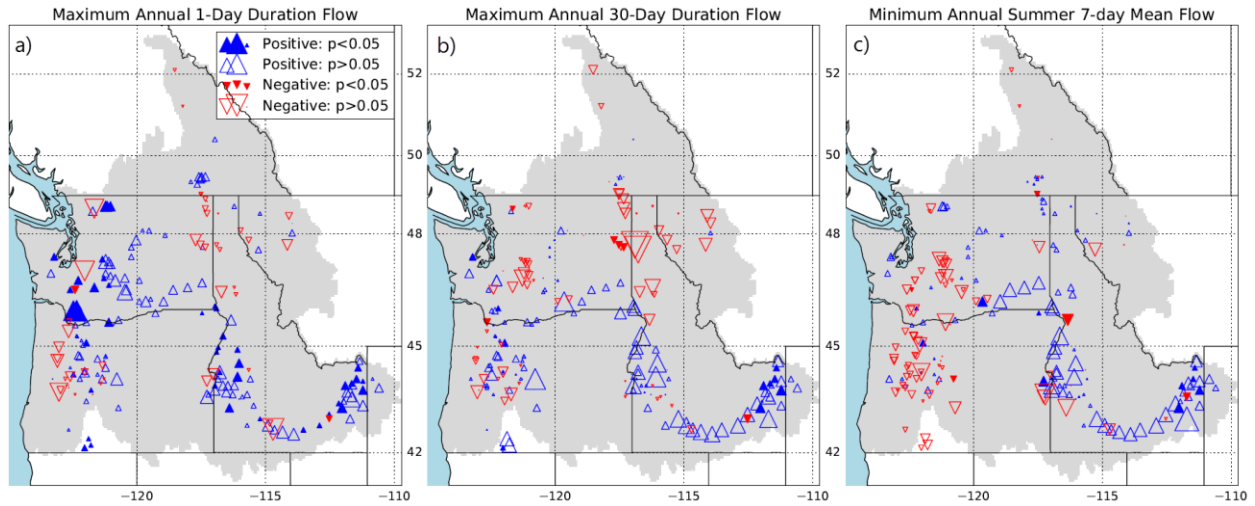


Figure 14: Monotonic trends for 1929-2008 identified in time series of (a) annual maximum 1-day duration, (b) annual maximum 30-day duration, and (c) minimum 7-day mean summer flows at NRNI locations. Blue upward pointing triangles indicate positive trends and red downward facing triangles indicate negative trends. The marker size is scaled by the magnitude of the trend present (slope in %, relative to all locations). Statistical significance (p-value) was calculated using the Mann-Kendal statistic and magnitude by Sen’s slope estimator.

3.5 Discussion

The development of the NRNI dataset was an iterative process as issues with how the data were derived were discovered and resolved as this research project progressed. The fourth iteration of the NRNI dataset, published in April 2017, was ultimately used for final calibration and bias-correction of the unregulated climate change flows.

One key finding during the process of converting the homogenous, regulated Modified Flow record to the NRNI dataset was that given the complex hydrology in the region and difficulties in accurately estimating irrigation depletions and returns, there are some parts of the basin where the NRNI flow calculations are more certain than others. This must be considered in evaluating the quality of the hydrologic model calibrations and even the climate change flow projections. In general, it is more difficult to estimate natural flows in areas where more intensive irrigation is employed. Application of statistical nonstationarity detection tests further demonstrates potential uncertainties in the reconstructed naturalized flows in these regions.

4.0 Hydroclimate Dataset Development

4.1 Introduction

To translate projected changes in climate into changes in streamflow, the research team used the modeling chain outlined in **Figure 15**. The individual steps are presented in more detail below, but the overall challenge is to convert the coarse-resolution output from the climate models into higher-resolution fields that can be used as input to hydrologic models and to ensure that the streamflow produced by these hydrologic models is consistent with observed streamflow. By doing this for a large number of climate model outputs, an ensemble of projected streamflow time series was produced, where each member represents a specific set of model options. The individual steps can be summarized as:

1. Select a set of Representative Concentration Pathways (RCPs);
2. Select a set of simulations from Global Climate Models (GCM);
3. Downscale the coarse-resolution GCM temperature and precipitation data to finer temporal and spatial scales;
4. Use the resulting finer-scale data as forcing data for hydrologic models, which represent snow accumulation and melting, glacier accretion and depletion, and other hydrologic processes that partition precipitation into changes in snow and soil moisture storage, evapotranspiration, and streamflow;
5. Post-process the modeled flows (“raw”) to mitigate or remove biases introduced in the modeling chain based on performance of the same modeling chain during a historical period for which streamflow observations exist; and,
6. Use bias-corrected streamflow time series as inputs to hydraulic models to account for anthropogenic flow modifications (*e.g.*, irrigation, reservoirs, hydropower, habitat/biological targets).

The research team selected multiple RCPs, GCMs, downscaling methods, hydrologic models, and model parameter sets in steps 1 through 4, and completed a simulation for each combination of these components, resulting in an ensemble of 172 distinct projections of future streamflow in the basin, as described in Section 4.7. This ensemble enables one to evaluate the impact of those model choices on the results. In other words, an ensemble of different model choices allows one to assess to what extent the methodological choices of a hydroclimate study affect the final projections.

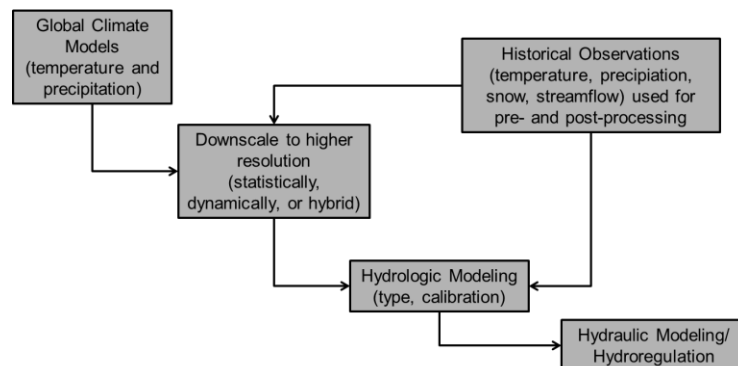


Figure 15: Hydroclimate modeling process flowchart.

4.1.1 Uncertainty and Ensemble Spread

Throughout this modeling process, and as envisioned in the project opportunity proposal, the objective was to *adequately capture the range of hydroclimate model uncertainty across the Columbia Basin as a whole*, and ideally capture modeling uncertainties in the largest tributaries (*e.g.*, Snake Basin, Upper Columbia Basin, Willamette Basin). However, it is important to make a distinction between “uncertainty” and “spread.” The streamflow projections from this project do not describe the true uncertainty of all possible future streamflows in the Columbia River Basin. In part this is because the numerical estimates of future climate are forced with assumed global-scale socioeconomic changes for multiple decades in the future, so not all forcing possibilities are considered. And in part this is because even state-of-the-science climate models, downscaling techniques, and hydrology models do not numerically represent all of the relevant geoscientific processes at the spatial and temporal scales where they occur. And if both those limitations were overcome, it would not be possible practically to construct complete model chains with all possible differences. Therefore, the true uncertainty is larger than the spread in the model simulations, which can be calculated based on these ensembles of projections. However, the spread of outcomes in these streamflow scenarios does provide insight into the effect of methodological choices in the modeling chain on the projections, and therefore captures some of the uncertainty associated with the climate projections. For these reasons, the project generally uses “spread” rather than “uncertainty” when describing the range of projected values. The magnitude of the spread varied across the basin, particularly by climate regime and basin size, and is very dependent on the metric of interest (*e.g.*, annual volume change, change in duration of low-flow periods).

4.1.2 Systematic Biases in Modeling Framework and Historical Datasets

A key assumption throughout the process is that historical temperature, precipitation, and streamflow datasets that were used for historical comparisons, climate model downscaling, hydrological model calibration, and post-processing, are used as the reference “truth.” However, as indicated in Section 2, observation-based datasets, such as the gridded meteorological forcing dataset used here, have known errors. These errors, which may affect downscaling and hydrologic model calibration, are not explicitly accounted for within the modeling chain of this particular project, and users of this dataset must be aware of this additional unknown during analysis.

Further, it is acknowledged that the development of this dataset was explicitly set out to be done at the regional scale of the entire Columbia Basin and its major sub-basins since that is the scale of the environmental decision-making these outputs were designed to inform. Accordingly, less focus was placed upon smaller sub-basins. Evaluations focusing on small catchments may benefit from studies directed toward those areas as opposed to the regionwide focus of this particular study.

4.2 Modeling Components

4.2.1 Representative Concentration Pathways (RCPs)

As detailed in the IPCC-AR5 report (IPCC, 2013), RCPs represent a range of projected carbon dioxide, methane, nitrous oxide, and other greenhouse gas concentrations that would result in a certain radiative forcing by year 2100. The IPCC-AR5 report included results from applications in GCMs of four RCPs (RCP2.6, RCP4.5, RCP6.5, and RCP8.5, named for the increase (in watts per

meter squared) in the radiative forcing at the top of the atmosphere in the year 2100 relative to pre-industrial values. This study used results from GCMs forced with two of those RCPs: RCP4.5 and RCP8.5. In general, RCP 4.5 represents a CO₂ concentration of around 538 ppm by 2100 but with levels stabilizing near 500 ppm by around 2050. RCP 8.5 represents a steadily rising CO₂ concentration to around 936 ppm by 2100. For comparison, atmospheric carbon dioxide levels were nearing 410 ppm in 2017, while in 1950 those levels were near 300 ppm (NOAA, 2018). The selection of these two RCPs was made based upon wanting to encompass a “business as usual” scenario (RCP8.5) as well as a more optimistic emissions reductions scenario (RCP4.5). **Figure 16** depicts the emissions pathways, projected concentrations of atmospheric carbon dioxide through 2100, and recent emissions trends from Fuss *et al.* (2014).

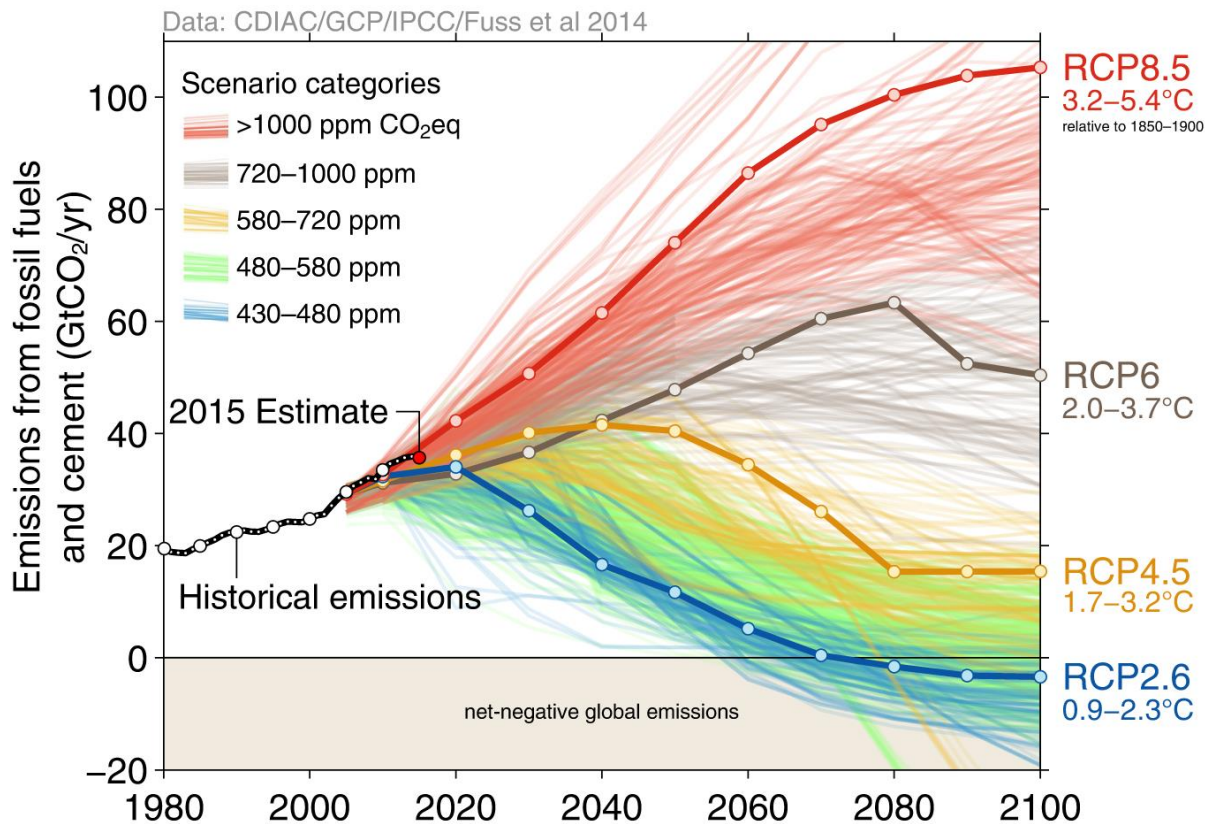


Figure 16: Emissions pathways used for the IPCC AR-5 climate modeling effort, and recent emissions trends through 2015. From Fuss *et al.*, 2014.

4.2.2 GCM Selection

At the time GCM selections were made for this project, outputs from 41 different GCMs were available for use—more than double the model sets available for RMJOC-I. In addition, most GCMs had several ensemble members also available for use. With such a large number of available GCMs, there was considerable discussion during the opportunity announcement phase whether to limit the number of GCMs that would be used for this modeling study. Ultimately, the opportunity announcement left it to the project team to make recommendations for both the number of climate models and their selection criteria.

Three initial screening criteria were applied to the initial set of 41. Because temperature, precipitation, and streamflow outputs were to be provided in daily time steps, the project team

reviewed only thirty-one GCM datasets that had complete (*i.e.*, 1950-2100) daily temperature and precipitation fields ready for downscaling. Because the Opportunity for Proposals required the use of at least two different Representative Concentration Pathways (RCPs) to account for uncertainty in future anthropogenic emissions, the team further narrowed the list to those GCMs which had outputs for two specific RCPs: RCP4.5 and RCP8.5.

The project team then applied a selection method based on Rupp *et al.* (2013) to the remaining 31 GCMs, which evaluated GCM performance in the historical period in the Pacific Northwest and over a broader region encompassing large portions of western North America and the northeast Pacific Ocean. In an acknowledgement of uncertainties in historical temperature and precipitation fields, the team used five observational datasets to compare GCM outputs to an initial set of 34 metrics. The team then narrowed the number of metrics to 18 after determining which had relatively small intra-GCM variability relative to the differences between GCMs (**Table 6**), and the metrics that had the most power to discriminate among GCMs.

Table 6: Performance metrics used for initial GCM selection (from Rupp *et al.*, 2013). MMM = DJF (December - February) or JJA (June - August).

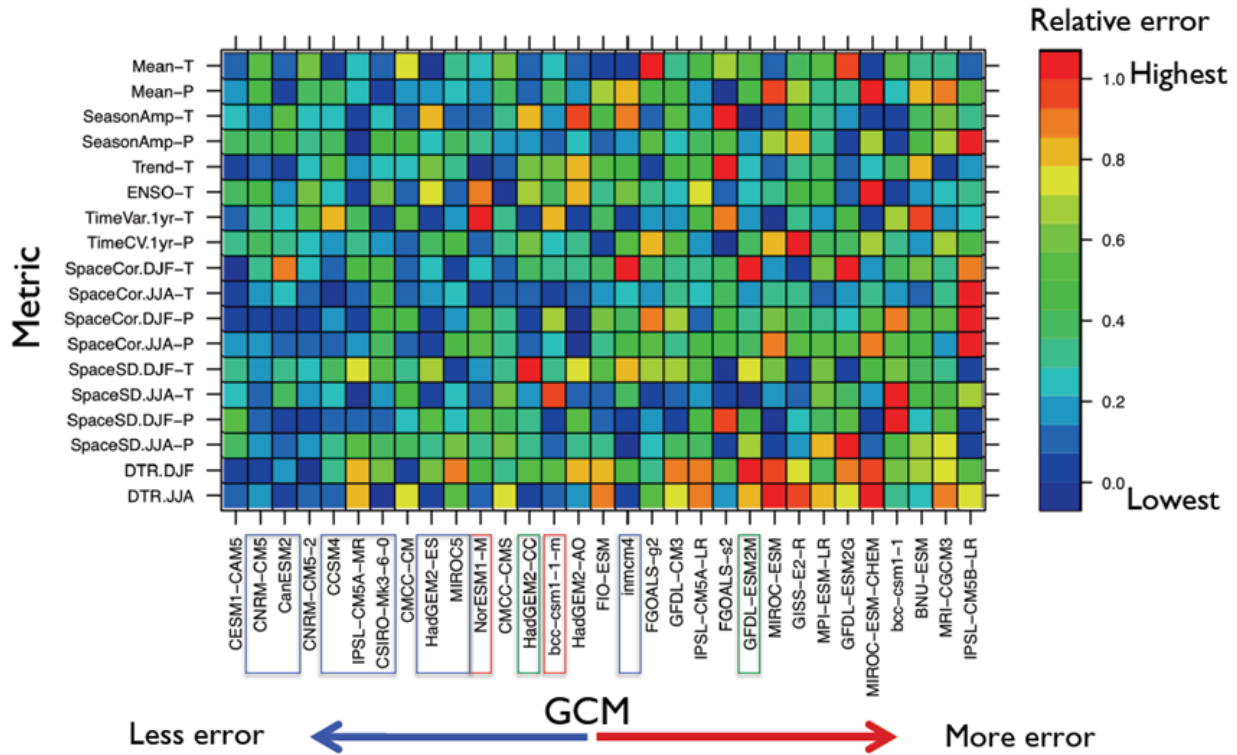
Metric Abbreviation	Historical Period	Description
Mean-T	1960-1999	Mean annual temperature
Mean-P	1960-1999	Mean annual precipitation
SeasonAmp-T	1960-1999	Mean amplitude between warmest and coldest months
SeasonAmp-P	1960-1999	Mean amplitude between wettest and driest months
Trend-T	1901-1999	Linear temperature trend
ENSO-T	1901-1999	Correlation of winter temperature with Niño 3.4 Index
TimeVar.1-T	1901-1999	Variance of temperature, 1 year frequency
TimeCV.1-P	1902-1999	Coefficient of variation of precipitation, 1 water year frequency
SpaceCor-MMM-T	1960-1999	Temperature spatial correlation versus historical
SpaceCor-MMM-P	1960-1999	Precipitation spatial correlation versus historical
SpaceSD-MMM-T	1960-1999	Temperature standard deviation of mean spatial pattern
SpaceSD-MMM-P	1960-1999	Precipitation standard deviation of mean spatial pattern
DTR-MMM	1950-1999	Mean diurnal temperature range by season

The output was visualized in a “Performance Quilt” which highlighted the relative performance of each GCM to each metric (**Figure 17**). This allowed the GCMs to be objectively sorted according to their performance. An additional check using Empirical Orthogonal Function analysis was applied to account for redundancy (autocorrelation) between metrics, and to reduce the number of metrics slightly when strong autocorrelation was found.

An initial recommendation for ten GCMs was shared in a technical RMJOC-II stakeholder workshop in year two of the project. Feedback from several participants suggested that the team revisit the GCM selection to ensure that the selected GCMs were also replicating large-scale atmospheric processes correctly during the historical period—specifically 500mb heights as a proxy for jetstream dynamics and processes near the layer of maximum upward and downward vertical motion in the atmosphere. This additional level of analysis prompted the team to replace two GCMs, which had shown adequate performance in temperature and

precipitation fields, with two other GCMs that exhibited better performance against historical 500mb heights in the northern hemisphere. The list of GCMs used for this project (Table 7) was then finalized in a subsequent project workshop.

GCM Performance Quilt



(Ordered by sum total of relative errors. All metrics treated equally.)

Figure 17: Global Climate Model Performance Quilt, prepared using methodology from Rupp *et al.* (2013) for overall historical performance in the Pacific Northwest. Two initial selections (NorESM1-M and bcc-csm1-1-m, highlighted by the red outlining of the model names) were replaced by HadGEM2-CC and GFDL-ESM2M (green outlining) in the final selection (blue plus green outlining).

Table 7: Global Climate Model (GCM) outputs used for RMJOC-II Study. All GCM data is from ensemble member r1i1p1 from each GCM dataset, except CCSM4 which is from ensemble member r6i1p1:

No	GCM	Global Climate Model (from CMIP-5/IPCC-5)	Country
1	CanESM-2	Canadian Earth System Model v2	Canada
2	CCSM4	Community Climate Systems Model v4	US
3	CNRM-CM5	Centre National de Recherches Météorologiques v5	France
4	CSIRO-Mk3-6-0	Commonwealth Scientific and Industrial Research Organisation Mk3.6.0 Climate Model	Australia
5	GFDL-ESM2M	Global Fluid Dynamical Lab Environmental System Model v2	US
6	HadGEM2-CC	Hadley Centre Global Environmental Model v2 – Carbon Cycle	UK
7	HadGEM2-ES	Hadley Centre Global Environmental Model v2 – Earth	UK

		System	
8	inmcm4	Institute of Numerical Mathematics Climate Model v4	Russia
9	IPSL-CM5-MR	Institut Pierre Simon Laplace Climate Model v5 – Medium Res.	France
10	MIROC5	Model for Interdisciplinary Research On Climate v5	Japan

4.2.3 Downscaling Methods and Characteristics

The spatial resolution of the native GCM modeled temperature and precipitation fields varied between 75-300 km, which is too coarse to adequately capture the complex terrain and highly varied climate across the Columbia River Basin. There are numerous downscaling methods available, which add local information to the coarse climate model output to create higher-resolution spatial fields that can be used for hydrologic modeling. All these methods have their relative strengths and weaknesses. New downscaling methods emerge and evolve as the state of the science advances. Downscaling techniques can be generally described in two broad categories: statistical and dynamical (Wilby and Wigley, 1997). “Statistical downscaling” develops statistical relationships between variables from the large scale output of the GCM and finer-scale meteorological data. Statistical techniques are often computationally efficient. Dynamical downscaling uses a regional climate or weather model to simulate finer-scale physical processes that are consistent with the larger-scale GCM output used as boundary conditions. Dynamical downscaling is computationally intensive, but it has the benefit of not relying on historical climate patterns to project future change.

As indicated in Section 2, there was recognition that different downscaling techniques introduce additional uncertainty in the climate modeling chain that must be considered when attempting to capture the reasonable range of future hydroclimate outcomes. Thus, three different downscaling methods were used in this study, which are detailed in this section.

4.2.3.1. Bias-Corrected Spatial Disaggregation (BCSD) Downscaling

For RMJOC-II as for RMJOC-I, the often-used Bias-Corrected Spatial Disaggregation (BCSD) downscaling method was applied to the temperature and precipitation outputs from the selected GCMs (Wood *et al.*, 2002; Wood *et al.*, 2004). BCSD downscaling has several advantages in that it is a well-tested and computationally quick and efficient method (Bürger *et al.*, 2012). Also, because it has been used for more than a decade in hydroclimate modeling, its characteristics, strengths, and weaknesses are well known. Using BCSD for both this study and RMJOC-I also allows users to compare RMJOC-I results with a subset of this dataset that used the same downscaling technique. BCSD used on a monthly time step for hydrologic applications in the region of the upper Colorado River basin was shown by Gutmann *et al.* (2014) to be largely unbiased for total wet-day fraction and extreme event incidence, and to scale well with increasing analytical domain size, relative to other widely used empirical-statistical downscaling methods. BCSD and all other empirical-statistical downscaling methods can be biased against observed climatology, especially in mountainous terrain or other domains with sparse historical data (Maurer and Hidalgo, 2008; Eum *et al.*, 2014). In terms of precipitation, Maurer and Hidalgo (2008) show that with respect to other statistical downscaling methods, BCSD downscaling tends to perform well in data rich-areas, particularly with respect to temperatures in the US portion of the basin.

The one key difference between BCSD processes in RMJOC-I and in this study is that the downscaling used a different, historical training dataset. In this iteration, a more recent temperature, precipitation, and wind dataset from Livneh *et al.*, 2013 (hereinafter referred to as the Livneh dataset) was used as the historical dataset for BCSD training and bias-correction. The Livneh dataset had a key advantage at the time because of its high gridded spatial resolution (1/16°), its use of more than 20,000 NOAA Cooperative Observers across the US and southern Canada, and its seamless extension into the Canadian Columbia Basin, where, at the time, high-resolution temperature and precipitation data up through 2011 was lacking. Although the dataset has a long period of record (1915-2011), there were concerns that the cooperative observer network was sparser before 1950, and as a result some spurious temperature and precipitation patterns were noted. Because the Statement of Work specified that the streamflow outputs would be for 1950-2099, a 1950-2005 subset was used for the BCSD training calculations.

4.2.3.2. Multivariate Adaptive Constructed Analog (MACA) Downscaling

The project also used a more recently developed downscaling technique from Abatzoglou and Brown (2012). The Multivariate Adaptive Constructed Analog (MACA) method utilizes a catalog of past meteorological sequences and looks for weather pattern commonality in the GCM outputs themselves. The RMJOC-II project used an existing dataset from the University of Idaho (<https://climate.northwestknowledge.net/MACA/index.php>), which was downscaled using the same Livneh dataset for the historical period that was used for the BCSD downscaling. Constructed analog downscaling methods have been used as another computationally inexpensive downscaling method. Because of the use of analogs, temperature, precipitation, and other synoptic meteorological fields for a particular GCM output are relatively well correlated and spatially consistent—including past individual, significant storm or drought events. Constructed analog methods are also apt to more adequately capture terrain-forced meteorological events like precipitation shadowing and inversions. Like the BCSD downscaling for this study, the MACA dataset used the Livneh historical temperature and precipitation fields from 1950-2005 for training and bias correction (Abatzoglou and Brown, 2012).

MACA downscaling does appear to exhibit greater skill for both temperature and precipitation in mountainous, data-sparse areas over BCSD (Abatzoglou and Brown, 2012). However, both downscaling methods perform much better than simple interpolation from the GCMs themselves. A couple of drawbacks identified with constructed analog techniques, though, are that they have been found to spatially spread out heavy precipitation events and thus dampen the resulting hydrologic signal. Precipitation averaging over larger basins can also generate too much drizzle or light precipitation (Pierce *et al.*, 2014), which in turn can translate to a wet bias in climatologically dry areas. One other potential issue is that one of MACA's strengths could also be a weakness since it relies on a catalog of past weather sequences. As climate change becomes more extreme, the risk of no analogs being found relative to a GCM output may increase over time (Abatzoglou and Brown, 2012).

4.2.3.3. Oak Ridge National Laboratory (ORNL) Hybrid Downscaling

As mentioned in Section 2, the Statement of Work envisioned the possibility that dynamically downscaled temperature and precipitation data might become available during the course of the project. In 2015, a new downscaled dataset became available for potential use in this study, developed for the Department of Energy's (DOE) SECURE Water Act Section 9505 Report to

Congress (DOE, 2017), documented in Ashfaq *et al.* (2016), Naz *et al.* (2016), and Kao *et al.* (2016). The processes for creating these simulations is briefly described here, but these runs were not compared against the empirical-statistical downscaling outputs described above.

The dataset, which includes daily temperature, precipitation, and wind speed time series from 1966-2005 and 2011-2050, was developed using a two-step downscaling process. The first step included the use of the Abdus Salam International Centre for Theoretical Physics Regional Climate Model (RegCM4; Pal *et al.*, 2007; Giorgi *et al.*, 2012), which was used on a set of ten CMIP5 GCMs—three of which were also selected for this study: CCSM4, GFDL-ESM2M, and MIROC5. The RegCM4 climate model dynamically downscaled temperature and precipitation information at an 18-km resolution over the Continental US and southern Canada (Ashfaq *et al.*, 2016). The ORNL team further statistically downscaled the temperature and precipitation fields using a quantile-based mapping method (Ashfaq *et al.* 2010; conceptually similar to the BSCD method from Wood *et al.*, 2002) to an approximate 4-km resolution for hydrologic modeling (Naz *et al.*, 2016). For the purposes of this study, the meteorological forcing data provided by ORNL was aggregated to 6km (same as Livneh) for application across the Pacific Northwest.

Besides the differences in downscaling technique, one other critical difference between the BSCD and MACA downscaling, and the hybrid dynamical-statistical ORNL dataset, is that ORNL used a combination of three historical datasets to support statistically downscaling (from 18 km to 4 km): the Parameter-elevation Regressions on Independent Slopes Model (PRISM) dataset from Oregon State University (Daly *et al.*, 1997; Daly *et al.*, 2002); the ORNL Daymet dataset (Thornton *et al.*, 1997), and for the Canadian portion of the basin, a gridded dataset from Hamlet *et al.* (2013) used in RMJOC-I. The decision was made because no single dataset was able to provide all required historical observations at the time of ORNL analysis. The Hamlet dataset was available for the Canadian part of the Columbia Basin at a time at which PRISM data from British Columbia was not yet available. A British Columbia PRISM dataset was published after ORNL's downscaling effort. See PCIC (2014).

4.2.4 Hydrologic Models

One of the cornerstones of this particular project was to investigate how the choice of the hydrologic models impacts the range of future streamflow projections. The project team chose to focus on two hydrologic models: the Variable Infiltration Capacity Model (VIC; Liang *et al.*, 1994) version 4.2.glaacier, and the Precipitation Runoff Modeling System, version 3.0.5 (PRMS; Markstrom *et al.*, 2015). A schematic comparing the two models from Mizukami *et al.* (2016) is shown in **Figure 18**.

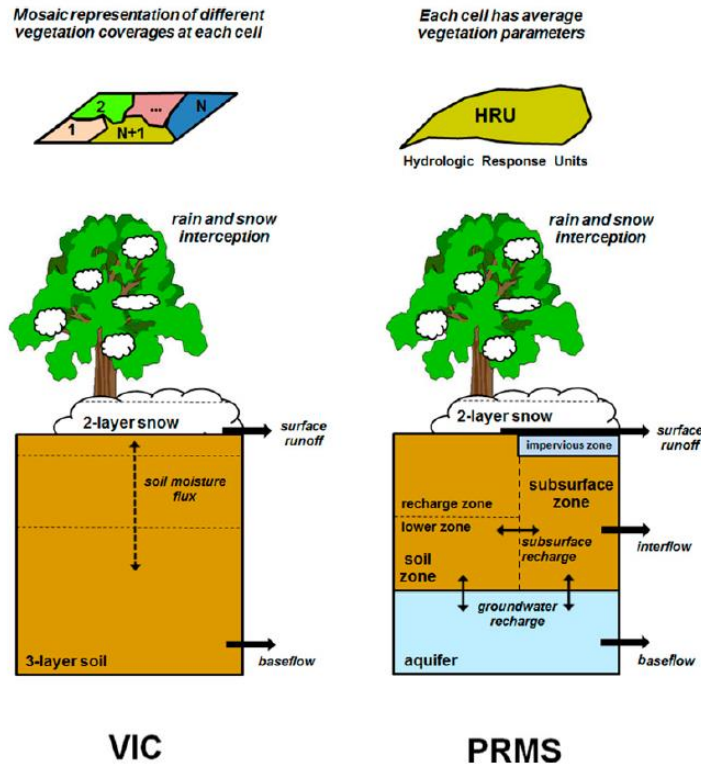


Figure 18: Schematic comparing VIC and PRMS soil and runoff processes, from Mizukami *et al.* (2016).

Fortuitously, as this project proceeded through initial tasks and stage gates, two other research projects were under way which also utilized the VIC model for hydroclimate analyses in the Columbia River Basin. Each of these implementations used different parameter sets, based on model calibrations that these research teams had performed independently. This allowed us to compare outcomes from two different hydrologic models as well as the effects of different parameter sets (based on different calibrations) within a single hydrologic model (VIC), resulting in four different hydrologic model setups.

Both VIC and PRMS were implemented at a spatial resolution of $1/16^\circ$, which corresponds to roughly rectangular grid cells that are 6 km or 3.5 mi on a side, resulting in 23,929 individual hydrological model elements (or grid cells) over the domain. Because all hydrologic modeling was conducted on the same spatial grid, the team was able to apply the same routing scheme to all simulations. The RVIC model (Hamman *et al.*, 2017) was used to route gridded surface water (VIC: surface runoff, baseflow; PRMS: surface flow, subsurface flow, groundwater flow) fields into and through the stream network. For all four hydrologic model setups, projections for streamflow were generated at 396 sites throughout the Pacific Northwest, including NRNI flow points provided by the RMJOC. Most of the sites are located within the Columbia River Basin, but the dataset also includes selected sites within the coastal drainages in Washington and Oregon.

All climate change simulations were run from water year 1950 through 2099, except for those based on the hybrid-downscaling method from ORNL. Four historical simulations using the Livneh *et al.* (2013) temperature and precipitation dataset were also completed for each model set from 1960 through 2011. Because the hybrid-downscaled meteorological forcings from

ORNL were available only for the time periods 1966-2005 and 2011-2050, the related hydrologic simulations are available only for those time periods.

Because of the different combinations of methodological choices, the final dataset consisted of 172 individual projections plus four historical simulations for each of the 396 streamflow locations. For a subset (190) of these locations, the University of Washington provided both raw and bias-corrected versions of the time series. In total, the streamflow dataset includes 103,136 individual streamflow time series. The importance of having an ensemble of possible climate futures created with a range of different models is an important development in hydroclimate applications, even when only small subsets of that ensemble can be used owing to restrictions on time and other resources.

4.2.5 Variable Infiltration Capacity Model (VIC)

The Variable Infiltration Capacity (VIC) model (Liang *et al.*, 1994; Gao *et al.*, 2010) has been extensively used for hydroclimate studies, including the RMJOC-I study in 2008-2011 (RMJOC-I, 2011; Hamlet and Lettenmaier, 1999). It is a semi-distributed hydrologic model, which simulates the land surface hydrology as a function of meteorological inputs and terrain-characteristics such as soil, land cover, and elevation. Within the model, no exchange of moisture and energy occurs between neighboring model elements (1/16° grid cells as implemented in this study). Instead, it is assumed that locally produced runoff will reach the river network within each grid cell and can be routed to locations of interest using a standalone routing model. For this study, the University of Washington used VIC Version 4.2.glaacier for all VIC model simulations.

Because the VIC model has been used for more than 20 years, its strengths and weaknesses for hydroclimate modeling are well documented. For example, Safeeq *et al.* (2014) show that while the VIC model generally represents temperature and precipitation effects on snowmelt and runoff quite well, the model does not perform as well in groundwater-dominated watersheds where water exchanges between surface/near surface water and groundwater are important, which can affect local/incremental flow estimates, particularly in smaller watersheds.

For most VIC research applications, permanent snow fields and glaciers are treated as a permanent snowpack that continues to accumulate indefinitely without redistribution to lower elevations (*i.e.*, no glacier transport). However, as part of the project, the University of Washington team implemented an explicit glacier accretion and melt component within VIC. The simple glacier subroutine uses an area-volume scaling relationship based upon Bahr *et al.* (1997). This model version was used for all VIC simulations conducted in the study.

4.2.6 Precipitation Runoff Modeling System (PRMS)

Changing hydrological model structure can introduce even greater spread in hydroclimate modeling results than model calibration and parameterization (*e.g.*, Poulin *et al.*, 2011). To account for this key uncertainty, the team used a different hydrology model to generate a set of completely distinct streamflow projections: the Precipitation-Runoff Modeling System (PRMS) from the US Geological Survey (Leavesley *et al.*, 1983; Markstrom *et al.*, 2015), which has also been heavily used for numerous hydrologic forecast applications, including hydroclimate projections (*e.g.*, Hay *et al.*, 2011; Jung and Chang, 2011). For this study, PRMS was implemented on the same grid as VIC. As a result, there was no exchange between neighboring

model elements, and runoff was expected to reach the channel network within each model grid cell. PRMS includes three main soil zones (surface, subsurface, and groundwater, see **Figure 18**). While there is an option to include larger aquifer systems within PRMS, this option was not implemented in this study. The decision to implement both VIC and PRMS on the same grid allowed the team to use the same calibration technique and routing scheme for both models. For example, as noted elsewhere in this report, aquifer interactions can be fairly significant in parts of the Snake Basin and the drainages of eastern Oregon, but these were not represented in this implementation of the PRMS model.

Like VIC, PRMS has been used for a wide range of applications, so the inherent strengths and weaknesses of the model are well documented. As one would expect given its ability to simulate groundwater exchange, PRMS may be well suited for some groundwater-dominated basins. However, Mizukami *et al.* (2016) indicated a tendency for PRMS to overpredict lengthy low-flow periods in the Pacific Northwest, along with a slight negative water balance bias.

4.3 Historical Data Sources and Characteristics

As mentioned in Section 2, what is “observed” in the past has a degree of uncertainty. Inherently, high-resolution gridded climatological fields are reconstructions based on a limited set of observations. Even “ground truth” observations are uncertain due to instrumentation uncertainty, gauge siting, and even observer bias (Daly *et al.*, 2007). In areas where observations are limited, particularly in complex terrain, the modeled gridded fields have less data for training and bias adjustment, which increases the risk for the historical data field to be more greatly influenced by assumptions of the model or interpolation methods, and to have larger potential biases.

Despite the relatively high quality of all the historical datasets used in this project, biases in these datasets were uncovered during latter stages of the streamflow generation tasks. In the case of the PRISM and Daymet datasets, because they have been used for numerous studies over at least a decade, possible temperature biases have been identified and studied, and are thus known to data users. Oyler *et al.* (2015) used a different observed TopoWx data product to highlight the possibility of warm biases in both PRISM and Daymet, particularly for maximum daily temperatures in the mountainous terrain of northeast Oregon, Idaho, and western Montana. McGinnis *et al.* (2011) found similar mountain temperature biases, and proposed that grid point elevations were the likely cause and thus could be at least partially corrected.

Because the Livneh dataset is newer, possible biases have not been investigated to any great degree. However, Mauger *et al.* (2016) identified the potential for substantial cold biases in mountains as a fixed lapse rate of 6.5°C/km was applied to low-elevation cooperative observation sites. In particularly moist locations like the mountains of western Washington, the bias can become significant, especially in winter months, when lapse rates are frequently less than 6.5°C/km in saturated maritime air masses (*e.g.*, Minder *et al.*, 2010). Daly *et al.* (2007) and Daly *et al.* (2010) also identified lapse rate concerns in that atmospheric decoupling and temperature inversions are common in the mountainous terrain of the Columbia Basin, which can lead to a warm bias in overnight valley low temperatures. Furthermore, Jiang *et al.* (2018) also found high elevations in the Livneh dataset to have significantly colder temperatures than other observational datasets in the Pacific Northwest.

Although not fully evaluated in this particular study, the possibility of temperature biases in the observed datasets used to calibrate and bias-correct downscaled climate projections needs to be considered by users of this hydroclimate dataset.

4.4 Hydrologic Model Calibration

Each of the four hydrological models was calibrated independently. The calibrations differed with respect to parameters used and reference streamflow datasets. UW VIC and PRMS used the same calibration technique and reference streamflow dataset, while ORNL and NCAR used different techniques. This diversity of approaches allowed an expanded potential representation of uncertainty stemming from calibration.

4.4.1 University of Washington Calibrations

As part of an innovation within the project, the team leveraged an inverse streamflow routing technique developed in the Ohio River Basin by Pan and Wood (2013). The NRNI streamflow dataset was used as a reference and disaggregated from time series at points along the river network into spatially distributed fields of runoff. Thus, a reference flow was available for every grid cell within the calibration domain. The hydrologic models were then calibrated to the runoff at every grid cell independently. The 10-year period WY 1992-2001 was used for calibration. This period was selected because it included a good representative hydrologic sample of streamflow in the Pacific Northwest. The calibration technique maximized the Kling-Gupta Efficiency (KGE) goodness-of-fit metric for the entire time series of 7-day mean streamflow.

The inverse routing method is in contrast to the traditional method of calibrating catchments in a lumped fashion, often from headwaters to river mouth. This “inverse routing” has the benefit of preserving streamflow-to-runoff balance in both time and space as one works up the river basins toward each headwater. Once the calibration is complete, flows are then routed back downstream and compared against historic records to confirm that the resulting hydrographs are reasonable. Such a technique does not obviate the need to have a well-functioning hydrologic model and rather high-density historical streamflow records. However, the inverse routing gave project teams the ability to recalibrate models reasonably quickly and objectively when historical records were updated, or new model versions became available during the modeling process.

The inverse routing technique proved quite valuable during the course of the project as the NRNI dataset was corrected and the BPA, USACE, and USBR technical teams conducted quality control of initial streamflow simulations. As unrepresentative streamflows in historical periods were discovered, the UW project team was able to quickly assess the quality issues, correct VIC model parameterizations in a relatively short period of time, and then rerun the simulations for further analysis. As mentioned above, despite best efforts to optimize calibrations, systemic biases still remain in hydrologic simulations. To accommodate this, the simulations still receive streamflow bias-correction as a final step where NRNI is available.

For this specific study, the University of Washington used the inverse routing technique to calibrate both the VIC and PRMS models. The selected calibration parameters, all relating to soil characteristics and processes, are shown in **Table 8**.

Table 8: Overview of calibration techniques used in study.

	VIC-UW	PRMS-UW	VIC-NCAR	VIC-ORNL
Calibrated parameters	b _i , depth of soil layers 2 and 3, Ksat, Nijssen (2001) parameters D1, D2, D3	slowcoef_sq, sat_threshold, pref_flow_den, gwflow_coef, ssr2gw_rate, snowinfil_max, soil2gw_max, soil_moist_max	See Mizukami <i>et al.</i> (2017)	See Oubeidillah <i>et al.</i> (2014)
Calibration methodology	Inverse calibration	Inverse calibration	Calibrated transfer functions	Lumped basin calibration
Base meteorological dataset	Livneh <i>et al.</i> (2013)	Livneh <i>et al.</i> (2013)	Maurer <i>et al.</i> (2002), updated in 2013	Daymet, PRISM, Hamlet <i>et al.</i> (2010)
Streamflow reference dataset	NRNI	NRNI	NCAR derived naturalized flows	WaterWatch

4.4.2 VIC-ORNL Calibration

During the course of this project, the DOE commissioned ORNL to conduct a nationwide assessment of climate change effects on Federal hydropower generation, as required under the SECURE Water Act of 2009 (Public Law 111-11). While the report and its underlying research were national in scope, because the Bonneville Power Administration’s generation capacity is by far the largest of DOE’s Power Marketing Administrations, special attention was given to the Columbia River Basin. Like the University of Washington, ORNL used VIC model version 4.1.1. to derive its hydrologic simulations (Naz *et al.*, 2016). However, ORNL’s calibration, in addition to employing the more traditional upstream-to-downstream calibration process, differed in two key areas which yielded different streamflow simulations, despite using the same downscaled temperature and precipitation forcings and same hydrologic model.

First, and perhaps most importantly, instead of using the NRNI dataset for calibration and bias correction, ORNL used the WaterWatch streamflow dataset from USGS (Brakebill *et al.*, 2011). Derived from the comprehensive National Water Information System (NWIS) gauge observations, WaterWatch runoff is the assimilated time series of flow per unit of area calculated for each conterminous US (CONUS) 8-digit hydrologic unit (HUC8). For each HUC8, multiple NWIS gauge stations located within the HUC8 or downstream are used to estimate the runoff generated locally at each HUC8, with gauge weighting factors determined by joint contributing drainage areas (both gauge-to-HUC8 and HUC8-to-gauge). This approach can effectively assimilate streamflow observations from multiple gauge stations as a real HUC8 runoff time series estimate that can be used to consistently calibrate VIC total runoff across all CONUS HUC8s (Oubeidillah *et al.*, 2014). However, since WaterWatch did not specifically filter out or “naturalize” regulated stream gauges, strong bias may exist in HUC8s under heavy regulation. Second, unlike the UW calibrations, ORNL used PRISM temperature and precipitation as its forcing dataset during the calibration process, which, as mentioned earlier, is

suspected to have a warmer bias in the complex terrain of the Pacific Northwest. Third, the VIC-ORNL calibrations were done on a monthly time step, which contrasted with the University of Washington's calibration to weekly time steps. See Naz *et al.* (2016) and Kao *et al.* (2016) for further details on the VIC-ORNL calibration process, and validation results relative to the WaterWatch streamflow dataset.

4.4.3 VIC-NCAR Calibration

A third climate change research project was under way at the National Centers for Atmospheric Research (NCAR) for several research purposes, including the USBR West-Wide Climate Assessments (USBR, 2016b). One research effort involved the development of a novel calibration routine that began by developing transfer functions to relate terrain features and parameter values based upon representative catchments (Mizukami *et al.*, 2017). These transfer functions were then calibrated and used to estimate parameters for the Continental United States.

4.4.4 Hydrologic Model Historical Performance

The project team expended considerable time and effort to robustly review and refine the hydrologic model calibrations to maximize their utility and represent hydrologically reasonable responses to the temperature and precipitation forcings. This was especially true for the UW-VIC and UW-PRMS hydrologic simulations, since the University of Washington team had the ability to recalibrate the underlying hydrologic models several times based on feedback from the RMJOC technical teams. While the ORNL-VIC and NCAR-VIC calibrations were generally kept as-is from their respective sources, snow melt parameters were adjusted for both calibration sets to match the UW-VIC simulations, with the maximum snow temperature and minimum rain temperature being set to 0.5 and -0.5°C respectively. Further, the VIC-ORNL implementation used a different vegetation and elevation band dataset (Kao *et al.*, 2016), while the VIC-UW and VIC-NCAR implementations used the same elevation and vegetation files.

In general for the mainstem Columbia and most large tributaries, because they were calibrated directly with the NRNI dataset, the UW-VIC and UW-PRMS performance versus the historical period is generally better relative to NRNI than the ORNL-VIC and NCAR-VIC historical flows. See **Figure 19** and **Table 9** for a summary of historical performance by each of the four models. In all four hydrologic model sets, performance relative to the historical period tended to be better along the mainstem of the Columbia than along smaller headwaters. Decreasing error with increasing spatial domain is common with applications of hydrology models.

The model performance was generally weaker in parts of the Snake, Deschutes, and a few tributaries into the lower Columbia River, including the Willamette Basin. This was expected in that land use and geological characteristics in these sub-basins make hydrologic modeling conducted for the entire Columbia Basin as a whole, as done for this project, more difficult. In much of southern Idaho and eastern Oregon, higher soil permeability allows a larger degree of surface-groundwater exchange, which is not measured easily, and is not captured well in the hydrologic models. In addition, this region has been under some form of irrigation for decades, with large in-river and groundwater withdrawal and some return flow from irrigated cropland back into the river system. These consumptive uses are also estimates as detailed in 2010 Modified Flows (BPA, 2011). Thus, in these parts of the Columbia Basin, the NRNI calculations themselves have greater uncertainty relative to the rest of the basin, which in turn can impact

the calibration of the hydrologic models themselves, and the post-processing/bias-correction on the flows. It is likely that many of the poorest performing lower bounds of the ranges of KGE values in these areas (**Table 9**) are attributable to uncertainties in historical NRNI data used to evaluate performance, rather than solely to the hydrological models' simulation of processes.

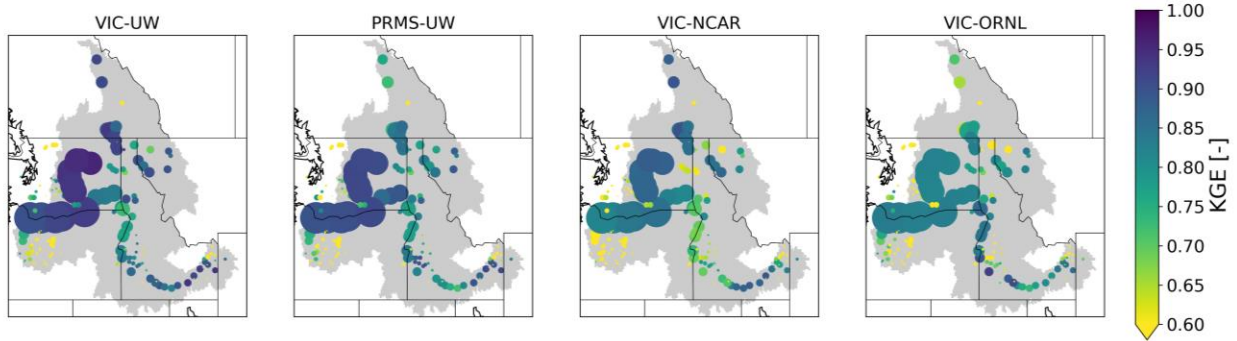


Figure 19: Historical performance of each of the four calibrated hydrologic models. Performance was calculated using the weekly Kling-Gupta Efficiency upon the period WY 1961-2005, removing the calibration period of WY 1992-2001.

Table 9: Median, minimum, and maximum (in parentheses) of Kling-Gupta Efficiency for weekly average flows WY 1961-2005, relative to the calibration period of WY 1992-2001.

	VIC-UW	VIC-ORNL	VIC-NCAR	PRMS-UW
<i>Mid-Columbia</i>	0.94 (0.81 - 0.96)	0.82 (0.33 - 0.82)	0.87 (0.66 - 0.88)	0.91 (0.75 - 0.92)
<i>Upper Columbia</i>	0.91 (0.90 - 0.93)	0.68 (0.63 - 0.77)	0.89 (0.86 - 0.90)	0.75 (0.72 - 0.83)
<i>Pend Oreille</i>	0.90 (-1.98 - 0.94)	0.82 (-1.86 - 0.85)	0.85 (-2.35 - 0.87)	0.85 (-1.91 - 0.89)
<i>Lower Columbia</i>	0.90 (-0.72 - 0.93)	0.83 (0.18 - 0.84)	0.82 (-0.46 - 0.85)	0.90 (-0.61 - 0.91)
<i>Kootenay</i>	0.87 (0.59 - 0.88)	0.78 (0.27 - 0.79)	0.85 (0.42 - 0.85)	0.86 (0.37 - 0.87)
<i>Lower Snake</i>	0.82 (0.69 - 0.91)	0.83 (0.62 - 0.86)	0.76 (0.61 - 0.84)	0.82 (0.64 - 0.89)
<i>Upper Snake</i>	0.81 (-4.0 - 0.94)	0.62 (-5.8 - 0.93)	0.65 (-5.0 - 0.89)	0.76 (-3.2 - 0.92)
<i>Spokane</i>	0.78 (0.68 - 0.79)	0.77 (0.68 - 0.78)	0.62 (0.54 - 0.64)	0.79 (0.70 - 0.81)
<i>Yakima</i>	0.75 (-6.0 - 0.84)	0.35 (-4.7 - 0.56)	0.60 (-6.3 - 0.77)	0.69 (-5.9 - 0.79)
<i>Willamette</i>	0.61 (-1.6 - 0.82)	0.68 (-3.1 - 0.80)	0.39 (-2.3 - 0.72)	0.58 (-1.64 - 0.77)
<i>Western Washington</i>	0.58 (-22.0 - 0.77)	0.39 (-18.8 - 0.83)	0.48 (-20.2 - 0.64)	0.56 (-22.8 - 0.81)
<i>Deschutes</i>	-0.9 (-7.0 - 0.57)	-0.37 (-4.4 - 0.56)	-0.80 (-5.34 - 0.18)	-0.77 (-6.8 - 0.48)

The performance of the models was also evaluated by comparing 10th, 50th, and 90th percentile daily flows to NRNI for the period of 1950-2005 (**Figure 20**). More pronounced seasonal biases are evident, and vary greatly between models and locations. For example VIC-ORNL (VIC_P2) shows strong positive biases in the spring freshet at Libby Dam (LIB) and strong negative biases at Arrow Lakes (ARD). In general, the timing of seasonal flows from VIC-NCAR (VIC_P3) and VIC-ORNL is delayed as compared with NRNI. In the groundwater-dominated Snake Basin (Brownlee Dam, BRN), three of the four models under-predict winter low flow periods. As noted above, VIC-UW (VIC_P1) and PRMS show the strongest agreement with NRNI.

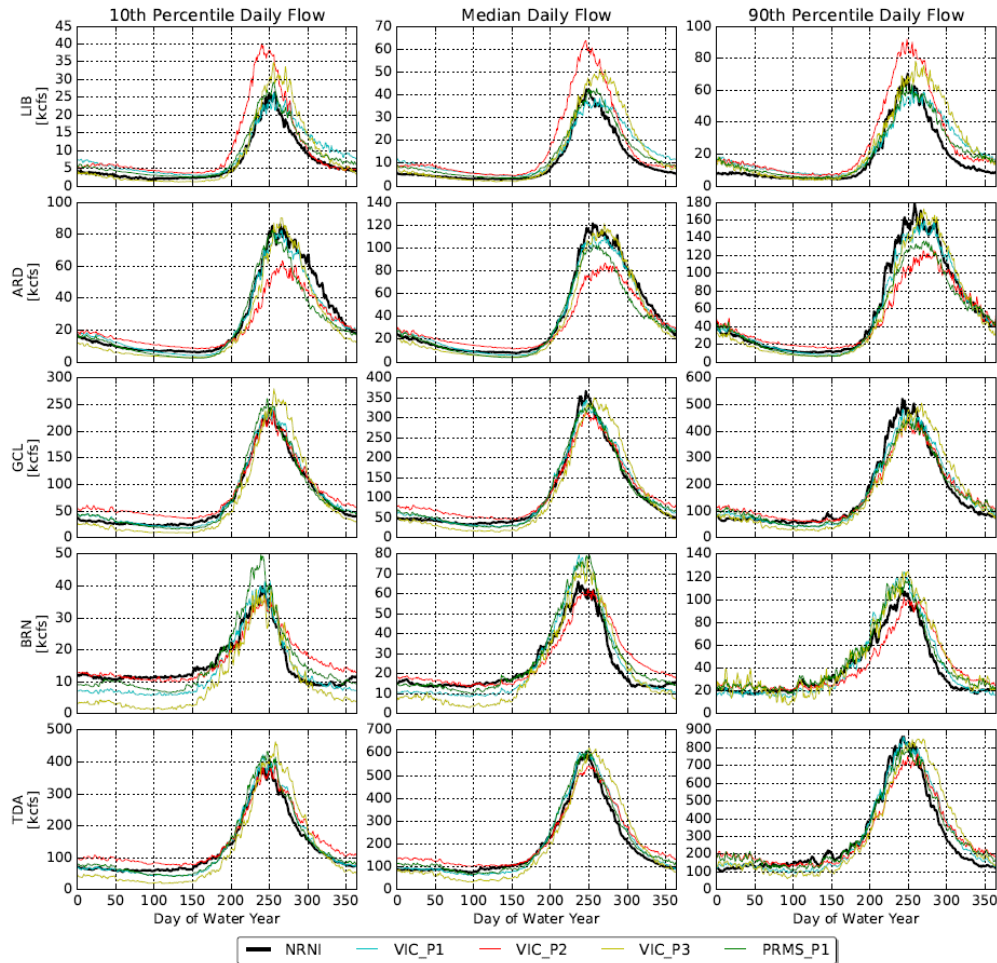


Figure 20: Comparison of modeled 10th, 50th (median), and 90th percentile daily flows from the four hydrological models (VIC_P1=UW; VIC_P2=ORNL; VIC_P3=NCAR) and NRNI data for the period of 1950-2005. The modeled flows are raw (no bias-correction was applied). Locations include Libby (LIB), Arrow Lakes (ARD), Grand Coulee (GCL), Brownlee (BRN), and The Dalles (TDA).

4.5 Streamflow Bias Correction

Because models, model parameters, and meteorological forcings are imperfect, the modeled streamflow time series still exhibit biases that may make them unsuitable for direct application in hydro-regulation models. For this reason, a final bias-correction is applied to the modeled flow values. For the RMJOC-I study (RMJOC, 2011a), a commonly used quantile mapping approach was applied (Snover *et al.*, 2003; Elsner *et al.*, 2010; Vano *et al.*, 2010). In that study, the post-processing was conducted in two steps: one to correct average monthly flows; and a second to correct for possible annual volume biases. The original intent and Statement of Work of this project envisioned that a nearly identical approach would be used. However, in the former study, daily NRNI flows were used as the reference historical streamflow dataset for 1951-2008, but were averaged to monthly time steps, and model evaluation was mostly performed at this monthly time step.

While the process was useful for the previous study, the strong desire to have bias-corrected daily flows in the current project highlighted a weakness with quantile mapping post-processing conducted on monthly time steps. At month and annual boundaries, the ratios applied on

monthly time steps were prone to overamplify bias-corrections in future periods, particularly as climate change causes seasonal shifts in volume and resulting streamflows. Distinct and hydrologically unrealistic drops or jumps in simulated flows were introduced, which did not resemble usual hydrographs, and did not conserve volume changes from upstream to downstream locations. In addition, as Cannon *et al.* (2015) suggested, quantile mapping can artificially drive future climate projections by imposing a past climate signal and can artificially dampen changes in extreme events.

When these issues were discovered in the quality control phase of the provisional streamflow datasets, new bias-correction techniques emerged which were then employed for the first time with this hydroclimate dataset. Pierce *et al.* (2015) proposed a modified quantile mapping method for bias correcting GCM temperature and precipitation outputs, which corrects for biases in historical periods, and also preserves model-predicted mean changes in future periods. This method was used as the basis for the development of a new streamflow bias-correction method for this project. A quantile mapping was developed for each streamflow scenario based on the entire control period (1951-2005). This mapping was applied to the entire time series to bias-correct the streamflow through the end of the 21st century. Then, a volume correction was applied to preserve streamflow volume changes between the future and control simulations. As a result, the bias-corrected streamflow time series exhibit the same increases or decreases in annual volumes as seen in the raw (not bias-corrected) streamflow time series.

This novel post-processing technique had several advantages which increased the overall quality of the bias-corrected streamflows for this project. Since the bias-corrections were performed directly on daily flows, unrealistic jumps in daily flows on month and annual boundaries were eliminated. In addition, the distribution of daily flows was nearly reproduced for the control period, so seasonal volume ratios between control and future periods were reproduced in raw and bias-corrected flows. Perhaps most importantly, changes to future flow timing induced by climate change were not artificially fitted to historical/past observations.

Although the bias-corrected flows inherited the expected streamflow changes caused by climate change itself, this new technique does not correct for other unrealistic artifacts that may exist in some of the raw simulations. Because the method is applied to each NRNI location independently, the same weakness with quantile mapping of volume inconsistencies between upstream and downstream points can still occur. Thus, for specific applications, particularly those requiring volumetric consistency between upstream and downstream locations, or precise flows in very small watersheds without an NRNI reference point, the raw streamflow scenarios could be more useful for hydroclimate planning.

4.6 Streamflow Scenarios and Naming Convention

The climate change streamflow dataset includes daily time series for 396 locations in the Columbia River Basin (**Figure 21**). At around 190 of those locations where NRNI data was produced and available, the raw streamflows were bias-corrected to the WY 1951-2005 historical period (see **Figure 10** in section 3.1). At each location, 172 separate streamflow scenarios were generated (plus four historic simulations). **Figure 22** details the characteristics for each streamflow scenario, sorted by parent RCP, GCM, downscaling technique, hydrologic model, and source of the model parameter set. For the streamflows generated using the hybrid downscaled dataset from ORNL, only three of the GCMs used by DOE (2017) overlapped with

the GCM selections for this particular project, and only for RCP8.5. The ORNL downscaled dataset was also generated only for years 1966-2005 and 2011-2050.

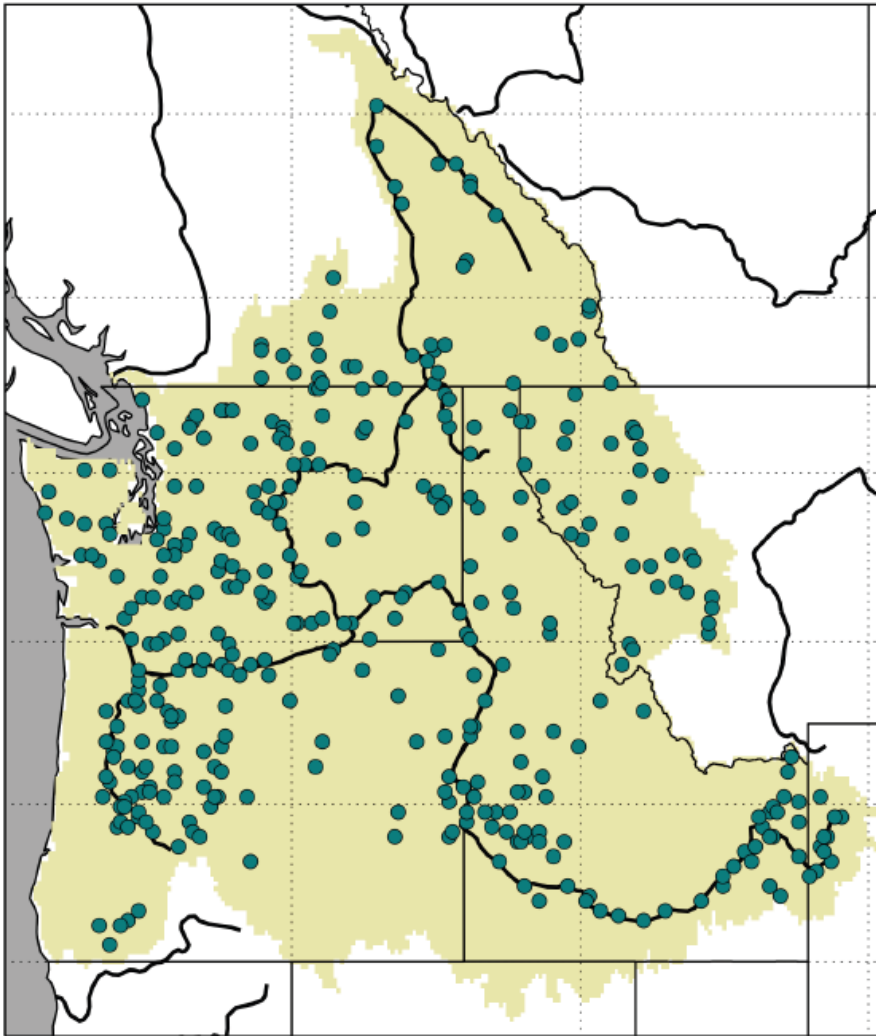


Figure 21: Raw streamflow locations. For bias-corrected flow locations, see Figure 9.

Streamflow Scenario Schematic

Hydrologic Model	Parameter Set Developer	BCSD Downscaling (statistical)		MACA Downscaling (statistical)		ORNL Downscaling (hybrid)
		RCP 4.5	RCP 8.5	RCP 4.5	RCP 8.5	RCP 8.5
VIC	UW (P1)					
	ORNL (P2)					
	NCAR (P3)					
PRMS	UW (P1)					

GCM:	CanESM-2	HadGEM2-CC
	CCSM4	HadGEM2-ES
	CNRM-CM5	inmcm4
	CSIRO-Mk3-6-0	IPSL-CM5-MR
	GFDL-ESM2M	MIROC5

Figure 22: Streamflow scenarios sorted by GCM, downscaling technique, hydrologic mode, and model parameter set.

Because so many scenarios were generated and made available for this project, a naming convention evolved allowing technical teams to quickly identify the source data used for each of the 172 streamflow scenarios. This naming convention will be referenced frequently in subsequent chapters and analyses. The convention follows the hydrologic model generation chain by including GCM used, downscaling technique, hydrologic model, and parameter set:

(Emissions Scenario) __ (Model Abbreviation) __ (Downscaling Method) __ (Hydrologic Model) __ (Parameter Set)

For example, RCP45_CanESM2_BCSD_VIC_P1 is the streamflow scenario is using the GCM data from the RCP4.5 run of the Canadian Earth System Model v2, downscaled using Bias Corrected Spatial Disaggregation, and used by the VIC hydrologic model that was calibrated by the University of Washington.

5.0 Downscaled Temperature and Precipitation Projections

5.1 Columbia Basin Summary

5.1.1 Temperature Trends

Consistent with numerous global and regional climate change studies outlined in Section 1.2, downscaled temperatures from the Global Climate Models (GCMs) used for this study show the Columbia Basin warming during the 1970-1999 historical period with warming continuing through the 2000s and 2010s (**Figure 23**). Both the magnitude and rate of warming are supported further by observational trends for the region summarized in volume one of the US National Climate Assessment (2017), the Climate Science Special Report (<https://science2017.globalchange.gov>) with about 1°C (1.4°F) of warming from the 1970s through 2010s. Based on the GCMs used for this study, continued warming in the Columbia Basin is nearly certain to continue, with even more warming if RCP8.5 carbon emission projections are realized.

Average annual daily maximum temperature across Columbia River Basin and Pacific coastal drainages (avg. across 10 models)

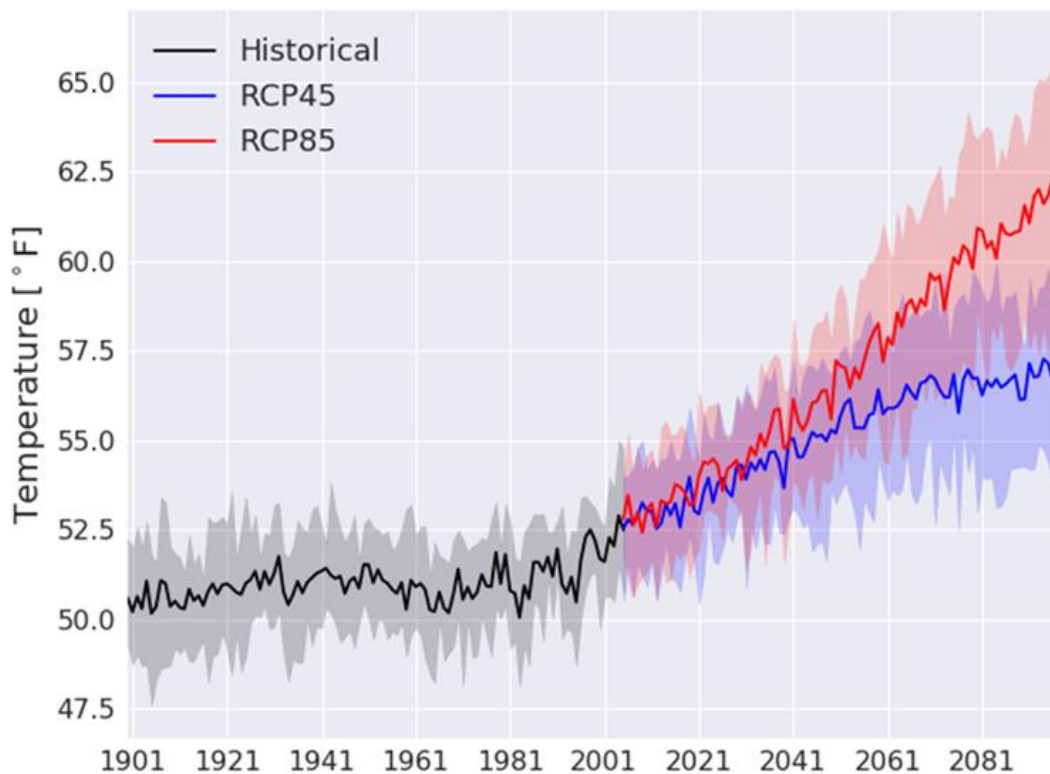


Figure 23: Average annual daily maximum temperatures, and 10th and 90th percentile temperatures, for the ten GCMs in this study for the Columbia River Basin and Pacific coastal drainages in Washington and Oregon. For RCP 4.5 and 8.5, from 1901-2100. The 20th century period (shown in black and gray) is the control period for each GCM and is used to evaluate performance. The GCM time series are also bias-corrected based upon the comparison of the latter half of the control simulation to a reference dataset.)

While basinwide warming over time is nearly certain, the rate and end-point of that warming will vary across the basin and by season. **Figure 24 and 25** compare temperature projections for the 2030s for both RCPs, all 10 GCMs, and all three downscaling techniques used in this study. Annual projected temperature increases from the historical period (1970-1999) to the 2030s (2020-2049) range from 2.0°F to around 5.5°F across the Columbia Basin for both RCP4.5 and RCP8.5 in the GCMs used for this study. While there are spatial trend differences between the three downscaling techniques and underlying GCMs, there is a general tendency for interior areas to warm more than areas near the Pacific Coast, where more modest warming of 1.5-2.5°F is projected through the 2030s. The range of temperature increases is also larger in the interior. This wider range of potential outcomes is apparent in all three downscaling techniques, although the ORNL hybrid downscaling method appears to show a somewhat narrower temperature range compared to the statistical BCSD and MACA methods.

By the 2070s (2060-2089), projected temperature trends become increasingly dependent on which RCP is realized, with much warmer temperatures projected for RCP8.5 compared to RCP4.5 (**Figures 26 and 27**). This is consistent with the design of the RCPs and with the established physical properties of GHG and their lifetimes in the atmosphere. However, the overall spatial distribution of the warming retains a similar pattern to the 2030s, with greater potential warming, and a greater range of potential warming, in interior portions of the basin.

The magnitudes and ranges of projected temperature changes also vary by season across the GCMs selected. In **Figures 28 and 29**, average seasonal temperatures show a wider range of possible outcomes in winter, spring, and summer, but with a tendency for greater warming in summer compared to the long-term mean than all other seasons. In all climate scenarios, though, general warming is predicted in all seasons.

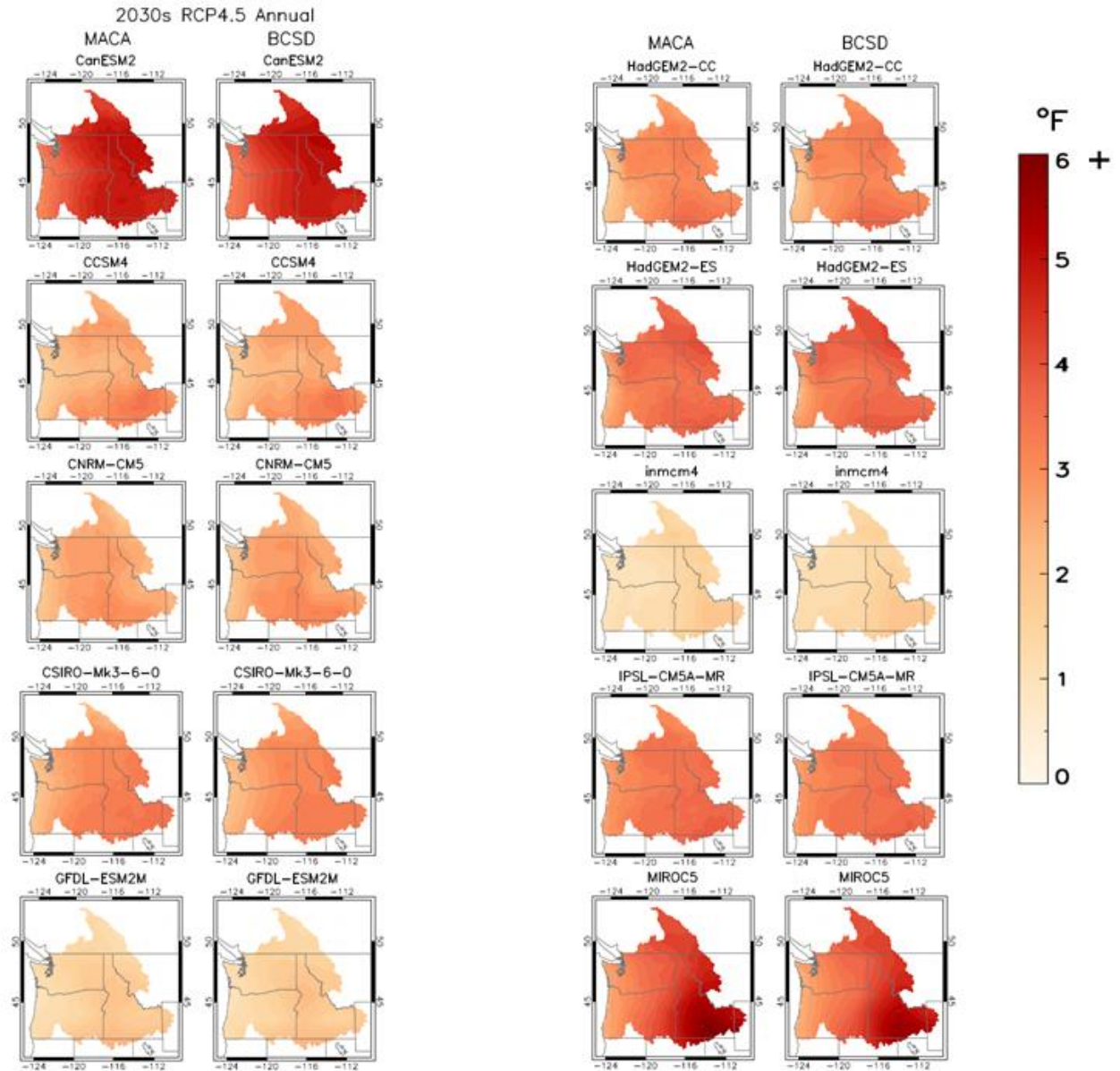


Figure 24: Annual temperature change (in °F) between historical period (1970-1999) and the 2030s (2020-2059) for RCP4.5, for all ten GCMs used for this study.

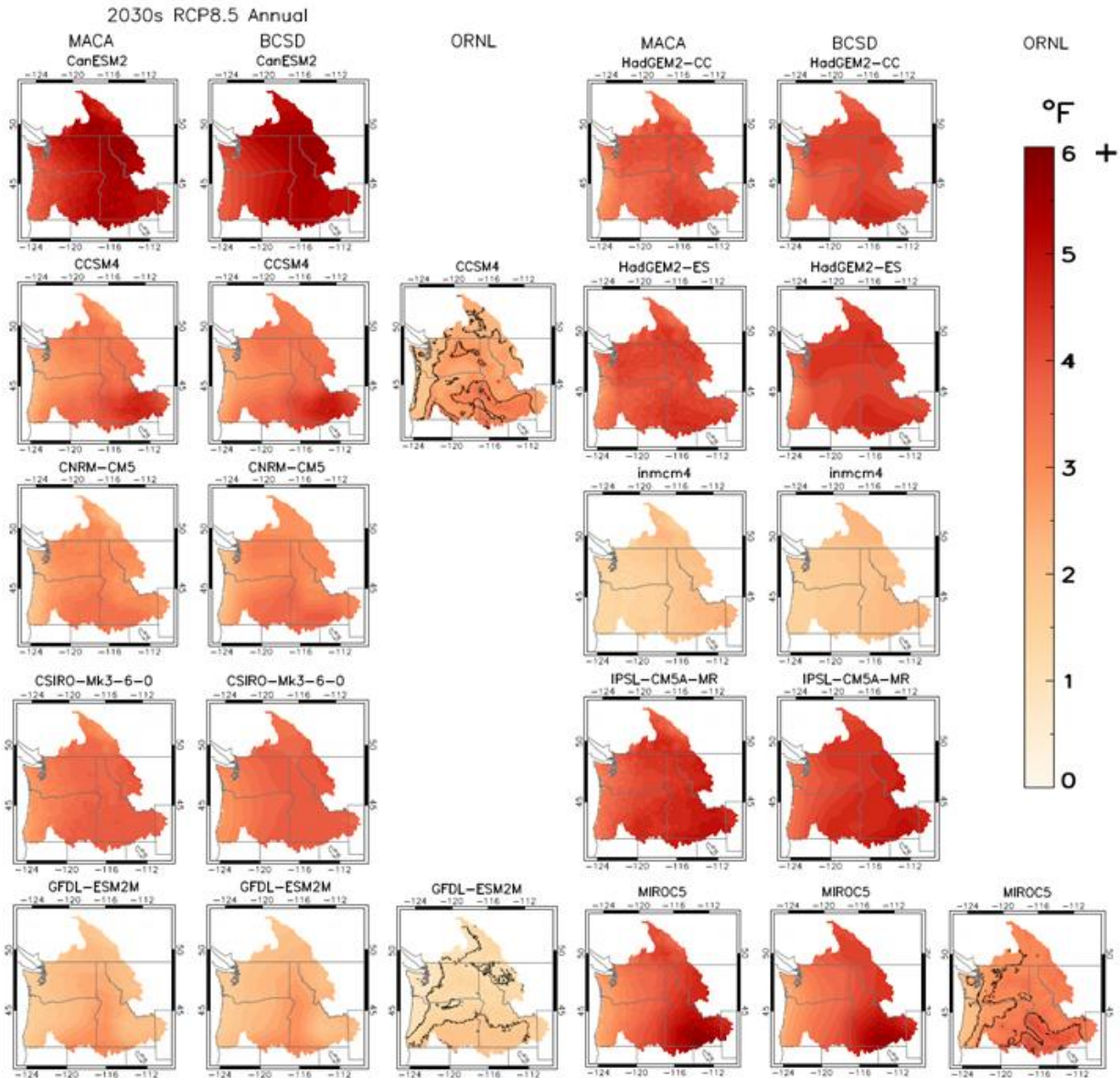


Figure 25: Same as Figure 24, except for RCP8.5. The temperature projections available from the hybrid dynamical downscaling by ORNL are included.

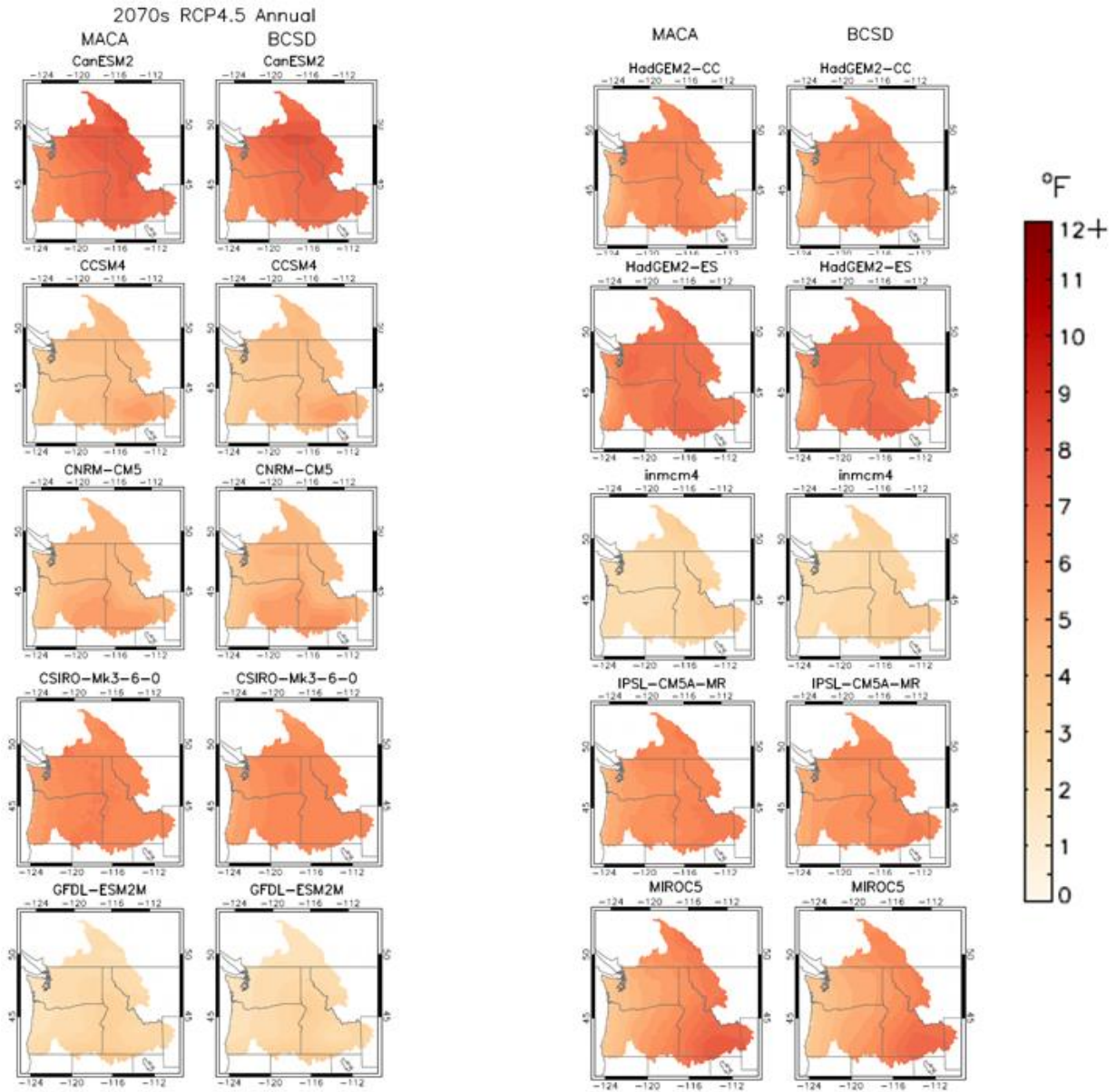


Figure 26: Temperature change (in °F) between historical period (1970-1999) and the 2070s (2060-2089) for RCP4.5.

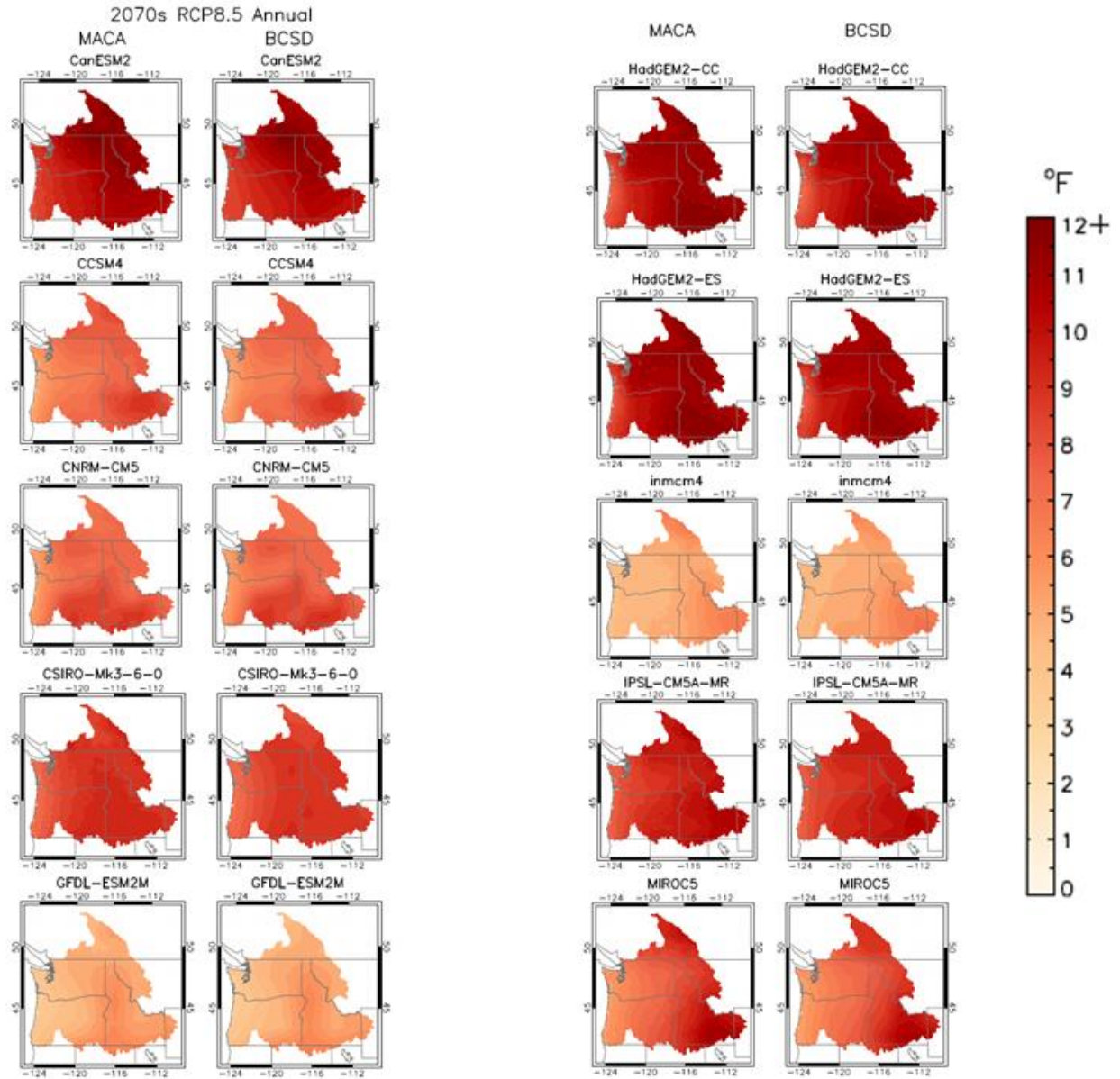


Figure 27: Same as Figure 26, except for RCP 8.5.

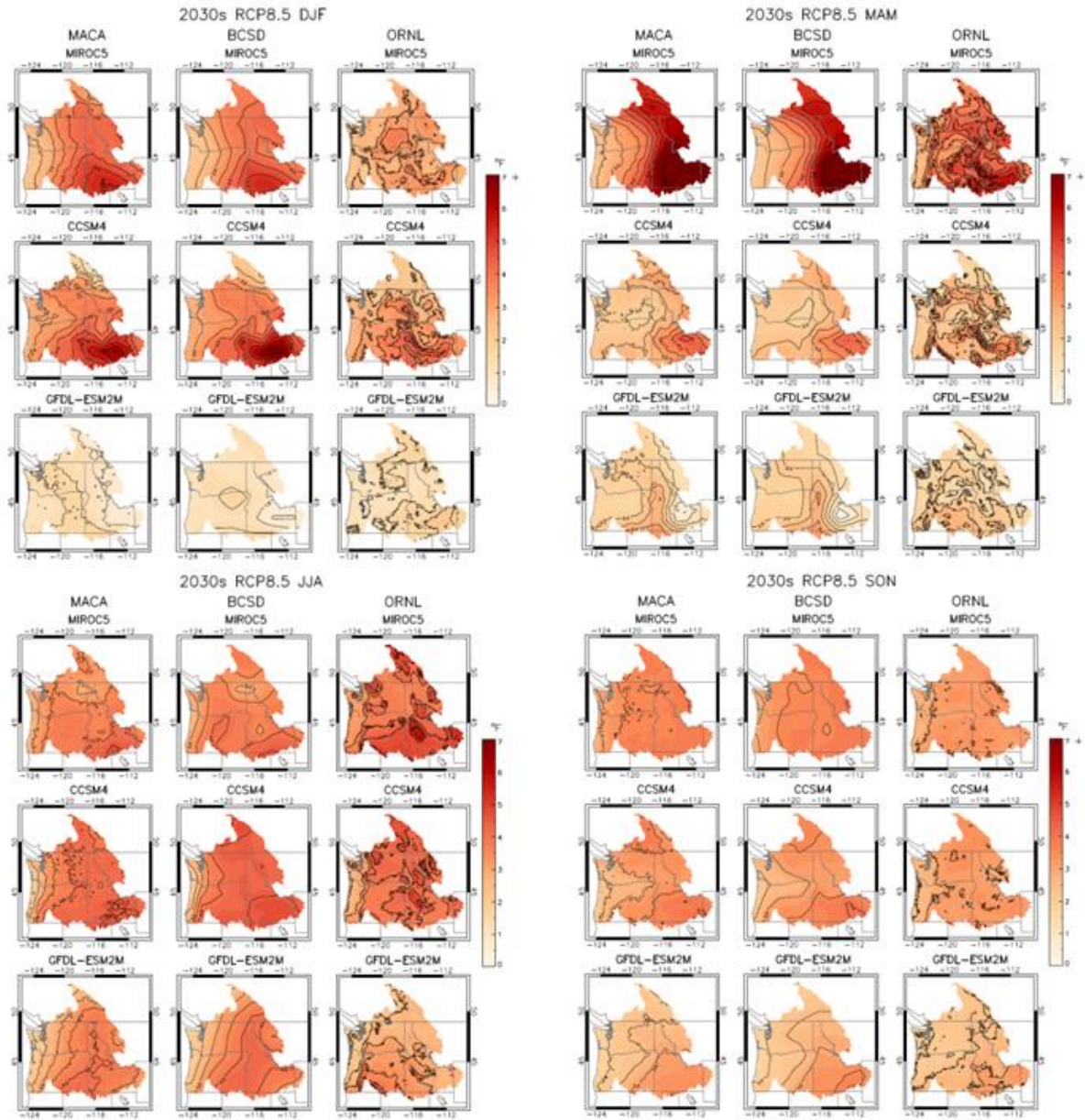


Figure 28: Seasonal change in temperature (in °F) between historical period 1970-1999 and the 2030s (2020-2039) for the three RCP 8.5 GCMs having data for all three downscaling techniques. DJF: December-February (winter); MAM: March-May (spring); JJA: June-August (summer); and SON: September-November (fall).

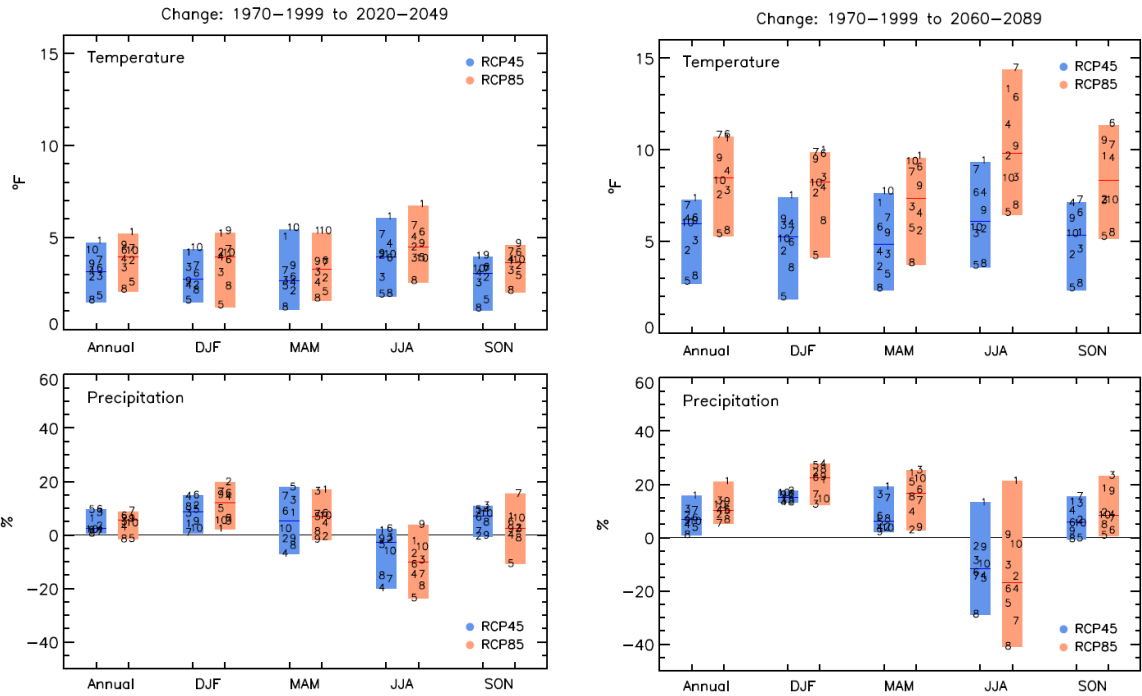


Figure 29: Average annual and seasonal temperature change (in °F) and precipitation (in %) relative to the long-term mean (1970-1999) for the 2030s (2030-2059, left) and the 2070s (2060-2089, right) above The Dalles, OR, for RCP 4.5 and RCP8.5. The individual GCM averages are indicated by numbers 1-10, with the median of the 10 marked by the thin horizontal line.

5.1.2 Precipitation Trends

Downscaled precipitation projections show more differences across models in space and time than projections of temperature. Despite this greater spread in projections, some important signals appear to emerge over time. Consistent with trends indicated in recent climate change studies (Section 1.2) near the Columbia Basin, a tendency for higher annual precipitation over time is apparent in a majority of the GCMs used in this study. While the already large year-to-year variability is projected to continue in climate model averages (Figure 30), by the 2030s, annual precipitation is likely to exceed the long-term mean more often than not for both RCP4.5 and 8.5 scenarios (Figures 31 and 32). For the basin as a whole, rather sizable percentage increases in precipitation are noted for most of the GCMs used in this study by the 2070s (Figures 33 and 34). Higher annual precipitation is projected more consistently for the Canadian portion of the Columbia Basin, and in middle and upper portions of the Snake Basin.

Annual precipitation across Columbia River Basin and Pacific coastal drainages (avg. across 10 models)

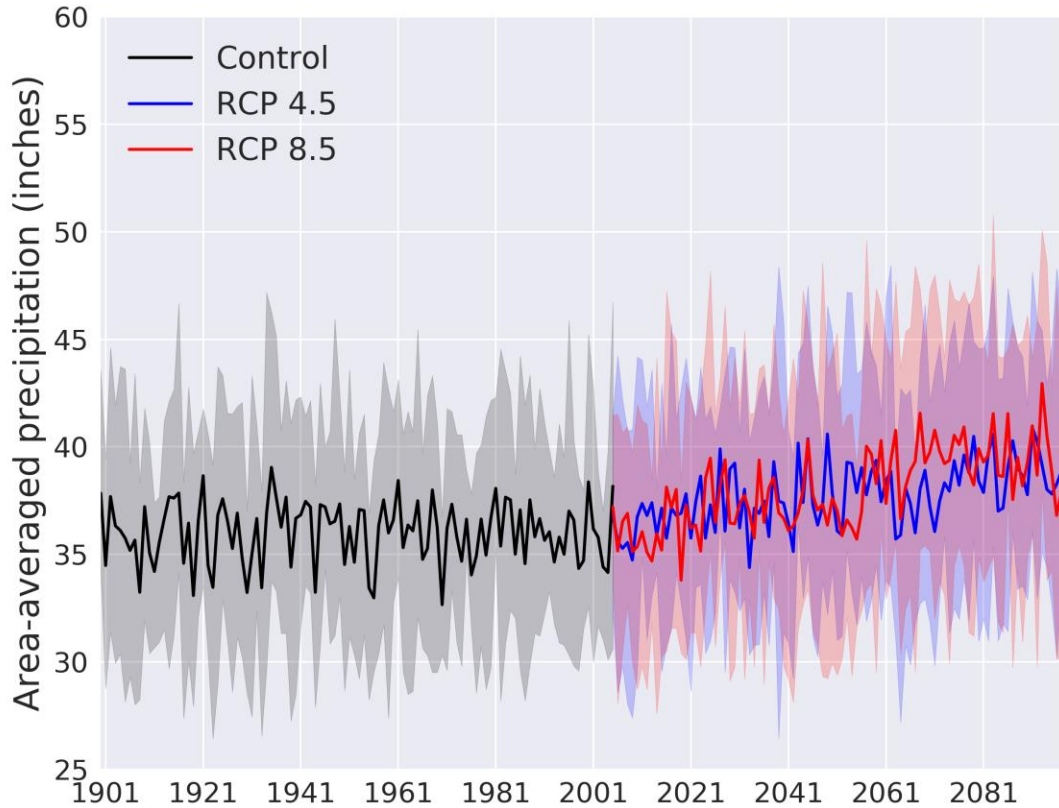


Figure 30: Average annual precipitation, and 10th and 90th percentile precipitation, for the ten GCMs in this study for the Columbia River Basin and Pacific coastal drainages in Washington and Oregon. For RCP 4.5 and 8.5, from 1901-2100 (1901-2004 as the historical period). The 20th century period (shown in black and grey) is the control period for each GCM and is used to evaluate performance. The GCM time series are also bias-corrected based upon the comparison of the latter half of the control simulation to a reference dataset.

While annual precipitation appears likely to increase, the projections appear to agree more substantially on seasonal trends, with most model projections indicating a tendency for higher winter precipitation and lower summer precipitation (**Figures 30 and 31**). However, since the region historically receives the bulk of its precipitation during the cool season, a percentage increase in winter precipitation is likely to offset even large percentage decreases in summer precipitation from an annual perspective. In addition, some projections imply that increased summer precipitation is still possible, particularly over the southern half of the basin.

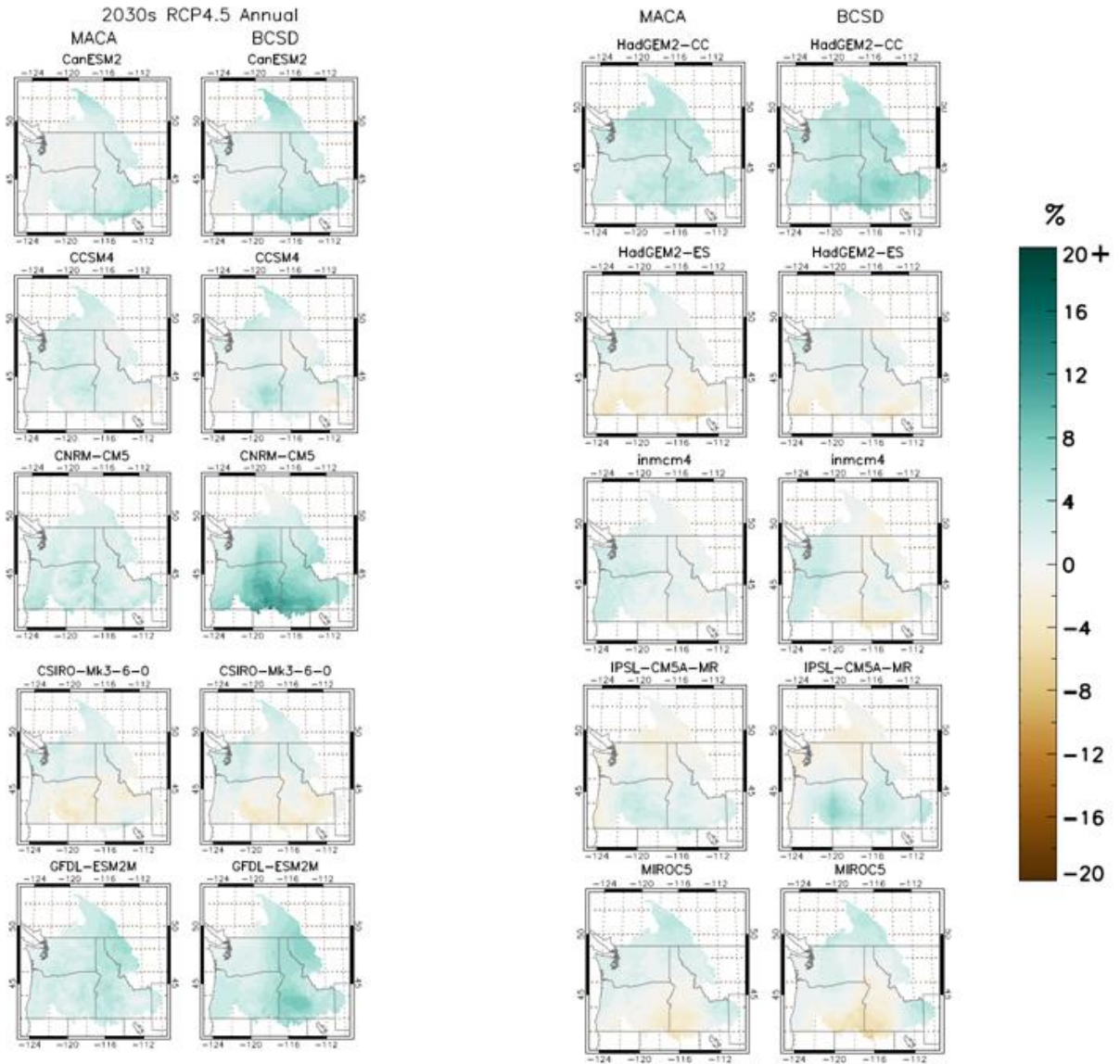


Figure 31: Annual precipitation change (in %) between historical period (1970-1999) and the 2030s (2020-2059) for RCP4.5, for all ten GCMs used for this study.

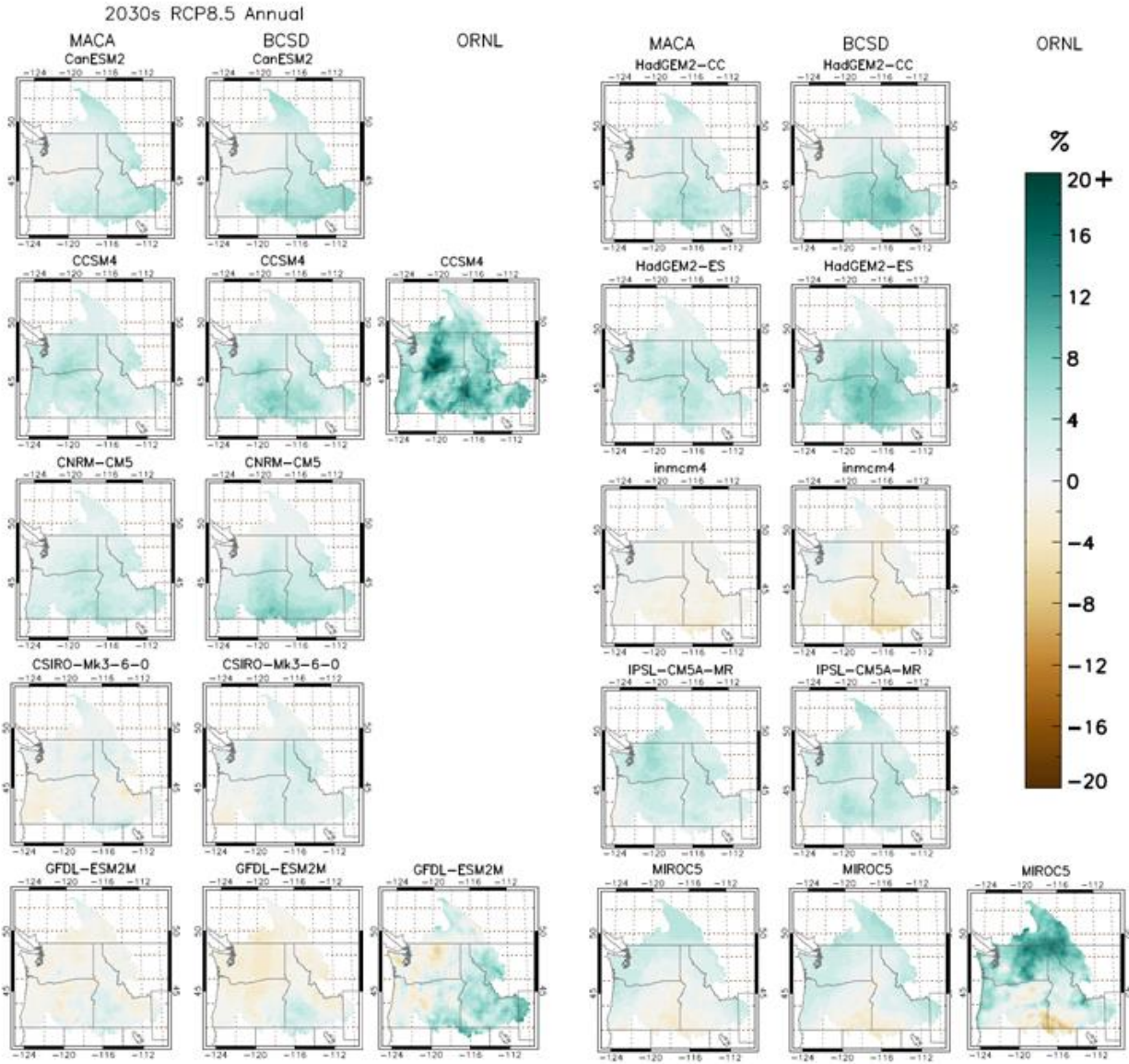


Figure 32: Same as Figure 31, except for RCP8.5.

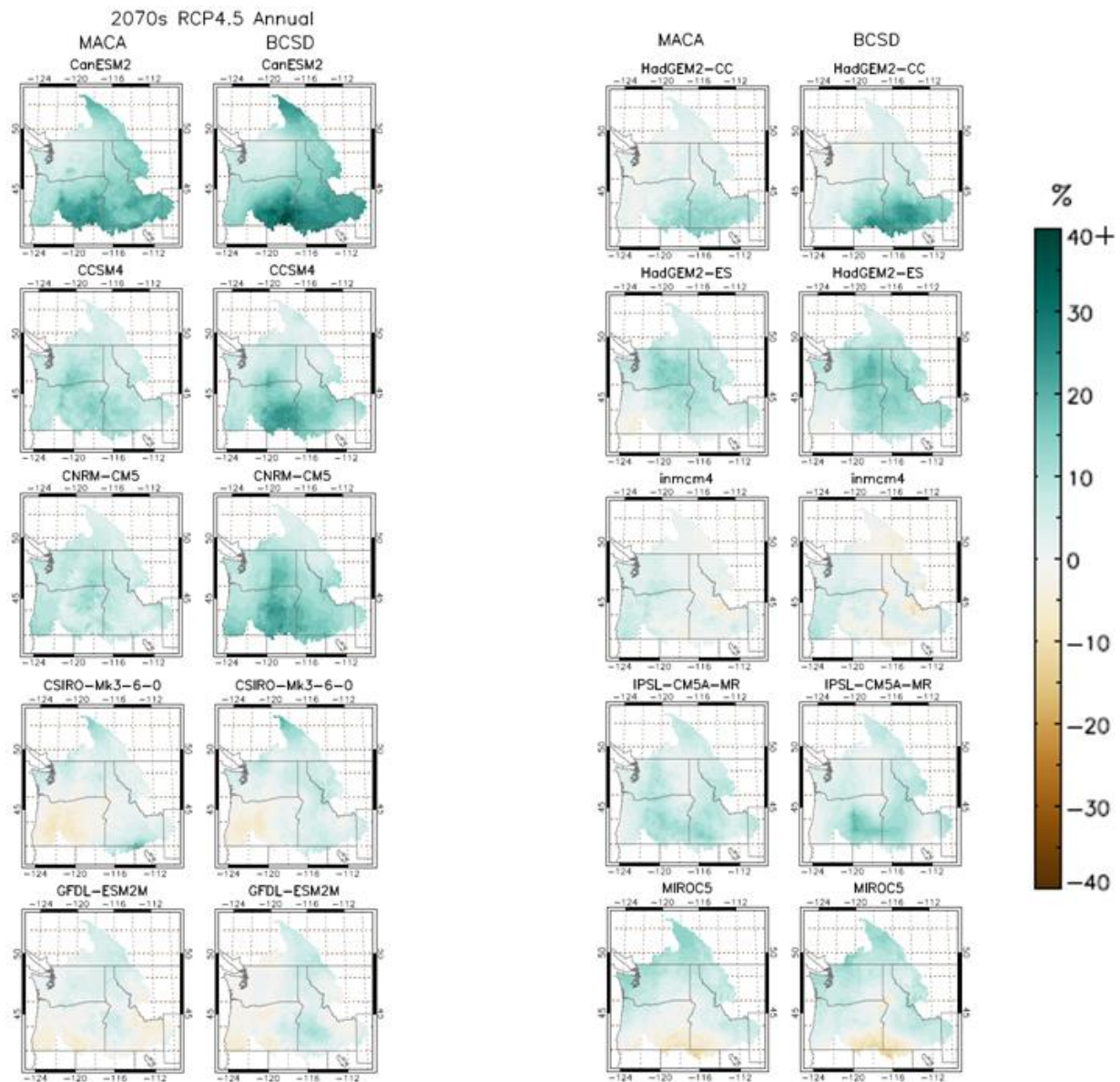


Figure 33: Annual precipitation change (in %) between historical period (1970-1999) and the 2030s (2020-2059) for RCP4.5.

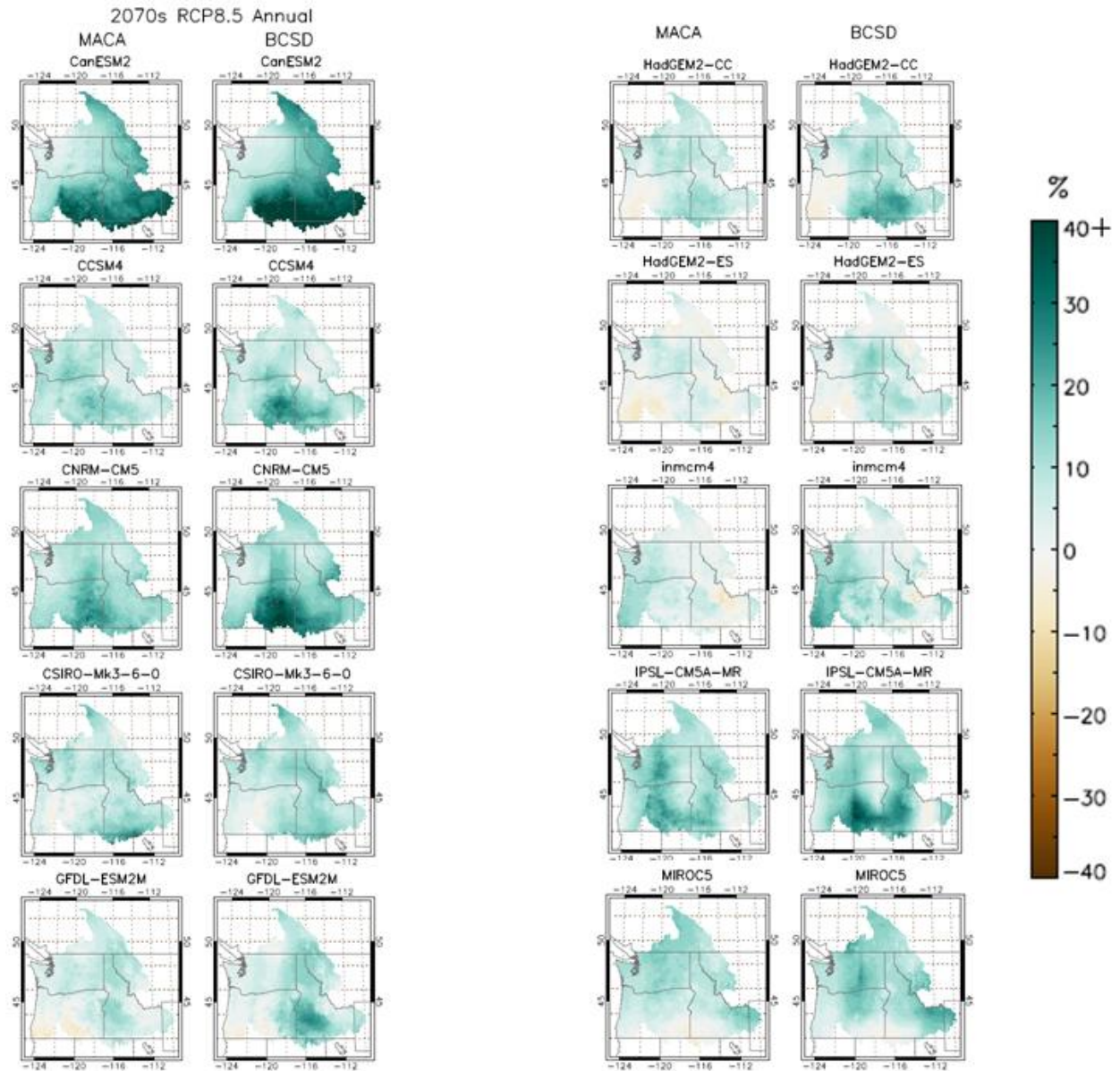


Figure 34: Same as Figure 33, except RCP 8.5.

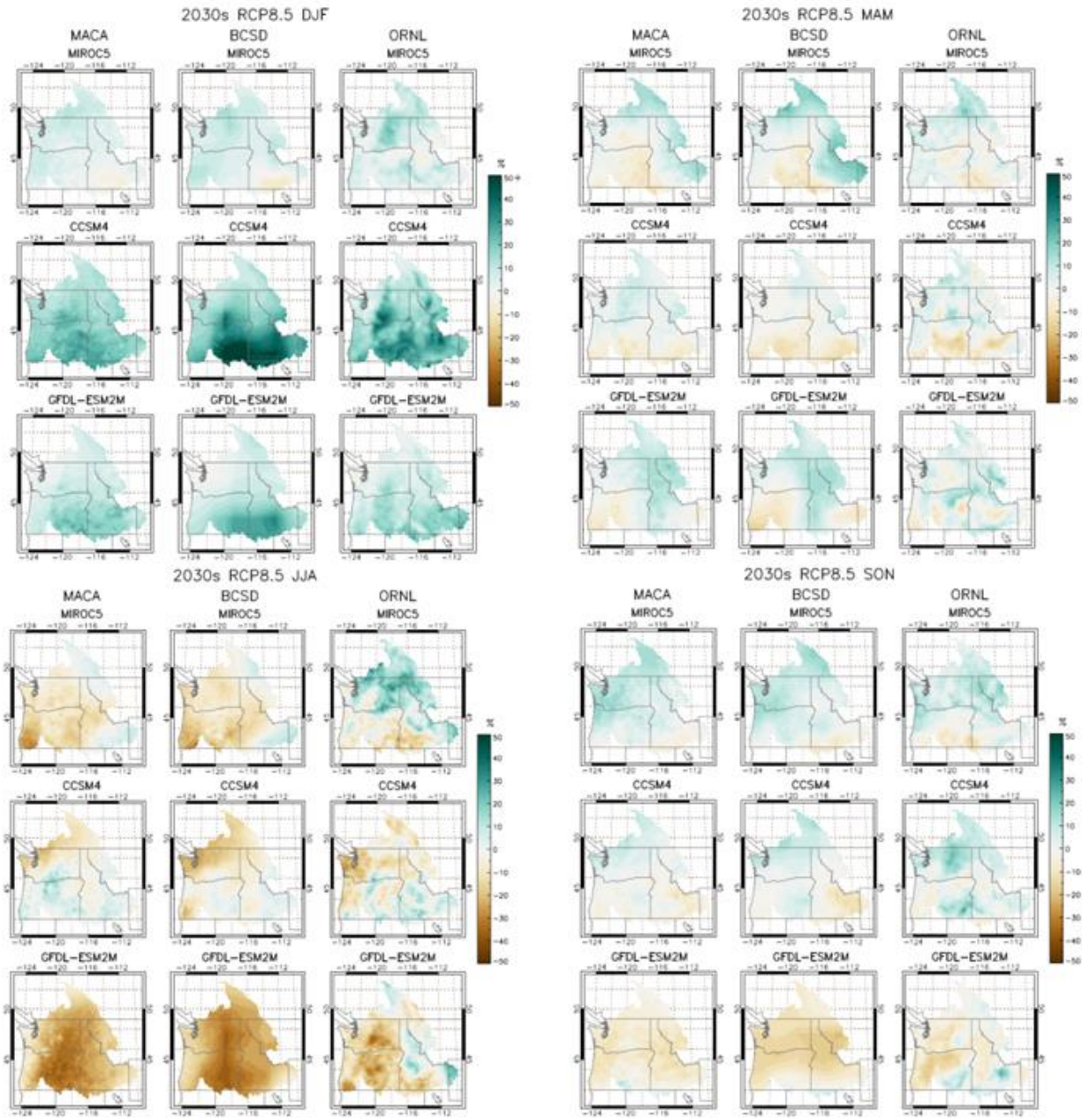


Figure 35: Seasonal change in precipitation (in %) between historical period 1970-1999 and the 2030s (2020-2039) for the three RCP 8.5 GCMs having data for all three downscaling techniques. DJF: December-February (winter); MAM: March-May (spring); JJA: June-August (summer); and SON: September-November (fall).

Figure 36 depicts the expected temperature and precipitation trends across the Columbia Basin from the different GCMs used, and the relative spread between temperature and precipitation outcomes. While all GCM outputs agree on basinwide warming into the 2030s, almost all outputs (16 out of 20) also show a tendency toward wetter basin conditions, with only one (inmcm4, RCP8.5) indicating some drying. By the 2070s, all but one scenario indicate wetter annual trends. It is also worthy to note that for the RCP8.5 scenarios in the 2030s, and both

RCPs for the 2070s, projected temperature and precipitation changes appear to show some correlation, with the warmer scenarios also tending to be wetter, with less warmer scenarios tending to be less wet on a basin average.

For comparison purposes, average GCM temperature and precipitation outputs from CMIP-3 are compared with those from CMIP-5 for the Columbia Basin (**Figure 37**). While there is sizable overlap between the two climate change datasets, and those used specifically for RMJOC-I and generated for RMJOC-II, the GCMs used for this study, along with the different driving emissions, projected conditions generally warmer and slightly wetter than the GCMs and emissions used in RMJOC-I. It is also noteworthy that the driest GCM used for RMJOC-I is a relative outlier compared to the GCMs selected for this study, while the warmest and wettest GCM used for RMJOC-I is closer to the median temperature and precipitation for RMJOC-II. Several GCMs evaluated for this study projected conditions as warm as or warmer than the warmest scenario used in RMJOC I.

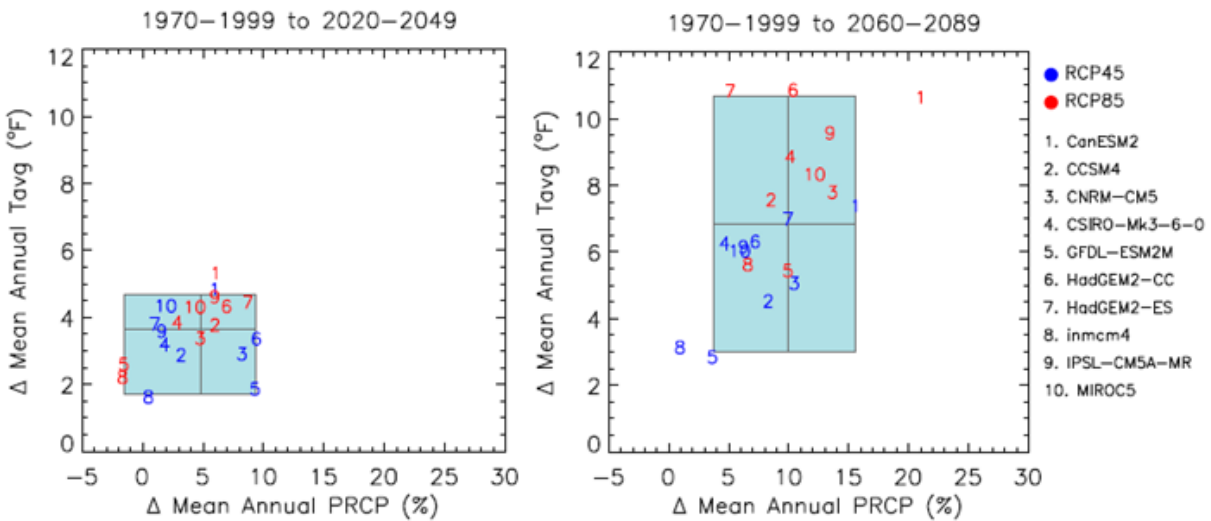


Figure 36: Change in annual temperature and precipitation between the historical period (1970-1999), the 2030s (2020-2049, left), and the 2070s (2060-2089, right) for each of the 10 GCMs used for this study, for RCP 4.5 and 8.5, above The Dalles, OR. The blue box denotes the 10 and 90 percentile changes in temperature and precipitation for all 20 scenarios. The blue lines in each box depict the median of all 20 scenarios.

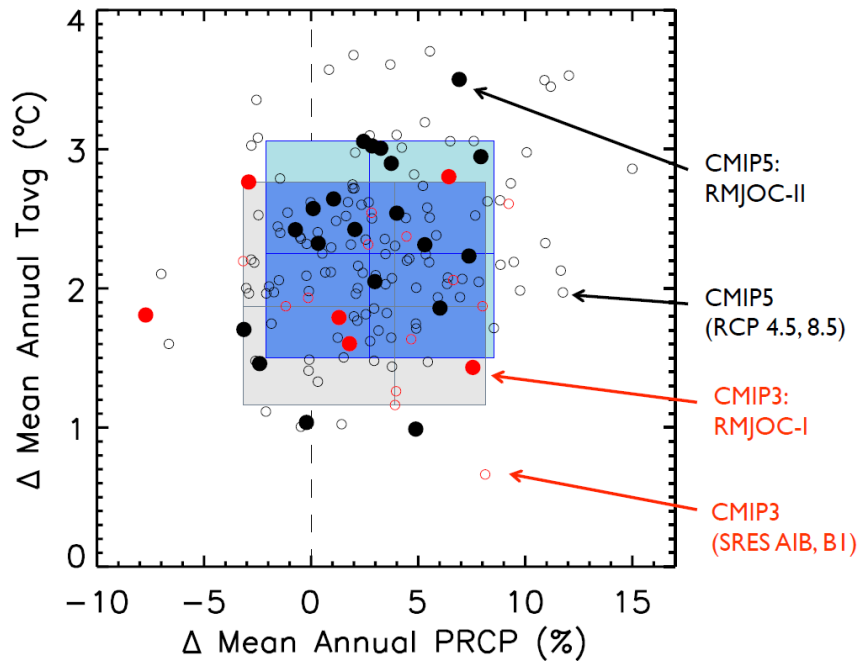


Figure 37: Comparison of annual temperature and precipitation trends between the historical period (1970-1999) and the 2040s (2030-2059) for RMJOC-I and RMJOC-II datasets. The blue box denotes the 10 and 90 percentile changes in temperature and precipitation for all GCMs available, including those not used for RMJOC studies. The gray box depicts the p10 and p90 changes in temperature (in °C) and percentage change in precipitation from CMIP-3 (2007) used for the RMJOC-I study, with the light blue box depicting p10 and p90 changes from CMIP-5 (2013) used for the RMJOC-II study. Red dots are scenarios used from the Hamlet et al. (2008) hydroclimate study for the first RMJOC study (2010). Black dots are scenarios generated for this study. The overlap between the two CMIP studies is in dark blue.

5.2 Upper Columbia River Basin Summary

For the upper Columbia Basin above Grand Coulee, WA, expected climate changes are similar to those depicted at The Dalles (**Figure 38**). Both annual and seasonal temperature increases are indicated in both RCPs used for this study. Most scenarios also project increased annual precipitation, mostly driven by increased precipitation in winter, spring, and fall, and only slightly offset by lower summer precipitation. It is worth noting that in the Canadian Columbia and Pend Oreille sub-basins, precipitation is historically substantial in June and early July, compared to the rest of the basin, which historically dries out during the early summer months. Thus, percent decreases in summer precipitation may be more significant in absolute terms compared to the rest of the Columbia Basin. However, as noted for the basin as a whole, the percentage increases in winter precipitation when it is already wet climatologically, appear to overwhelm the drier summers in terms of annual precipitation.

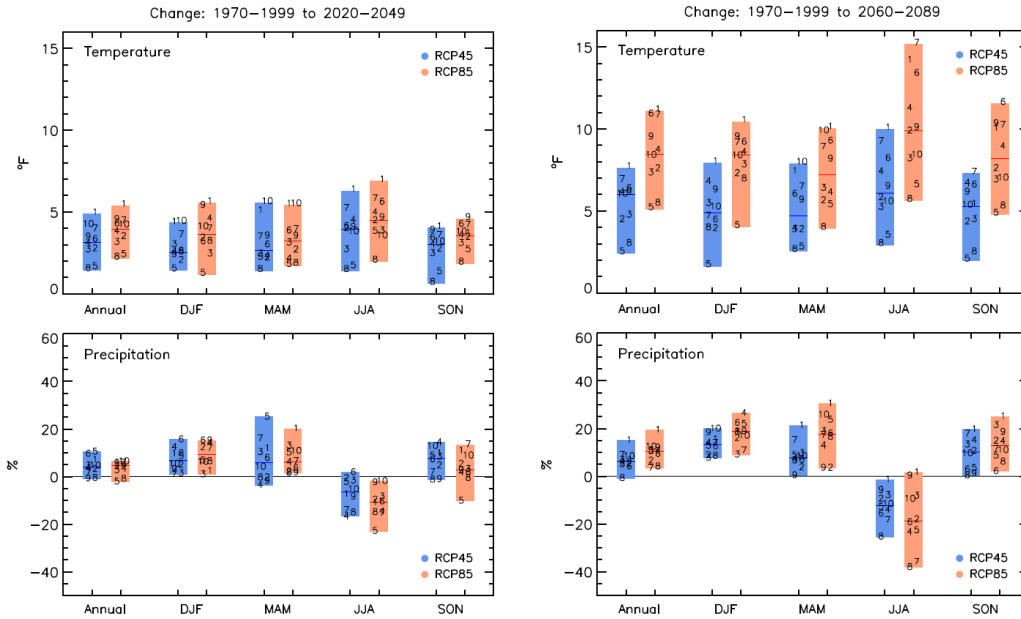


Figure 38: Basin average changes in temperature and precipitation above Grand Coulee Dam, WA, from the historical period to the 2030s (left) and 2070s (right).

5.3 Snake River Basin Summary

In contrast to the upper Columbia, a somewhat different and hydrologically important signal is apparent in the Snake River Basin. **Figure 39** shows that most scenarios used for this study project even greater warming relative to the historical period in both the 2030s and 2070s compared to the upper Columbia and Willamette basins, both seasonally and annually, and for both the spring and summer months. However, the range of expected warming is wider in the Snake Basin compared to elsewhere in the Columbia Basin, which indicates somewhat greater uncertainty. In addition, while precipitation is projected to increase in both winter and spring, a drier summer signal indicated elsewhere in the region is less certain in the Snake basin, with several scenarios indicating the potential for wetter summers. It is also important to note that some parent GCMs that are wetter in the upper Columbia Basin in both winter and spring (*e.g.*, CanESM-2 and MIROC5) are drier on a percentage basis in the Snake Basin. This means that while one GCM may be the warmest and wettest “bookend” in the upper Columbia, it may not be in the Snake Basin. This has important implications for the hydrologic scenarios one may use for hydropower planning purposes.

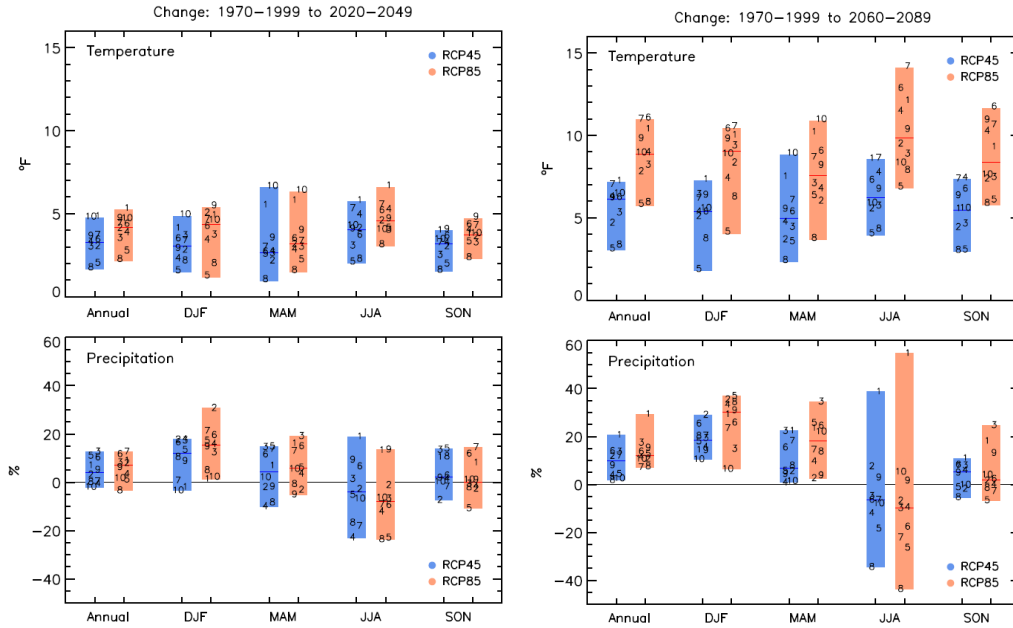


Figure 39: Same as Figure 38, except for above Lower Granite Dam, WA, for the Snake River Basin.

5.4 Willamette River Basin Summary

Consistent with the spatial analyses in **Figure 40**, the range of projected annual temperature increases in western Oregon and the west side of the Cascades is not as great as east of the Cascades on an annual basis, with a narrower range in the spring period relative to the rest of the Columbia Basin. Like the Snake Basin, the range of future precipitation changes in the spring, summer, and fall is rather wide and uncertain, with the GCMs differing on whether precipitation will increase or decrease in these seasons. Despite the spread among the models, precipitation is projected to increase in the Willamette Basin, and like the rest of the Columbia Basin, virtually all GCMs used in this study indicate increasing precipitation in the winter months, particularly in the 2070s. Unlike other parts of the Columbia Basin, temperature and precipitation projections are similar between RCP4.5 and RCP8.5 GCMs in the Willamette Basin in the 2030s, and closer to each other by the 2070s.

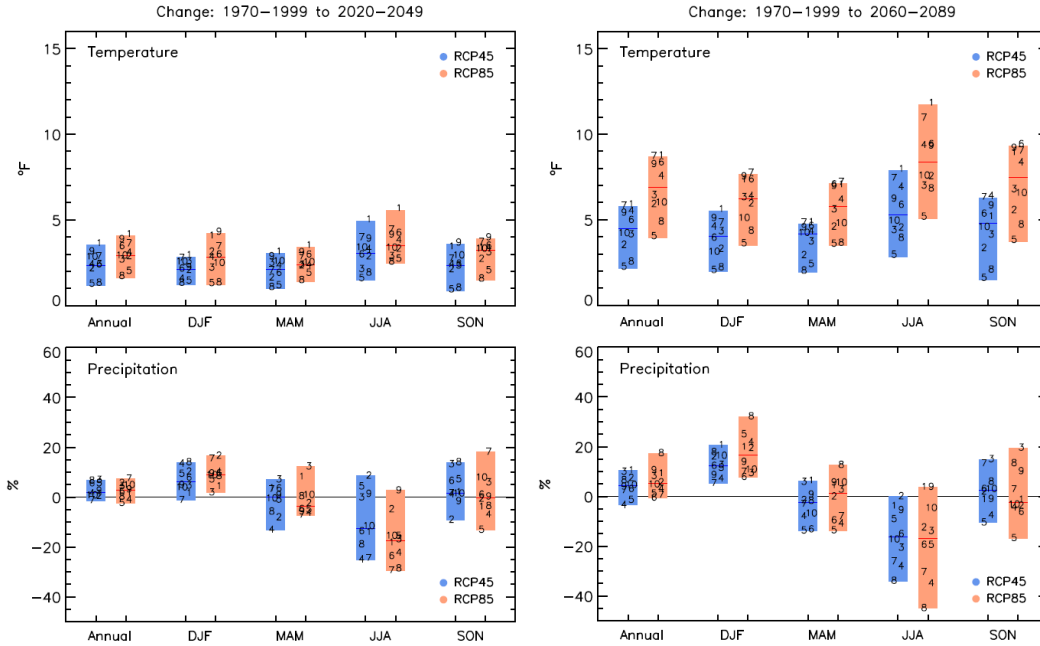


Figure 40: Same as Figure 38, except for above Willamette Falls, OR for the Willamette Basin.

5.5 Discussion

The downscaled data from the GCMs used in this study are unanimous in showing that, consistent with global and regional trends and numerous other projections, regionwide warming will continue through the 2030s under either RCP used here. Since RCP 8.5 was created to produce more warming with larger emissions than in RCP 4.5, RCP 8.5 naturally projects more warming by the 2070s than RCP 4.5.

One key difference between RMJOC-I and this study is that the former did not identify any significant precipitation trends relative to the already large inter-annual variability across the Columbia Basin. In this study, though, the GCMs selected project increasing precipitation over time, regardless of which downscaling technique is used. The precipitation changes are not likely to be seasonally uniform, with the wettest time of year in the Columbia Basin (winter) likely to become even wetter, and probably overwhelm any projected decreases in summer precipitation.

Another important consideration from this study is that while, in general, the warmest and wettest GCM outputs are generally the warmest and wettest across the entire basin, both the magnitude and rate of temperature and precipitation changes vary by sub-basin between GCMs. For example, the “least warm/driest” GCM outputs (e.g., GFDL-ESM2M) in the Canadian Columbia Basin are not necessarily the “least warm/driest” GCM in the Snake (e.g., Inmcm) or Willamette Basins (e.g., CSIRO-Mk3-6-0). *This underscores the importance of utilizing the full range of temperature, precipitation outputs, and their resulting snowpack and hydrologic outputs, to better capture the range of future hydroclimate trends.*

6.0 Cryosphere Projections

6.1 Basin Snowpack Projections

As has been indicated in many previous studies (e.g., Hamlet *et al.*, 1999; Nolin and Daly, 2006; Hamlet *et al.*, 2013) and in RMJOC-I, perhaps the greatest hydroclimate change the Columbia Basin will encounter over time will be in regional snowpack. Historically, most of the Columbia River Basin hydrologic regime has been snow-dominated, with at least half of its annual precipitation falling as snow. In the coastal drainages in lower elevations of the Cascades and Coast Ranges, most precipitation already falls as rain, but even there, winter snowpacks do develop and are an important contributor to spring and summer streamflows.

Even with the possibility of more winter precipitation, warming regional temperatures are very likely to result in declining snowpacks available to support spring and summer runoff. **Figure 41** depicts expected losses in April 1 snowpack as simulated with the VIC model for the ten GCMs downscaled using BCSD. April 1 is historically near the peak of annual winter snowpacks for most of the US portion of the Columbia Basin. By the 2020s, April 1 snow water equivalents (SWE) are projected, as averaged across these ten projections, to be between 10 and 60 percent lower in the Cascades, coastal mountains, and lower portions of the Clearwater and Spokane basins in central Idaho and eastern Washington. By the 2050s, the hydrological model simulations (based on the downscaled GCMs) indicate decreases of more than 70 percent in these same areas, and a 90 percent decrease by the 2080s.

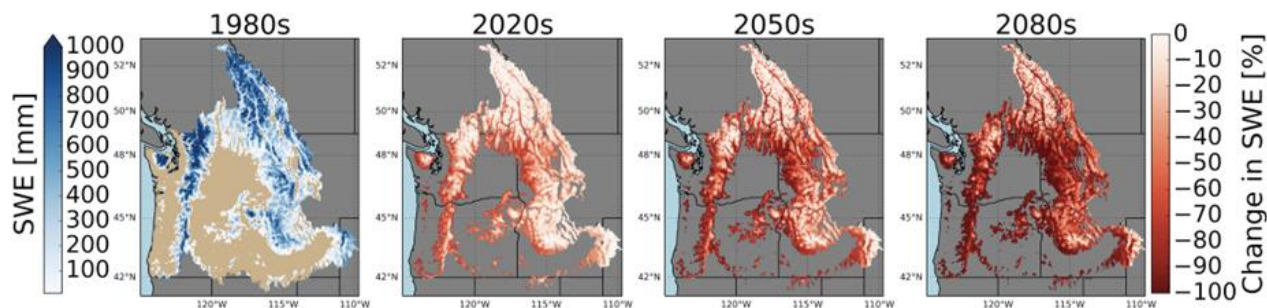


Figure 41: Columbia Basin Snow Water Equivalent (SWE) in the 1980s, and average SWE changes by the 2020s (2010-2039), 2050s (2040-2069), and 2080s (2070-2099) on April 1, for the 10 GCMs using RCP8.5 and downscaled via BCSD. Areas in tan historically have less than 10 mm of snow-water equivalent.

Figure 42 displays the 20-year running means of spatially aggregated Snow Water Equivalent (SWE) for three hydrologically distinct regions of the basin. SWE is presented as the fractional change from the historical mean of SWE for the first day of five months of the melt season. The referenced historical SWE was taken from the respective projection simulation. In the Yakima Basin (YAK), a basin with warm winters historically, the model projections indicate decreasing February-June SWE over the historical period, and in March and February as early as the 2020s. In some projections June and May SWE is entirely diminished as early as the 2060s. A similar but less extreme pattern is projected for the area upstream of Brownlee Dam (BRN). An important exception to these trends is apparent in the Canadian portion of the Columbia Basin as noted in the spread of projections for the area upstream of Arrow Lakes, BC (ARD). Because average winter temperatures in the Canadian portion of the basin are historically colder than the rest of the Columbia Basin, the degree of warming expected through the 2030s is not likely to be enough to lead to significant changes in May or June SWE until after the 2030s. Lesser impacts of warming are evident in February to April SWE later in the century. These spatially

aggregated trends clearly indicate diverse sensitivities of snowpack to warming throughout the basin.

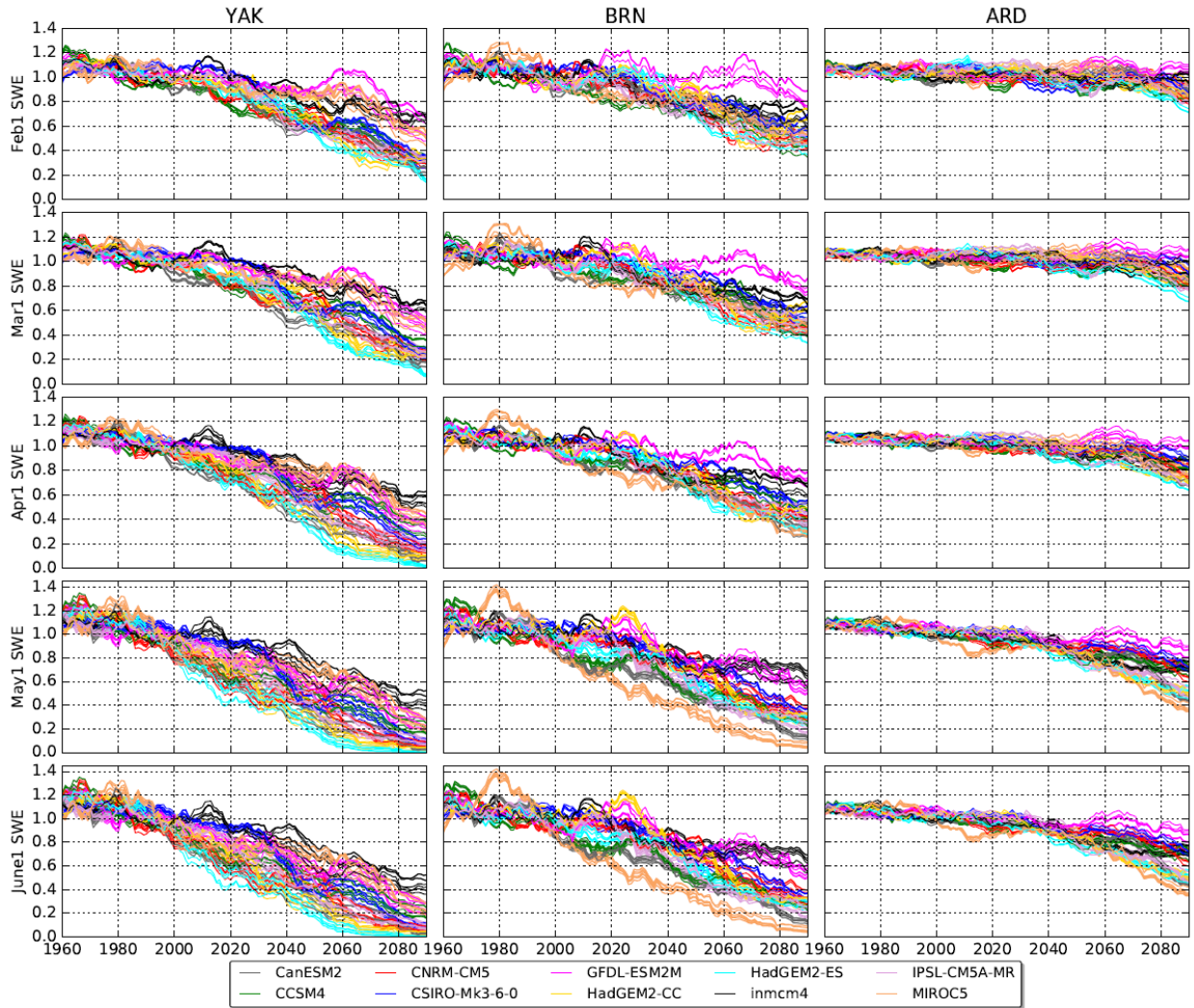


Figure 42: Fractional changes in 20-year centered mean SWE (relative to 1950-2010 mean). The SWE fields represent spatial aggregates of the areas upstream of the Yakima River at Kiowa, WA (YAK), Brownlee Dam, ID (BRN), and Arrow Lakes, BC (ARD). Each trace indicates one of the 80 RCP8.5 projections. The colors indicate the GCM used for the individual projection.

6.2 Upper Columbia Glacier Projections

As indicated in Section 4, a more explicit glacier subroutine model was developed specifically for this project, and used within each of the three VIC simulations. The representation of glaciers was not included in the PRMS model application. Thus, instead of allowing the model to build an infinite snowpack where snow fails to melt in a given year, it evolves into glacier ice which can be transferred to lower elevation zones where it is available to melt. This additional glacier melt then contributes to local runoff until cooler fall temperatures and seasonal snow arrest glacial melt until the next year. The glacier model as implemented here leverages a volume-area scaling relationship (Bahr *et al.*, 1997). This consists of a calibrated power law relationship that directly relates ice volume to ice area.

As shown in **Figure 43**, the glacier subroutine in the VIC-UW calibration accurately developed glaciers in the historical period. Blue colors indicate locations where VIC places a glacier where there was one observed. The 21 yellow grid cells indicate locations where VIC failed to simulate a glacier where there is one observed. There were no locations where VIC simulated the presence of a glacier where one did not exist in observations, so there is a lack of any red pixels in **Figure 43**. More importantly for the Upper Columbia Basin, the spatial coverage of the area's glaciers was well depicted in the main part of the Columbia Basin where summer flows have historically been maintained, and even enhanced by glacial melt during unusually hot summers.

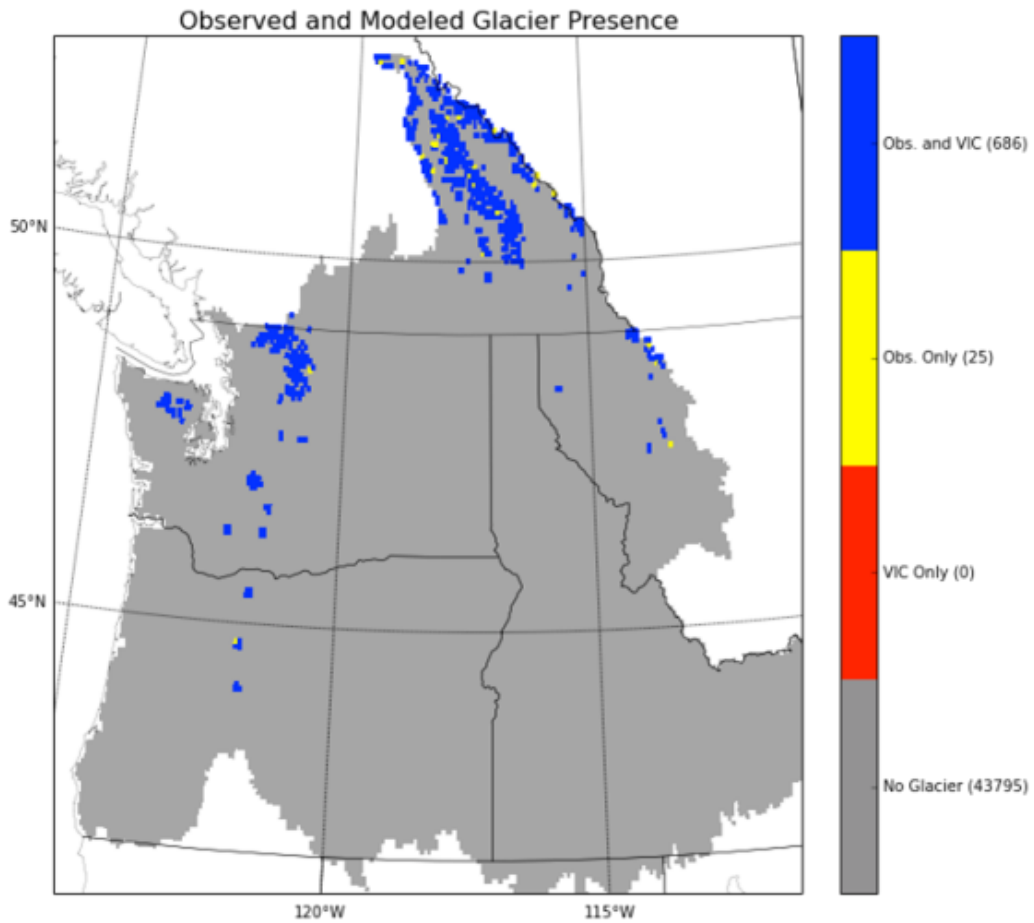


Figure 43: Comparison of observed versus modeled glacier presence in the Columbia Basin for the historical period (1976-2005).

7.0 Streamflow Projections

The bias-corrected streamflow projections generated in this study support the same three broad trends which were described in RMJOC-I, the Fourth National Climate Assessment, Volume 1 (2017), the Department of Energy 9505 Assessment (2017), and the USBR 9503 Assessment (2016). By the 2030s, the Columbia Basin will very likely experience:

- higher average winter flows,
- earlier peak spring runoff, and
- lower average summer flows, and/or a longer period of low summer flows.

By the 2070s, as temperatures continue to rise, these trends will increase in magnitude, especially if the higher RCP8.5 greenhouse gas levels are realized. The range of changes indicated by streamflow projections derived from RCP 8.5 GCMs and the two statistical downscaling techniques used for this study are shown in **Figure 44**.

However, there are projection differences depending on the methodological choices within the modeling chain, and between the different sub-basins. These differences are described in the following subsections.

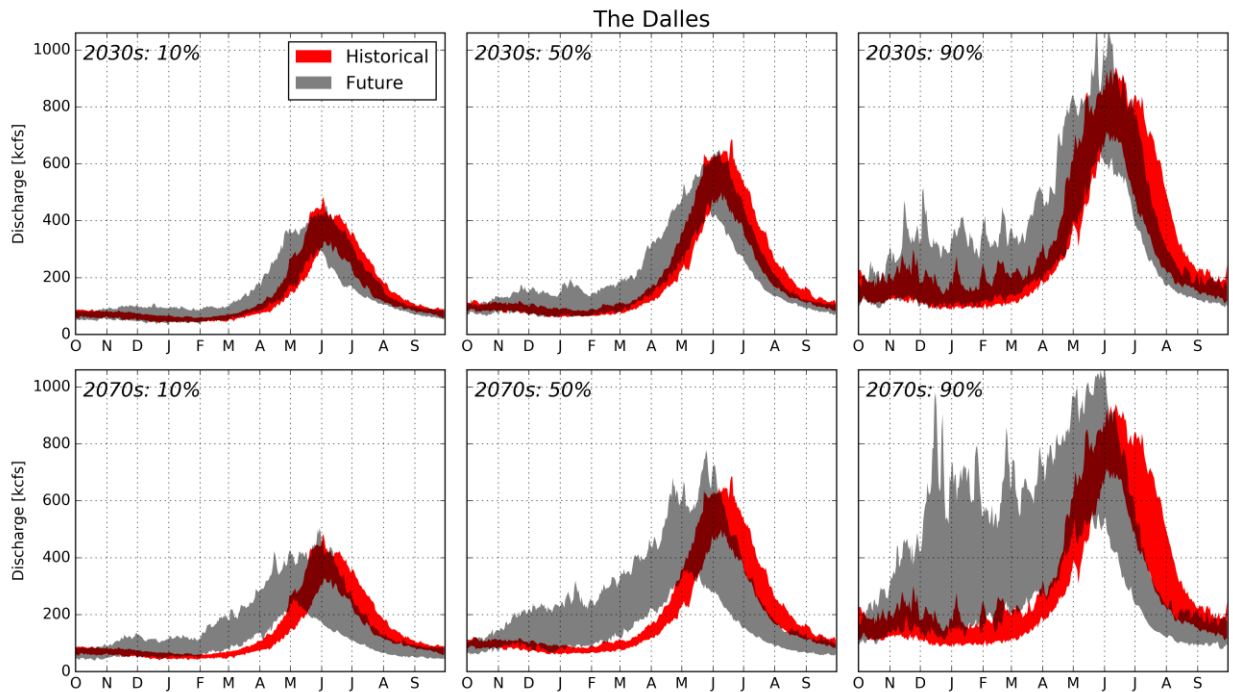


Figure 44: Range of 10/50/90 percentile flows at The Dalles, OR (TDA, Lower Columbia Basin), for each day of the water year for the historical (1976-2005) and future periods. These ranges represent the 80 statistically downscaled RCP8.5 projections.

7.1 Modeling Chain Elements Influence on Projection Spread

As hypothesized in the project design, specific and important details depicted by each streamflow projection differed from each other, at least in part, due to the methodological choices used to generate each sequence. The influence of each of the methodological elements

on the overall spread of projections was analyzed to understand sources of and magnitudes of uncertainty stemming from steps in the modeling chain.

7.1.1 Emissions Scenario

As discussed in Section 5, temperature trends between RCP4.5 and RCP8.5 are similar through the 2030s, although RCP8.5 GCMs tend to be slightly warmer in that time period, and much warmer by the 2070s. Meanwhile, precipitation trends for both RCP4.5 and RCP8.5 generally show an increase over time, particularly in the winter months. These basin trends are generally reflected in both monthly-averaged streamflows in **Figure 45 and 46** at The Dalles, OR. As early as the 2030s (WY 2020-2049), winter flow increases, spring snowmelt peaks are higher and occur earlier, and summer flows are lower, consistent with the results in RMJOC-I. These changes become more pronounced through the rest of the century, especially for the warmer RCP8.5 scenarios. By the 2070s (WY 2060-2089), average winter flow changes range from near zero to more than double the historical period (WY 1970-1999), with all RCP8.5 scenarios showing winter flow increases and July-August flow decreases by the 2070s.

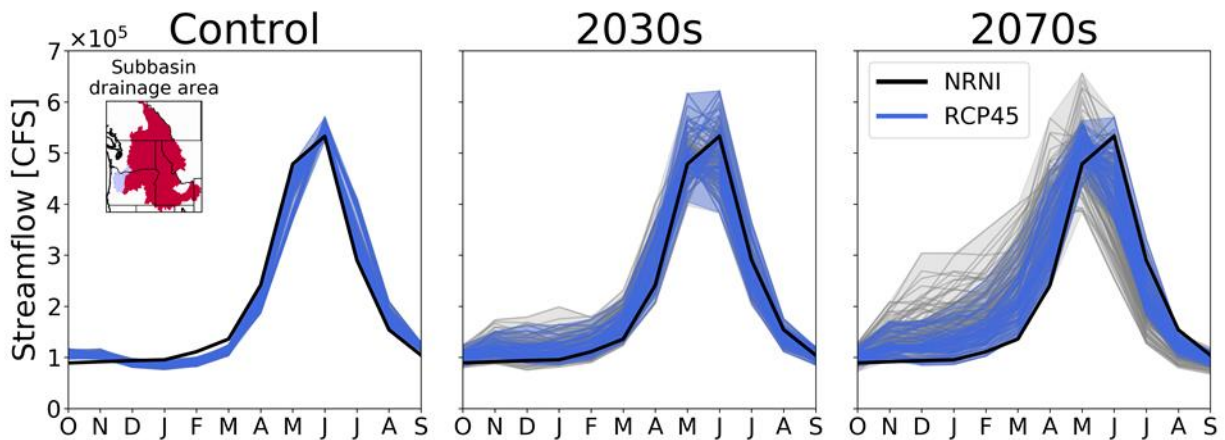


Figure 45: Average monthly flows for each streamflow scenario derived from BCSD and MACA downscaling using all GCMs and all hydrologic models, aggregated by RCP 4.5 for the Control period (WY 1951-2005), the 2030s (WY 2020-2049), and 2070s (WY 2060-2089) at The Dalles, OR.

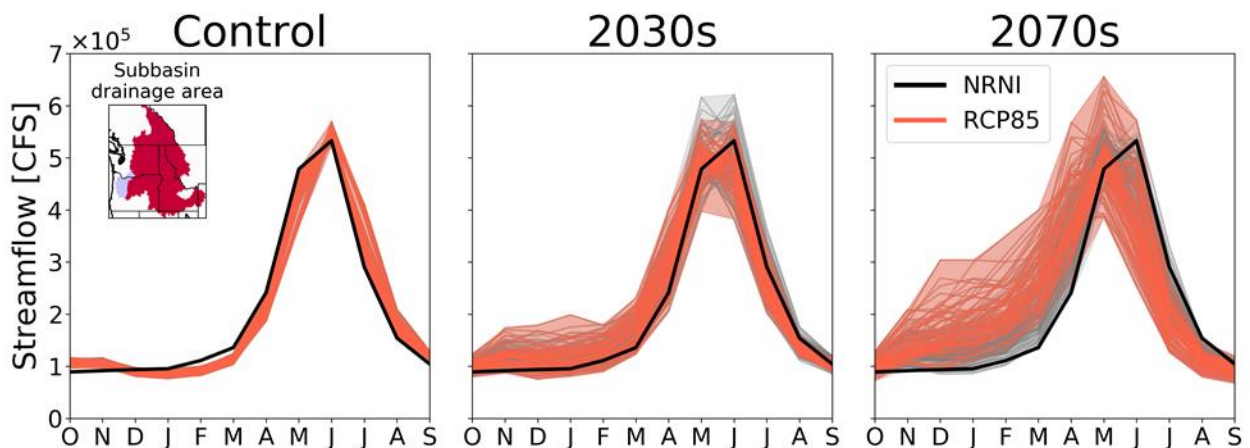


Figure 46: Same as Figure 45, but for RCP 8.5 (in red).

7.1.2 Global Climate Model

Projected average streamflow trends are mostly consistent with the temperature and precipitation trends from each GCM, as depicted in Section 5. For example, **Figure 47** shows the streamflow outcomes from the CanESM-2 GCM, which tends to be the warmest and wettest GCM used in this study, while **Figure 48** shows the outcomes from the GFDL-ESM2M GCM, which tends to be a less warm but drier GCM in this study. The choice of GCM in this case has a large impact on the shift in seasonal hydrograph. Simultaneously, however, the choice of hydrologic model can have a large impact on the projected changes in streamflow, particularly in smaller catchments (Chegwidden *et al.*, in preparation).

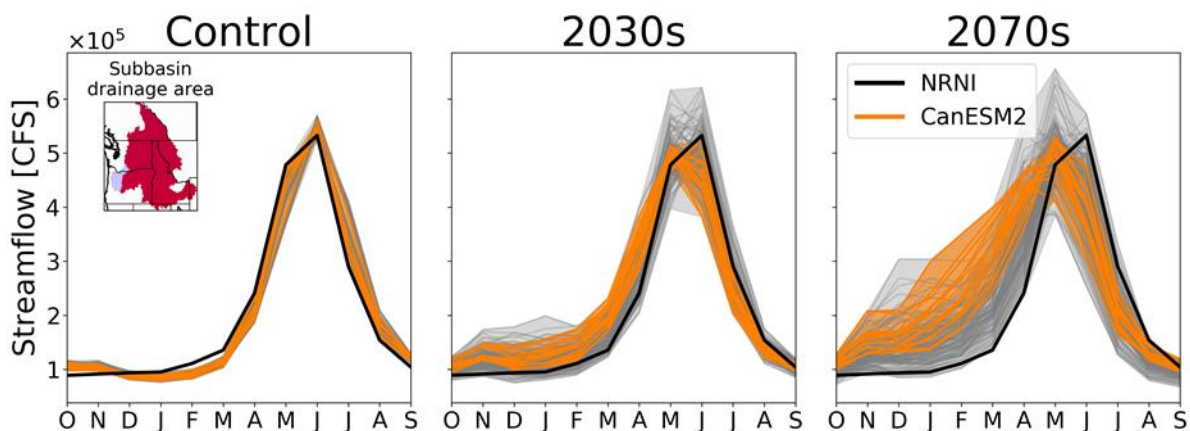


Figure 47: Average monthly flows for each streamflow scenario (gray), aggregated by GCM CanESM-2 (in orange), derived from both RCP4.5 and RCP8.5, for BCSD and MACA downscaling, and all hydrologic models for the Control period (WY 1951-2005), the 2030s (WY 2020-2049), and 2070s (WY 2060-2089) at The Dalles, OR.

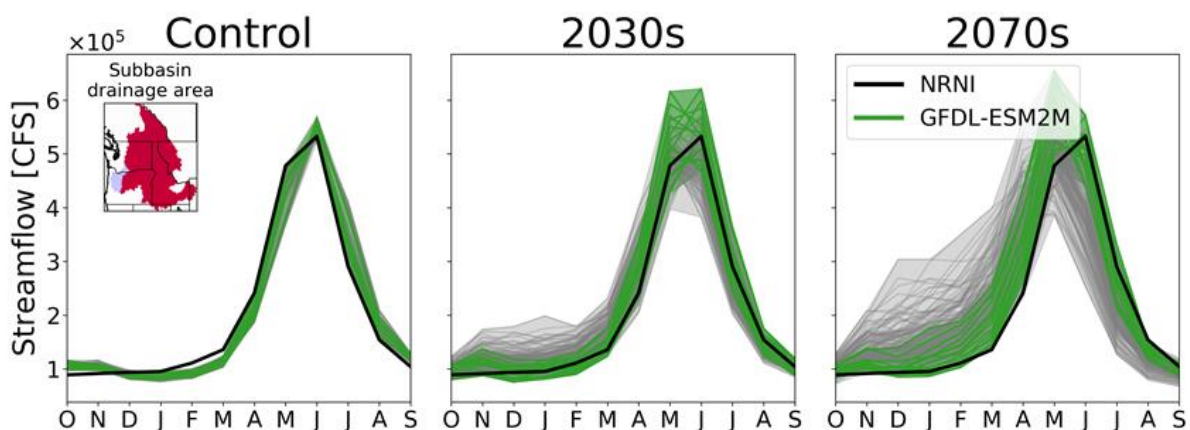


Figure 48: Same as Figure 47, but for GCM GFDL-ESM2M (in green).

For a somewhat different view, **Figure 49** shows day-averaged flows for each GCM, but for a single RCP (8.5) for the analysis periods planned for subsequent hydropower studies (2030s and 2070s). In general, the warmer the GCM, the more runoff timing tends to shift earlier in the year. Also in general, the wetter the GCM, the more flows and volumes increase in the winter, spring, and annually.

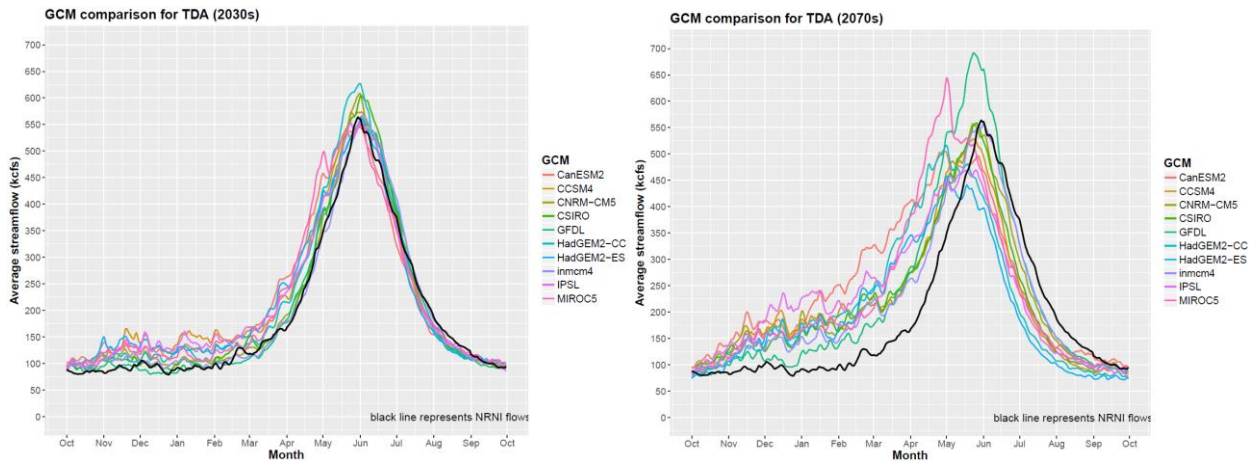


Figure 49: Day-average streamflows (in kcfs), by climate model, for RCP 8.5, BCS and MACA downscaling, for all four hydrologic model sets, at The Dalles, OR. Black line is the historical NRNI average (1976-2005). Left is for the 2030s (2020-2049). Right is for the 2070s (2060-2089).

These differences can be amplified at upstream locations. As discussed in Section 5, the GCMs used for this study show the greatest spread in both temperature increases and precipitation changes in the Snake Basin, which leads to greater spread in projected volume and flow changes. For example, average flows derived from the less warm and drier GCMs in this basin (inmcm4 and GFDL-ESM2M), result in slightly lower projected winter and early spring flows by the 2030s, while warmer and wetter GCMs like CanESM2 and MIROC5 show higher winter flows, and spring flow peaks shifting as much as a month earlier by the 2030s relative to the historical period (Figure 50).

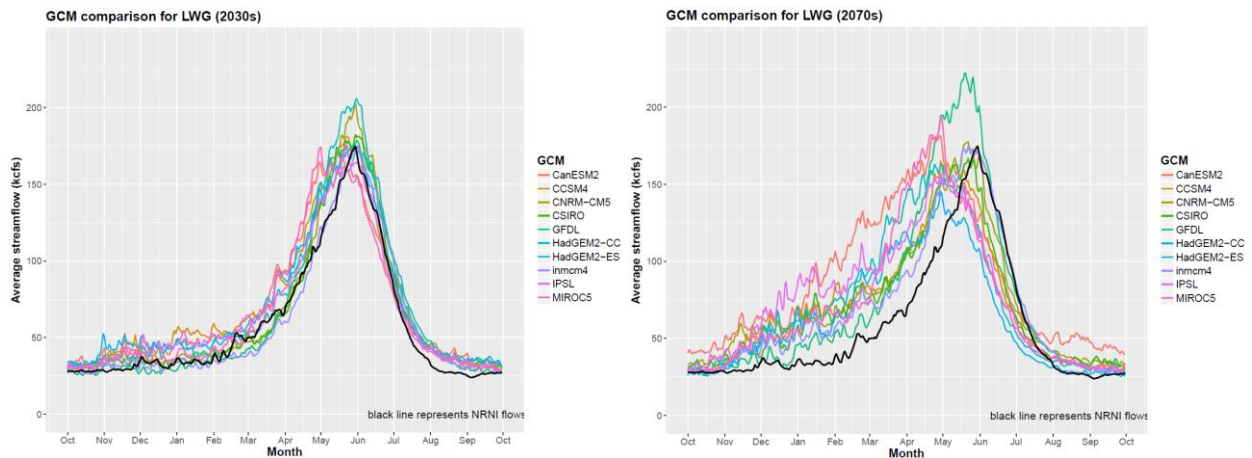


Figure 50: Same as Figure 49, but for Lower Granite Dam, WA. Left is for the 2030s (2020-2049). Right is for the 2070s (2060-2089).

7.1.3 Downscaling Technique

These streamflow trends are consistent and rather similar between downscaling methods. Figures 51 and 52 compare results for both BCS and MACA downscaling for both RCP4.5 and RCP8.5 and for all GCMs. At The Dalles, OR, a few scenarios derived from BCS-downscaled data show a tendency for higher winter flows compared to MACA. However, by and large, the two statistical downscaling methods tended to yield similar results on a large basin level and

multi-decadal averages. Analyses to this point have not assessed the extent to which the selection of downscaling method impacts the frequency or magnitude of extreme high- or low-flow events.

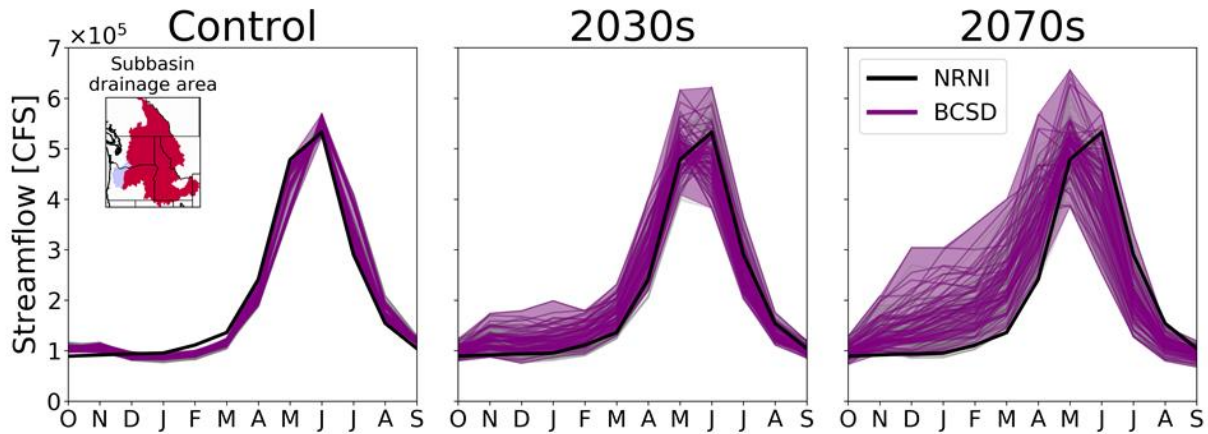


Figure 51: Average monthly flows for each streamflow scenario (gray), aggregated by the BCSD downscaling (in purple), derived from both RCP 4.5 and 8.5 for all GCMs, and all hydrologic models for the control period (WY 1951-2005), the 2030s (WY 2020-2049), and 2070s (WY 2060-2089) at The Dalles, OR.

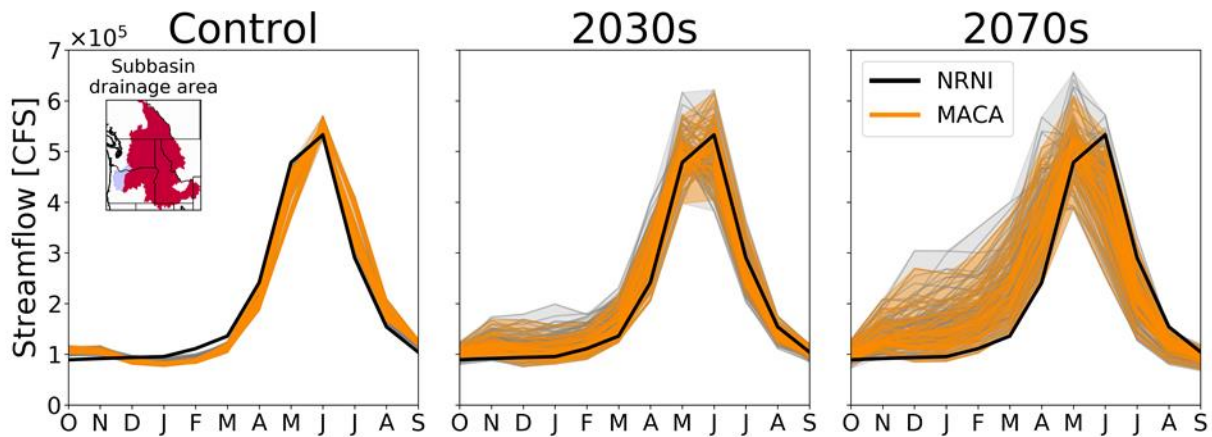


Figure 52: Same as Figure 51, but for MACA (in orange).

There are significant streamflow differences, however, between those derived from statistically downscaled projections, and the 12 RCP8.5 streamflow scenarios derived from the ORNL hybrid dynamical-statistical downscaling method. **Figure 53** shows that even in the historical period, the hybrid downscaled flows from the CCSM4, GFDL-ESM2M, and MIROC5 GCMs were much higher in winter compared to their BCSD and MACA downscaled counterparts and to NRNI historical flows. One potential driver contributing to this difference is suspected to result from different observation data sets used by two approaches. While both BCSD and MACA are based on Livneh *et al.* (2013), which is also used by UW-VIC calibration, the ORNL hybrid projection uses multiple different background temperature and precipitation datasets (PRISM, Daymet, and Hamlet). This difference would affect the magnitude of downscaled data and further the simulated streamflow. There are other possible causes for these large differences; however,

these could not be fully explored and diagnosed from the final set of outputs from the hybrid dynamical-statistical downscaling products available. Given the large differences in flows relative to NRNI flows in the historical period, the streamflow scenarios derived from the ORNL hybrid downscaling in this particular study should be used with caution in the context of regional hydroclimate studies.

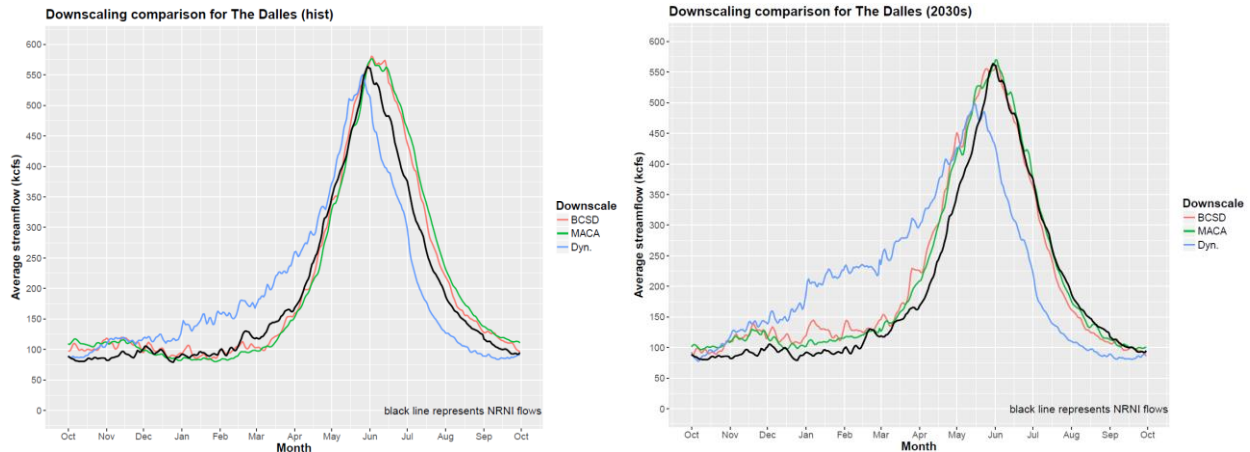


Figure 53: Day-average streamflows (in kcfs), by BCS, MACA, and ORNL Dynamical-Hybrid downscaling, from CCSM4, GFDL-ESM2m, and MIROC5 GCMs, for RCP 8.5, at The Dalles, OR. Solid black line is the historical NRNI average (1976-2005). Left is for the historical period (1976-2005). Right is for the 2030s (2020-2049).

7.1.4 Hydrological Model and Parameterizations

Although the overall trends in future streamflow timing are similar across hydrologic models and parameter sets, somewhat different outcomes are apparent between them. These differences also tended to vary by sub-basin, which is described in subsequent sub-basin overviews. For the Columbia Basin as a whole, the UW-VIC (**Figure 54**) and PRMS (**Figure 55**) scenarios tend to more closely reflect NRNI flows in the historical period, which is expected since these parameter sets were calibrated to NRNI historical flows, while ORNL-VIC (**Figure 56**) and NCAR-VIC (**Figure 57**) flows used different historical flows for their calibrations. Additionally, NCAR-VIC and ORNL-VIC were calibrated using different meteorological forcing (**Table 9**, in Section 4.4.4). Meteorological forcing data can have a strong influence on calibrated parameters, as the parameters will adjust to compensate for any underlying biases in the meteorological data in order to capture the hydrological mass balance represented with streamflow volumes. While all four hydrologic model sets have similar timing trends through the 21st century, ORNL-VIC and NCAR-VIC streamflows tend to exhibit the increases in winter and early spring flows later in the century compared to the other calibrations. This slight trend is also apparent when flows from each hydrologic model set are averaged by day (**Figure 58**). In this comparison, flows from UW-VIC and PRMS show slightly larger increases in winter flows as the 21st century proceeds, compared to flows generated from the ORNL and NCAR VIC parameter sets. While the multi-year averaged streamflow differences between hydrologic models and their calibrations are noteworthy, at large locations they are generally smaller than the differences imposed by GCM forcings, but larger than differences in the downscaling methods used in this study (with the important caveat involving the ORNL hybrid downscaling results). Choice of hydrologic model can have a large impact on projections at smaller locations or with analysis of more specific metrics like low flows (Chegwiddden *et al.*, in preparation).

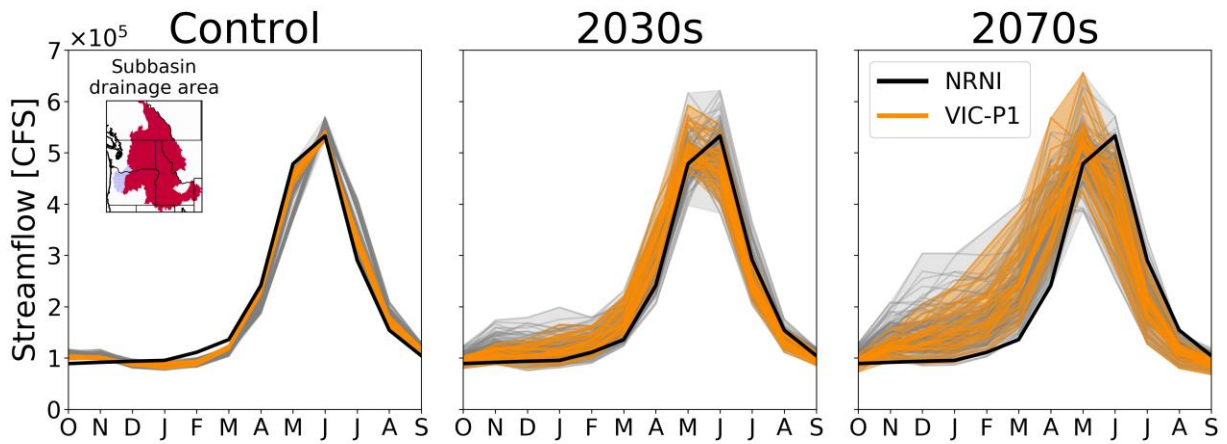


Figure 54: Average monthly flows for each streamflow scenario (gray), aggregated by the VIC calibration from UW (P1, in orange), derived from both RCP4.5 and RCP8.5, for BCS and MACA downscaling, for the Control period (WY 1951-2005), the 2030s (WY 2020-2049), and 2070s (WY 2060-2089) at The Dalles, OR.

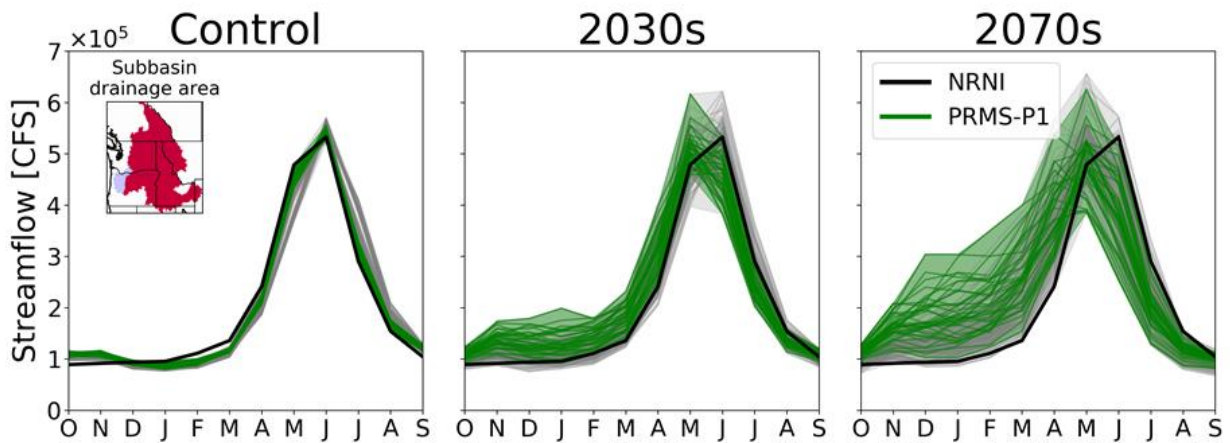


Figure 55: Same as Figure 54, expect for PRMS calibration from UW (P1, in green).

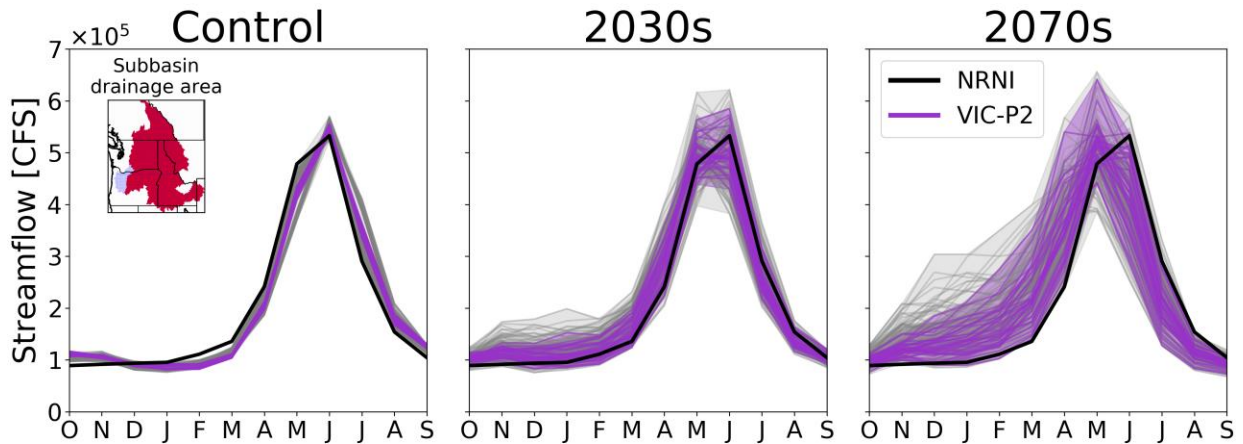


Figure 56: Same as Figure 54, expect for VIC calibration from ORNL (P2, in purple).

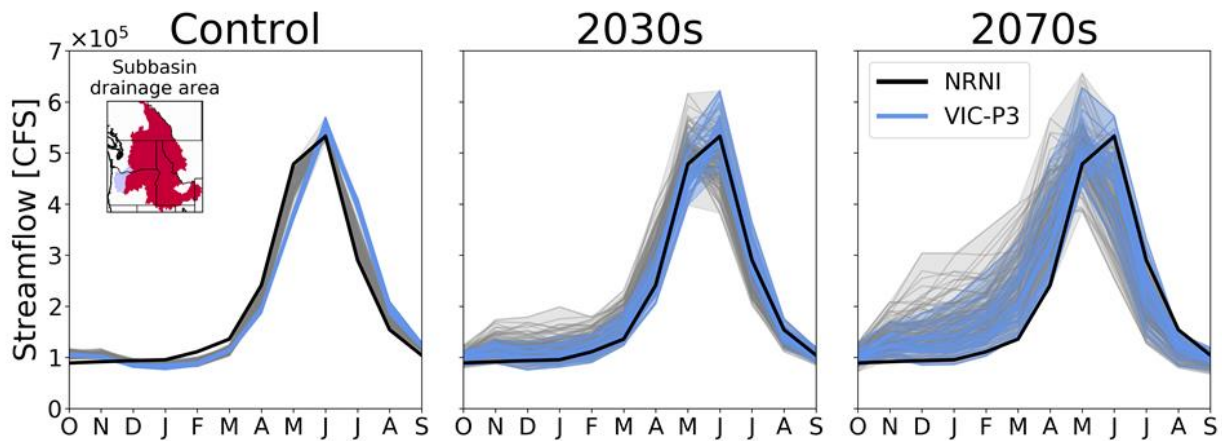


Figure 57: Same as Figure 54, except for VIC calibration from NCAR (P3, in blue).

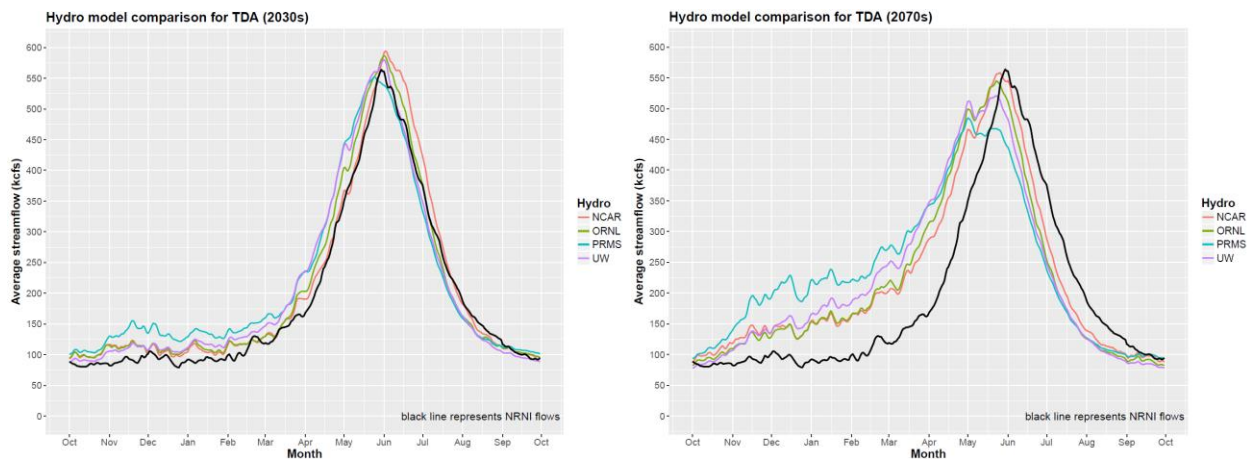


Figure 58: Day-averaged streamflows (in kcfs), by hydrologic model set, for all RCP 8.5 GCMs, BCS and MACA downscaling, at The Dalles, OR. Black line is the historical NRNI average (1976-2005). Left is for the 2030s (2020-2049). Right is for the 2070s (2060-2089).

The different hydrologic models and parameter sets produce notable differences in their resulting streamflow projections in some of the upstream basins. For example, in the Upper Columbia for most scenarios, particularly those generated with UW-VIC, July and August streamflows are projected to decline by the 2030s, which is historically the time of year when glacier melt is an important contributor to flows in this portion of the basin. Because the VIC simulations (as opposed to the PRMS simulation) also include a glacier subroutine, it was hypothesized that at least for these scenarios, late summer flows would not decrease for some time. However, averaged VIC flows in the historical period show much lower summer flows relative to both the historical period and the other hydrologic model calibrations. By the 2030s, though, regardless of hydrologic model and whether they treat glaciers as ice or permanent snowpack, averaged flows for all 10 GCMs show sizeable decreases in mid-July through mid-September flows relative to the historical period (Figure 59).

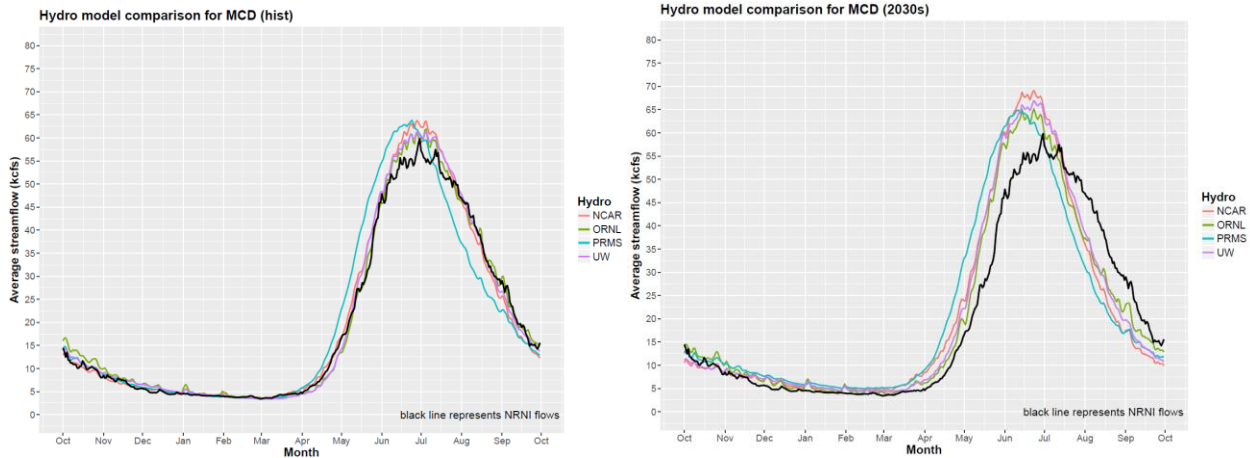


Figure 59: Day-averaged streamflows (in kcfs) by hydrological model set, for all RCP8.5 GCMs, BCS and MACA downscaling, at Mica Dam, BC. Black line is the historical NRNI average (1976-2005). Left are the averaged flows in the 1976-2005 historical period. Right is for the 2030s (2020-2049).

7.2 Streamflow Projections

The analysis and discussion in the above section sets the stage for further demonstration of the spread of projections throughout the basin. In the subsequent sections, the spread of projections presented represents 80 streamflow projections from the RCP8.5 emissions pathway scenario, the two statistical downscaling techniques, and four hydrological modeling approaches.

7.2.1 Basinwide Projections

The general tendency for precipitation to increase in the Columbia Basin, particularly in the already wet winter months, is reflected in future annual and seasonal volume projections (Section 5.1.2). **Figure 60** shows the mean of expected volume change and amount by location (and by the size of each circle) for each location. Not only do the projections show average increases, but agreement among the 80 streamflow projections is rather high, regardless of downscaling technique or hydrologic model (**Figure 61**). The largest increases, averaged across the RCP 8.5 ensemble, are indicated in the middle Snake Basin. However, as noted by circle size, annual volumes in this part of the basin are smaller compared to the mainstem Columbia Basin below Grand Coulee. The spread in annual volume projections is also larger in the Snake Basin compared to other parts of the region (**Figure 62**). The largest disagreement in annual volume change is noted in the Kootenay Basin of northwest Montana and southern British Columbia, and in a few of the tributaries originating in the Washington Cascades. However, the flow volume represented by these drainage areas is small compared to other parts of the Columbia basin.

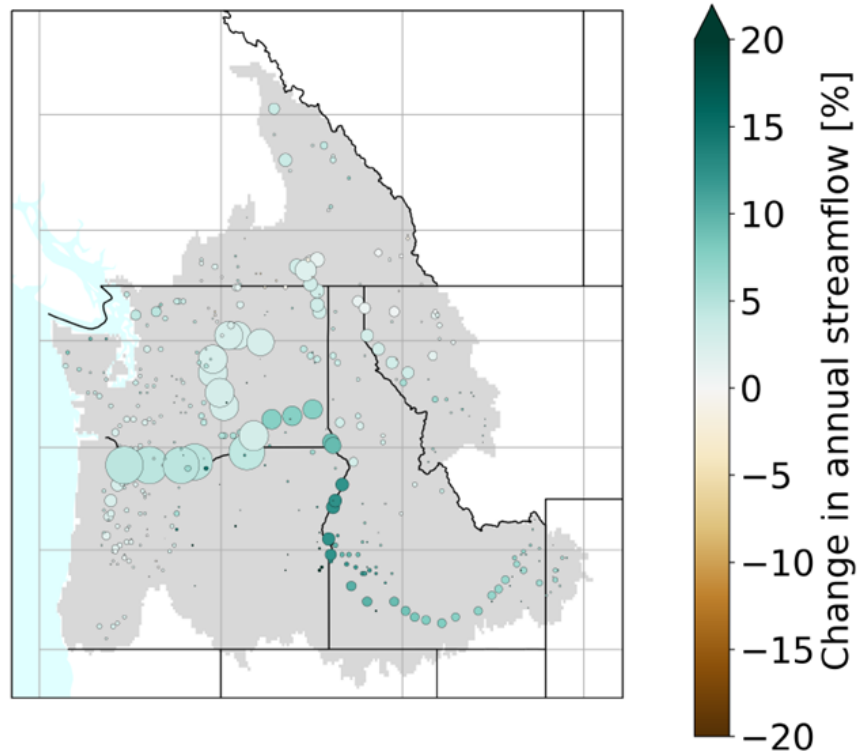


Figure 60: Percent change in annual volume from the historical period (1976-2005) for the 2030s (2020-2049), averaged for the 10 RCP8.5 GCMs used for this study, and using BCS and MACA downscaling. Each circle is an NRNI control point, with circle size denoting relative annual volumes in the historical (1976-2005) period.

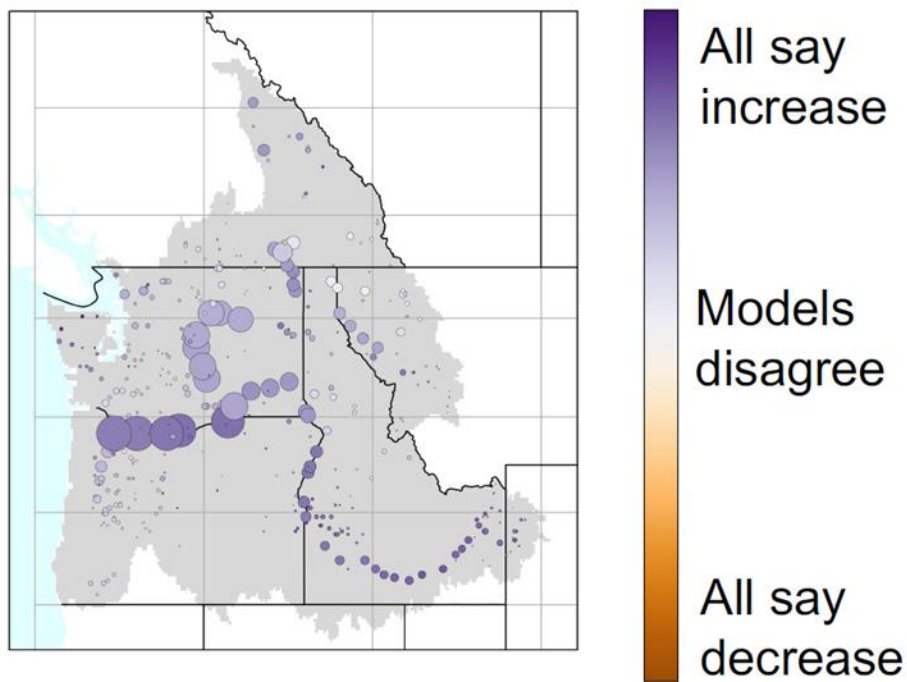


Figure 61: Generalized depiction of scenario agreement for annual volume changes from the historical period (1976-2005) and the 2030s (2020-2049), averaged for the 10 RCP8.5 GCMs used for this study, and using BCS and MACA downscaling. Each circle is a NRNI control point, with circle size denoting relative annual volumes in the historical (WY 1970-1999) period.

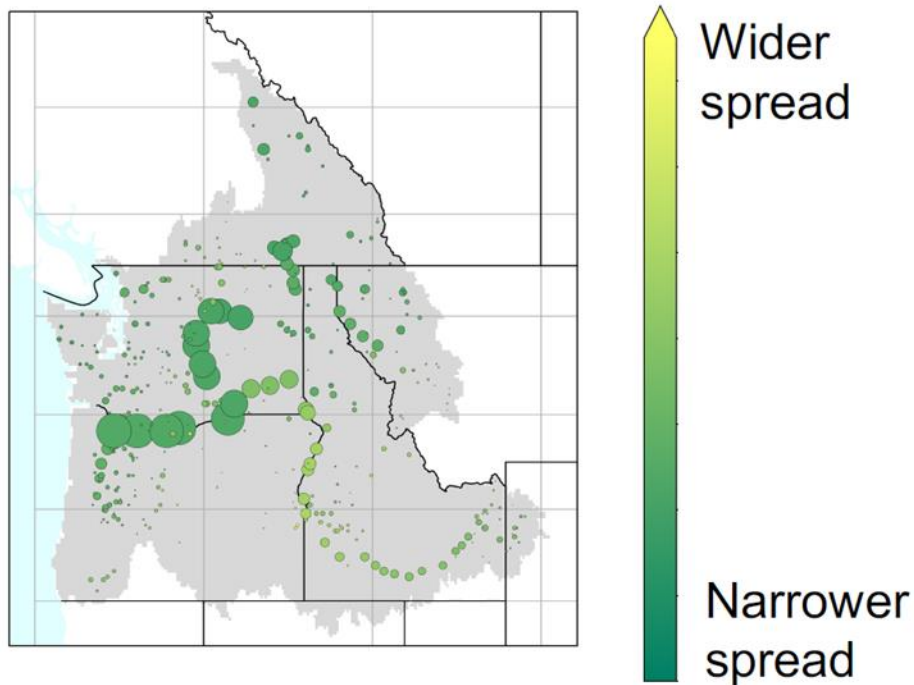


Figure 62: Generalized depiction of scenario spread for annual volume changes from the historical period (1976-2005) and the 2030s (2020-2049), averaged for the 10 RCP8.5 GCMs used for this study, and using BCSD and MACA downscaling. Each circle is an NRNI control point, with circle size denoting relative annual volumes in the historical (1970-1999) period.

Consistent with precipitation trends noted in Section 5, changes in volume are concentrated by season, with higher winter and spring volumes, and generally lower summer volumes (mostly driven by lower June and July volumes) (**Figure 63**). The relative scenario agreement and spread is also depicted in **Figures 64 and 65**, respectively. There are important timing exceptions outside of the Columbia Basin, particularly in tributaries fed by the west side of the Cascades and the Oregon and Washington coastal mountains. For example, while most of the scenarios indicate higher spring flows in the Columbia Basin, there is a tendency toward lower spring flows in the Willamette Basin and some coastal drainages. Also note that while there is a large amount of agreement in higher winter flows in the Columbia Basin, the spread between scenarios is also quite large, with large spreads also noted in the spring months in Canada and the upper Snake Basin. Finally, despite most GCMs showing drying across the Columbia Basin by the 2030s (see Section 5), some disagreement in summer and especially fall flows is noted in the Snake Basin, where less than half of the scenarios show the possibility of increased summer and fall streamflows.

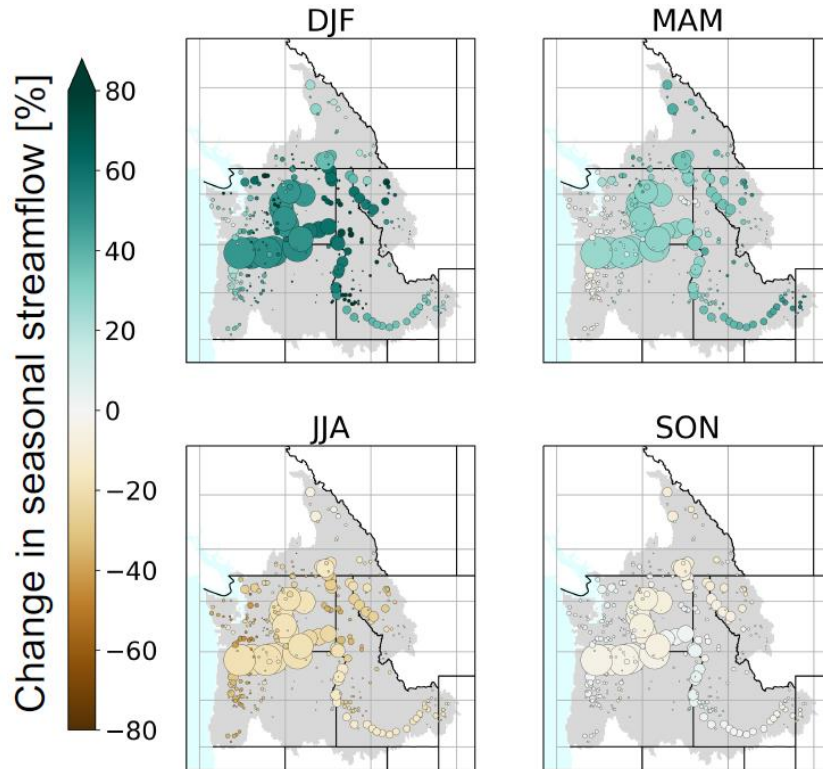


Figure 63: Same as Figure 60, but by season (DJF: December-February/Winter; MAM: March-May/Spring; JJA: June-August/Summer; SON: September-November/Fall).

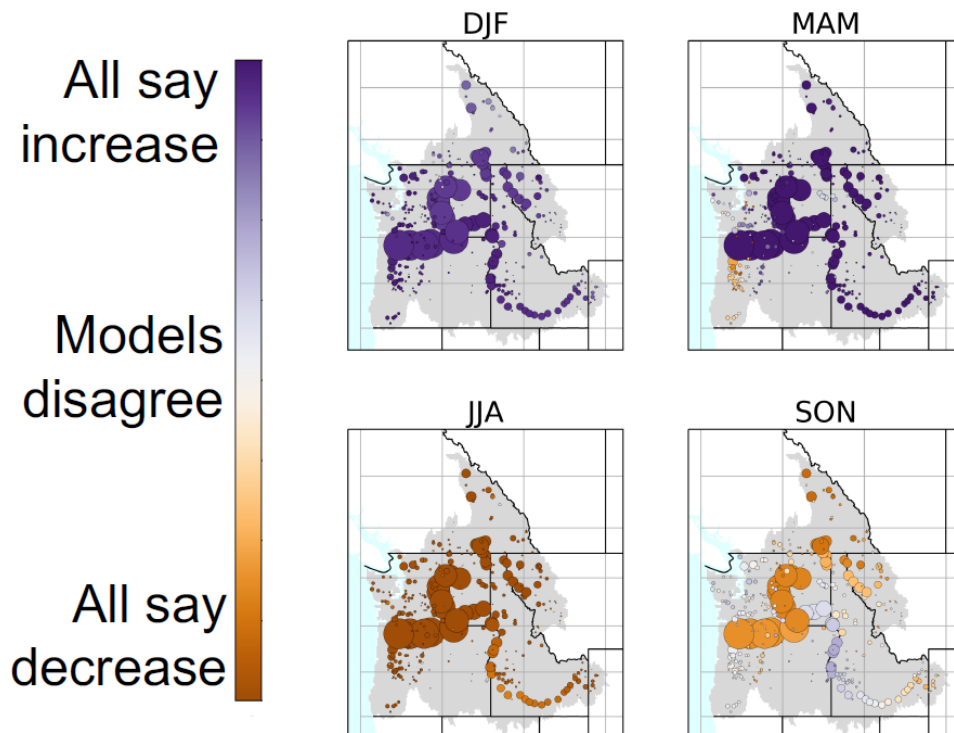


Figure 64: Same as Figure 61, but by season (DJF: December-February/Winter; MAM: March-May/Spring; JJA: June-August/Summer; SON: September-November/Fall).

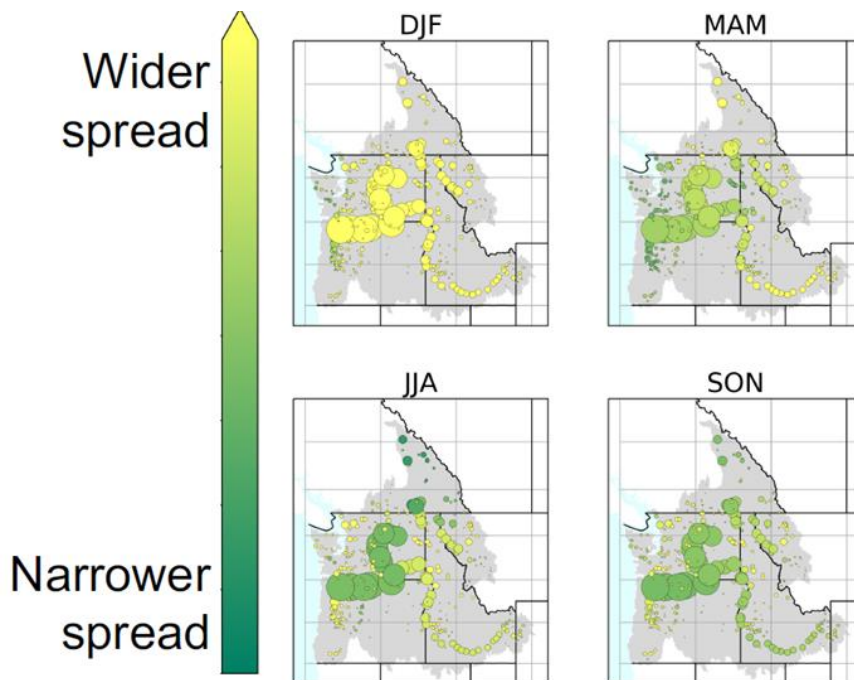


Figure 65: Same as Figure 62, but by season (DJF: December-February/Winter; MAM: March-May/Spring; JJA: June-August/Summer; SON: September-November/Fall).

In summary, for the Columbia Basin as a whole, increasing basin temperatures are very likely to result in higher winter flows and earlier spring flow peaks later in the 21st century according to the hydrologic model simulations. Moreover, warming temperatures will likely result in either slightly lower summer flows as a whole, or a longer period of low summer flows. This overall outcome is projected almost universally by the 172 streamflow scenarios, regardless of which representative concentration pathway, climate model, downscaling technique, or hydrologic model is used. However, the details of this overall evolution vary depending on the different model and methodological choices. In many cases, the differences are substantial and indicate that subsequent hydroclimate planning studies using this dataset should explore and understand the differences in model spread.

Although the signal is not as pronounced, there is a general tendency for increasing annual volumes over time, with the largest increases in the winter offsetting decreases in summer volumes. However, there are some spatial and seasonal differences in this tendency, particularly in the Snake and Willamette basins, which are discussed below.

7.2.2 Upper Columbia, Kootenai, and Pend Oreille River Basins

This northernmost part of the Columbia Basin includes the mainstem Columbia in British Columbia, and the Kootenai River, a large tributary draining southeast British Columbia. In this part of the basin alone, the streamflow projections show modest change well into the 21st century, in large part because precipitation in all but the lowest valleys will continue to fall as snow for some time. Even here, though, spring and early summer streamflow changes are noted in **Figures 66 to 68**. Some of the projections indicate higher spring freshet peaks, which tend to occur one or two weeks earlier by the 2030s as precipitation increases in this part of the basin and the climate warms. Decreasing summer volumes are pervasive throughout these basins.

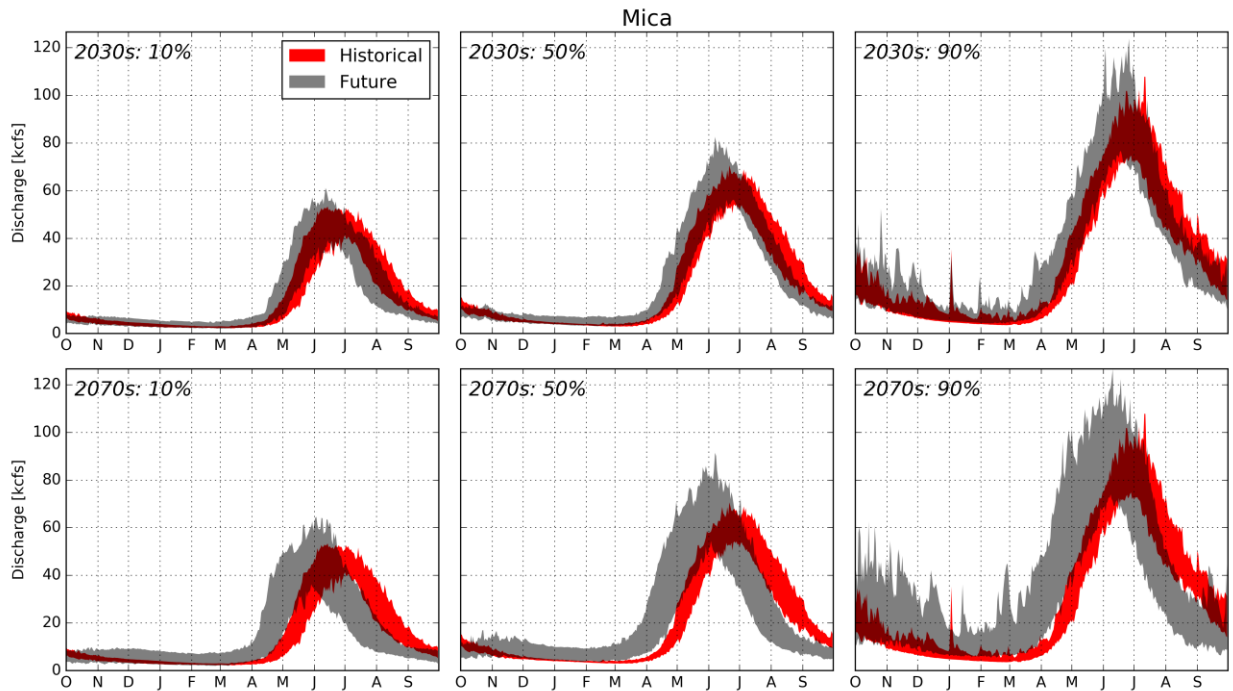


Figure 66: Range of 10/50/90 percentile flows at Mica, BC (MCD, Upper Columbia Basin), for each day of the water year for the historical (1976-2005) and future periods 2030s (WY 2020-2049) and 2070s (WY 2060-2089). These ranges represent the 80 statistically downscaled RCP8.5 projections.

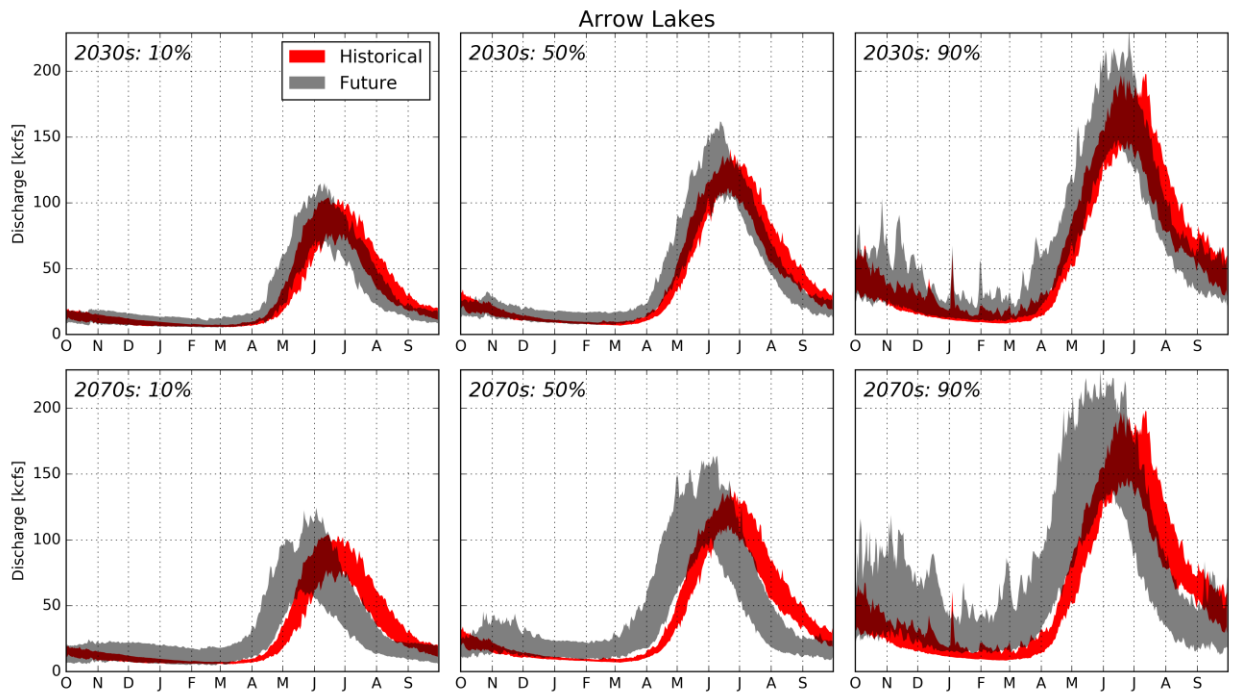


Figure 67: Same as Figure 66, except at Arrow Lakes, BC (ARD, Upper Columbia Basin).

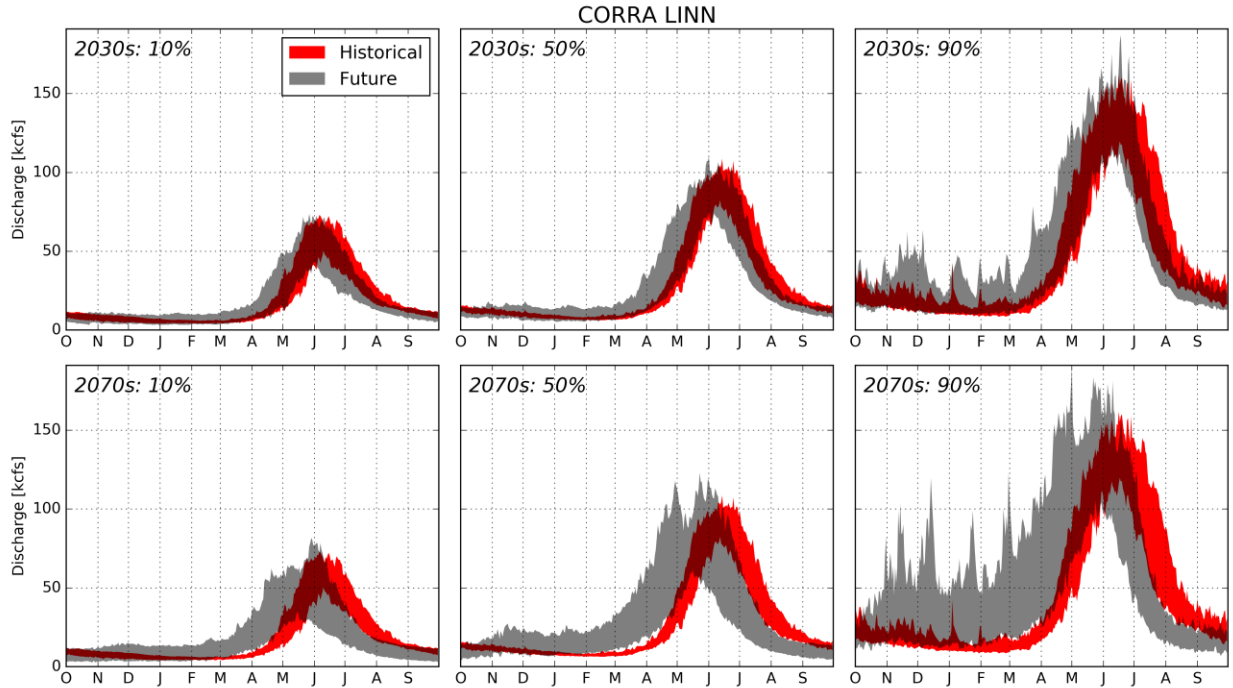


Figure 68: Same as Figure 66, except for Corra Linn, BC (COR, Kootenay Basin).

The Pend Oreille River starts in Western Montana with tributaries of the Clark Fork and Flathead Rivers. The river flows through Northern Idaho, eastern Washington and enters the Columbia mainstem above Grand Coulee near the border with Canada. At the headwater, changes in inflows to Hungry Horse Dam are relatively modest by the 2030s, with slightly earlier timing and intensified high flows in winter and early spring (**Figure 69**). In the 2070's, the freshet occurs earlier, and some projections indicate higher freshet peaks. Winter and early spring flows increase substantially, and summer flows decrease. These patterns translate downstream with increased intensification on winter extreme flows earlier in the century (**Figure 70 and 71**).

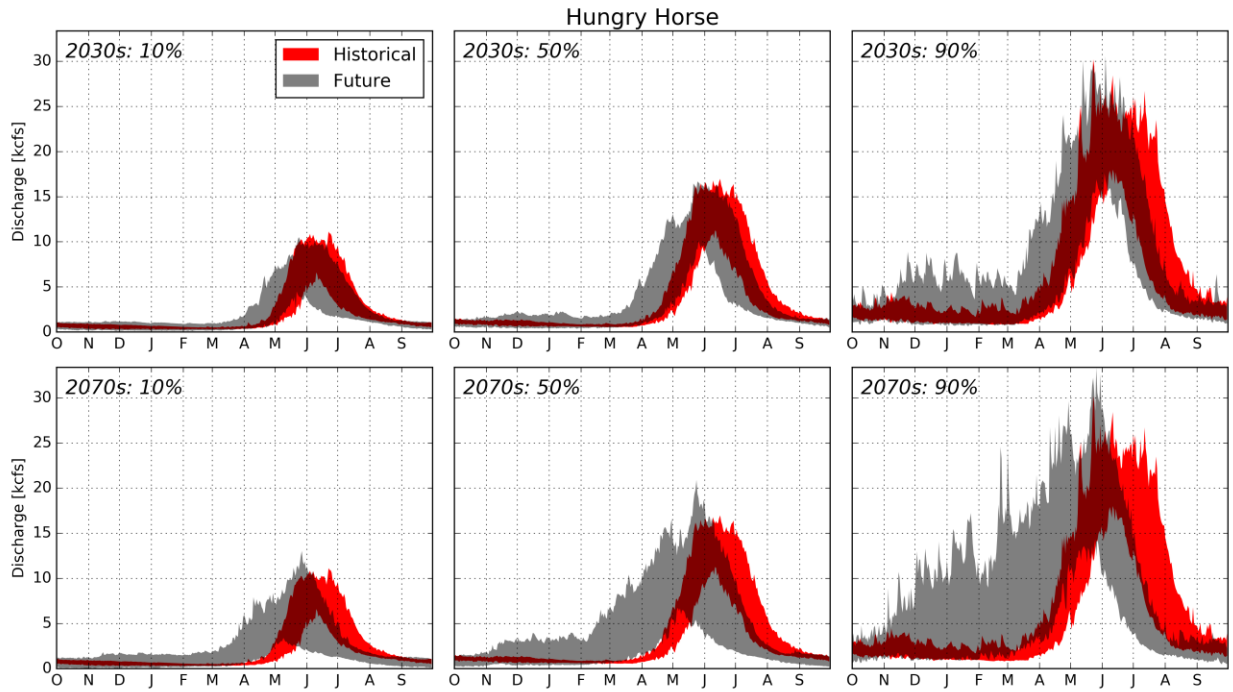


Figure 69: Same as Figure 66, except at Hungry Horse Dam, MT (HGH, Flathead Basin).

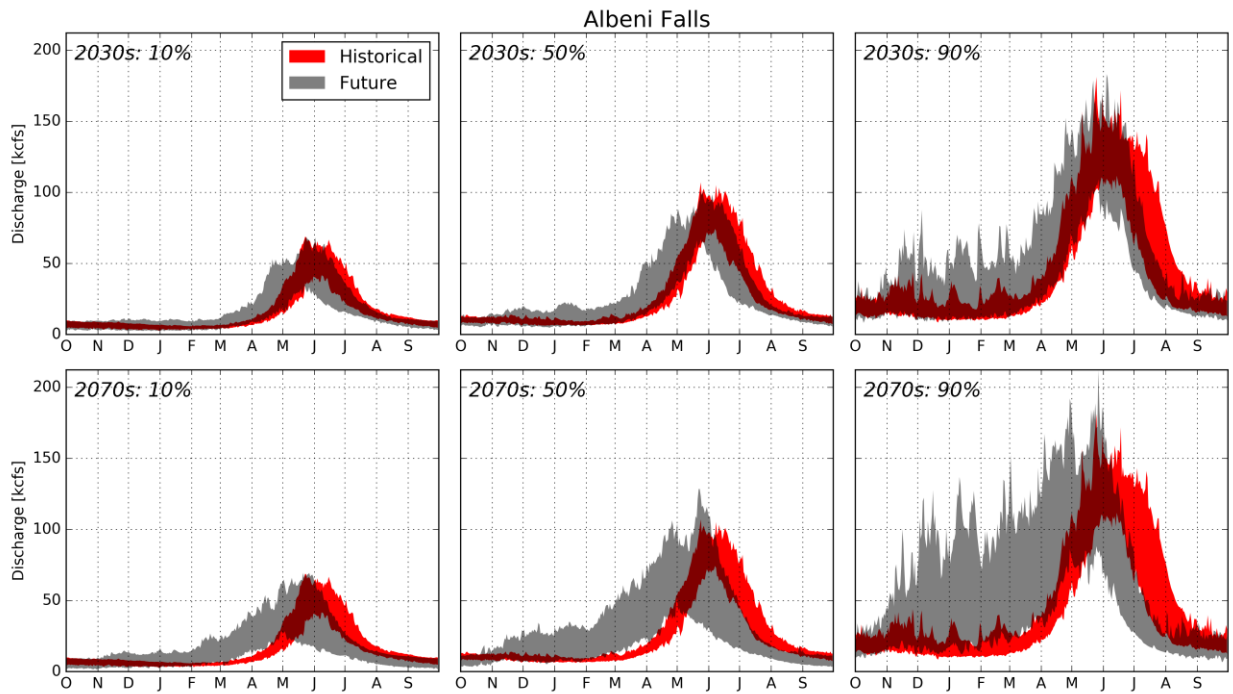


Figure 70: Same as Figure 66, except at Albeni Falls Dam, ID (ALB, Pend Oreille Basin).

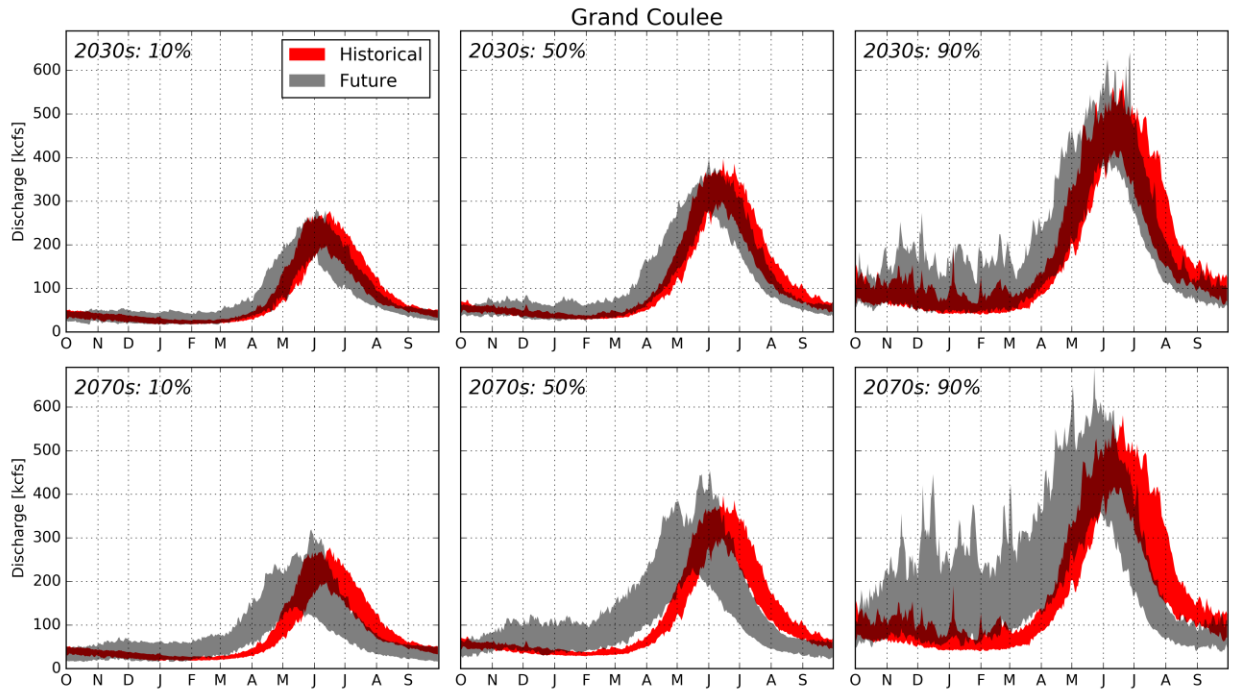


Figure 71: Same as Figure 61, except for Grand Coulee Dam, WA (GCL, mid-Columbia Basin).

7.2.3 Snake River Basin

This part of the Columbia Basin includes the Snake River and its tributaries above. Tributaries include the upper Snake River, which drains southern Idaho and extreme northwest Wyoming, the Salmon River, which includes the high mountains of central Idaho, and the Clearwater Basin, which drains middle elevations of central Idaho. In this sub-basin, overall trends of higher fall and winter flows, earlier and higher spring flow peaks, and the period of low summer flows shifting earlier into the summer are all noted (**Figures 72 to 74**). However, as discussed in Section 6, the Snake River Basin includes key areas where winter snowpacks are likely to decrease as early as the 2020s. Thus, the flow timing responses tend to occur earlier in Snake River scenarios compared to the upper Columbia. In addition, as regional warming continues, many of the scenarios show an increasing tendency for multiple freshet or rain-on-snowpack events throughout the winter and spring—some of which rival the historical spring snowmelt peaks later in the spring. The cumulative effect of these increasing and multiple winter flow peaks impacts daily average flows over time, such that by the 2070s, daily average flows for each GCM show greater variability, with multiple flow peaks in the winter months, and annual flow peaks occurring several weeks or even months earlier than historically observed.

In addition to the greater temperature and precipitation variations between GCMs in the Snake River Basin, historical flow calculations and surface hydrologic modeling were particularly challenging in this area. Similar to what was found in the upper Columbia Basin, climate change streamflows in the historical period exhibited the possibility of a cool bias in more snow-dominated sub-basins like the Clearwater Basin above Dworshak Dam. However, other uncertainties arose due to the fact that the Snake Basin has considerable surface-groundwater exchange, along with decades of crop irrigation. What was “observed” in the historical period is more uncertain in this part of the basin, as is the hydrologic modeling result dependent on those observations.

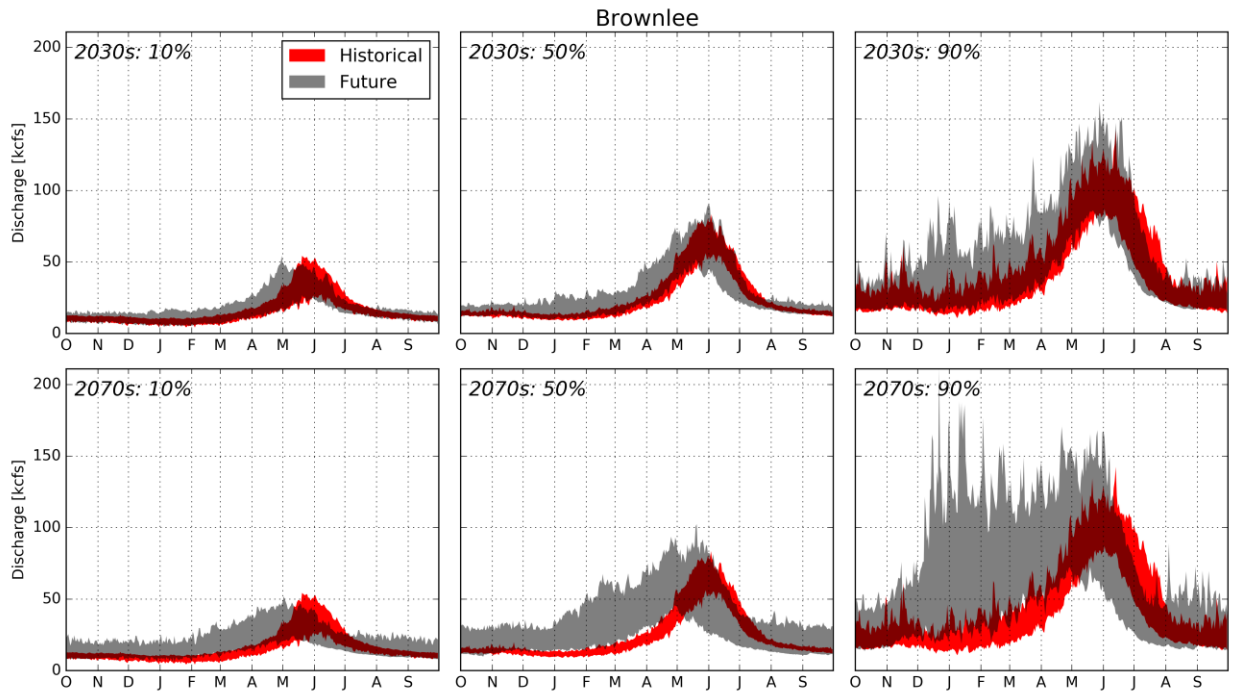


Figure 72: Same as Figure 66, except at Brownlee Dam, ID (BRN, Upper Snake Basin).

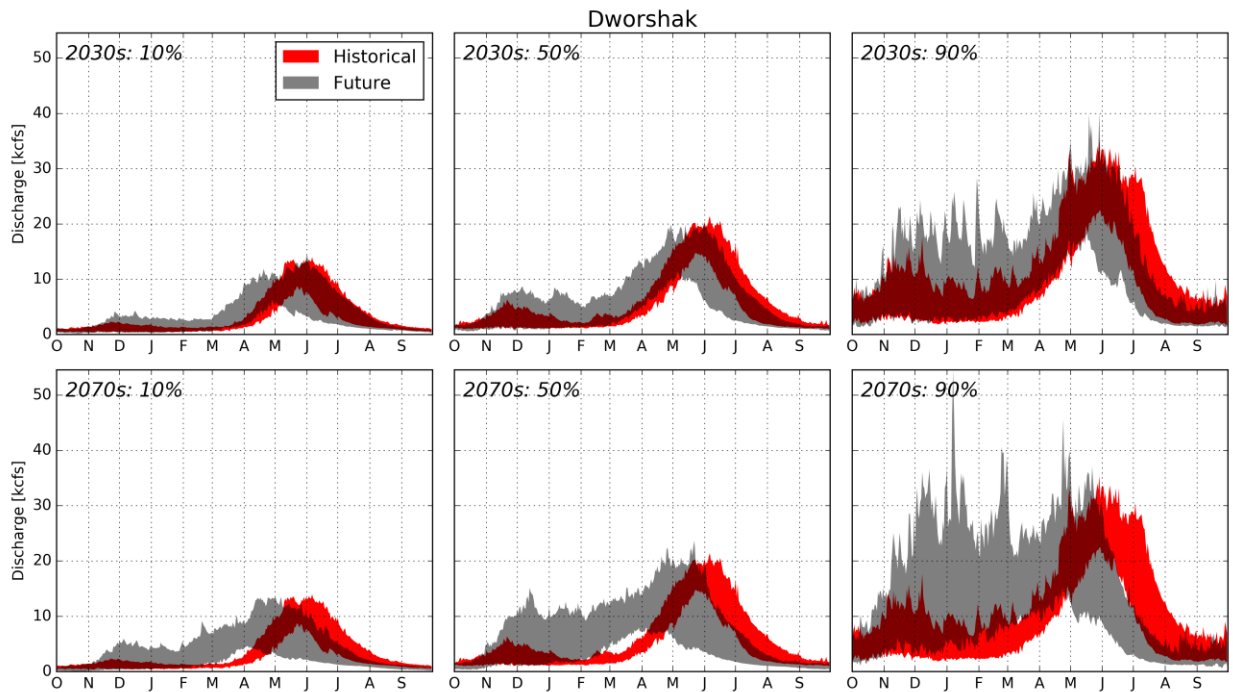


Figure 73: Same as Figure 66, except at Dworshak Dam, ID (DWR, Clearwater Basin).

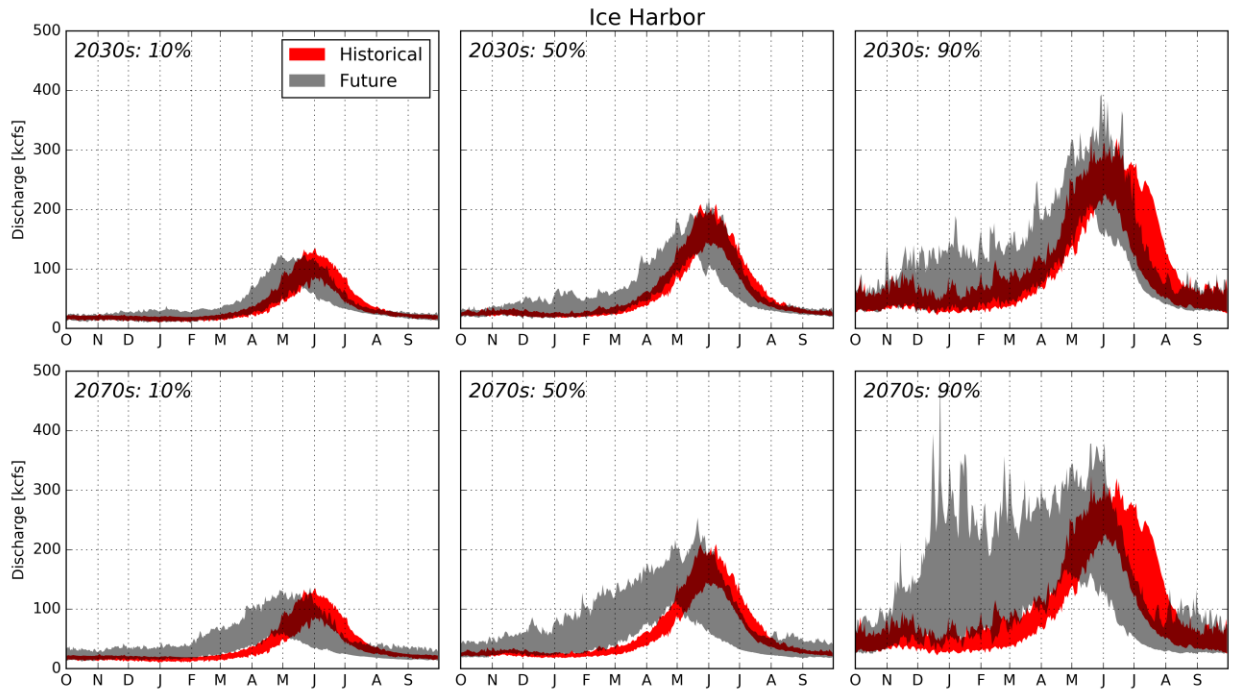


Figure 74: Same as Figure 66, except at Ice Harbor Dam, WA (IHR, Lower Snake Basin).

Despite these modeling challenges, useful information can still be derived from this streamflow set. While the modeling uncertainties and outcome spreads are largest relative to the historical period, the Snake Basin appears to be the most likely to encounter changes in streamflow timing earlier in this century than other parts of the basin. Also, despite the modeling differences, there is fairly good scenario agreement that both winter and spring flows will increase over time in this basin. There may also be some indication that instead of already rather low summer flows becoming even lower over time, the period of low summer flows which historically extended from mid-July to October may shift earlier with time.

7.2.4 Willamette River Basin

The Willamette River empties into the Columbia River at Portland, OR, and is similar to several small tributaries that drain the west side of the Washington Cascades. Unlike the rest of the Columbia Basin, the Willamette and west side basins are historically rain-dominant, which means peak flows have historically occurred each year in the winter months, with only a modest spring snowmelt peak. In most cases, floods in this part of the basin only occasionally coincide with spring freshet flows in the Columbia Basin. However, with the projection for higher winter flows coming out of the Columbia River over time, this part of the basin was given considerable attention in this study. The projections indicate increasing median and extreme winter flows and decreasing later spring and summer flows (Figure 75).

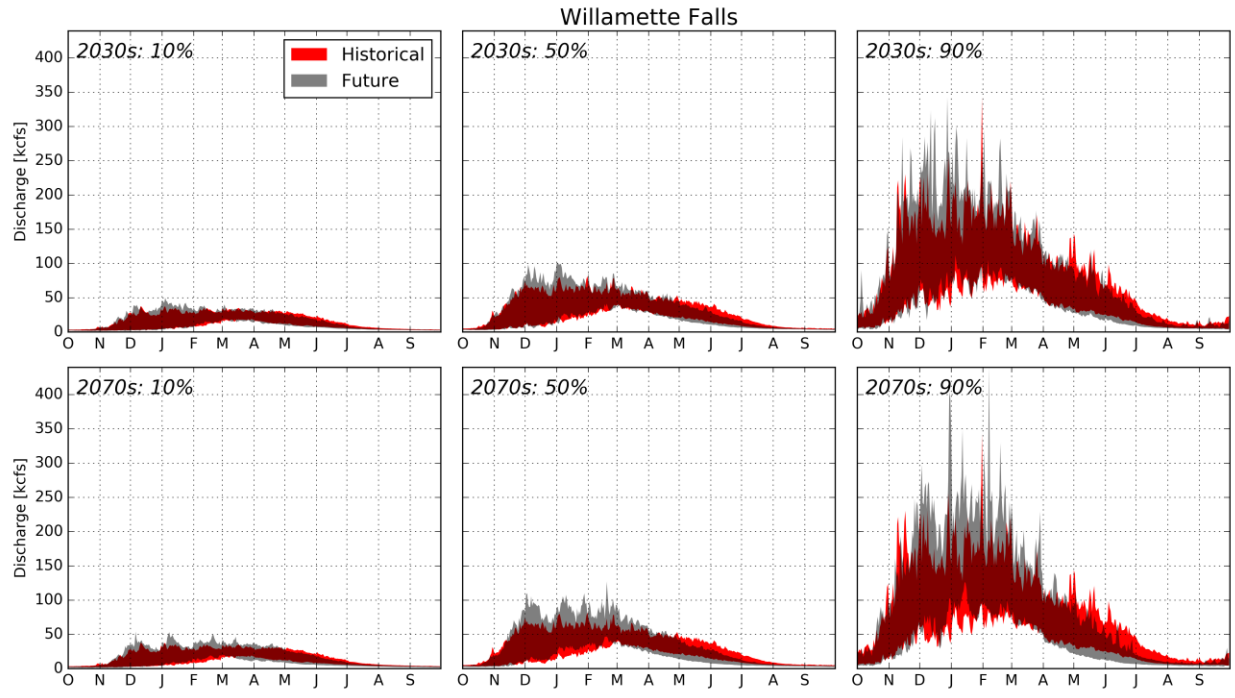


Figure 75: Same as Figure 66, except at Willamette Falls, OR (Willamette Basin).

8.0 Dataset Selection for Hydroregulation Modeling

8.1 Introduction

While it is desirable to use all 172 projections for hydroregulation analyses, some hydroregulation processes require considerable time and resources to complete. Therefore a representative subset of the entire ensemble of projections will be used in hydroregulation modeling analyses for hydropower studies. The first step in narrowing the full ensemble for hydroregulation studies was to consider only the streamflow scenarios members generated utilizing the RCP 8.5 emissions scenario. Based on the current trajectory of global greenhouse gas emissions (Sanford *et al.*, 2014) and the potential for the IPCC RCPs to under-represent potential warming (Brown and Caldeira, 2017), reservoir modeling for Part II of this report will be limited to the projections from the higher emissions-based RCP8.5 scenario. Focusing on RCP8.5 scenarios was also recommended by policymakers for conducting regional studies (e.g., NOAA, 2016).

Additionally, the projections that used GCM-based meteorological forcing downscaled using the hybrid downscaling method were also removed from consideration for the hydroregulation subset. As discussed in Section 7.1, the meteorological forcings and hydrological output from these projections displayed inconsistencies with the hydroclimatology of the region over the historical period.

When these projections are excluded, the ensemble of 172 projections was narrowed to 80 projections. These 80 projections represent a single emission scenario (RCP8.5), 10 GCMs, two statistical downscaling techniques (MACA and BCSD), two hydrology models (VIC and PRMS), and three hydrological model parameter sets of the VIC model.

8.2 Subset Selection for Hydropower Analyses

The outcome of climate-changed hydrometeorological impact analyses can be largely dictated by choice of individual projections selected to represent future conditions (e.g., Harding *et al.* 2012; Vano *et al.* 2014). Despite this fact, climate change assessment studies have often relied on analyzing only a small number of scenarios out of a larger ensemble of hydrometeorological projections due to resource constraints. Several methods for selecting subsets of climate change projections have been suggested in recent literature. The majority of methods are centered on selection of GCMs based on projections of temperature and precipitation (e.g., Snover *et al.*, 2003; Mote *et al.*, 2011) and ranking of the performance of GCMs for simulating historical climate at the regional scale (e.g., Brekke *et al.*, 2008; Rupp *et al.*, 2013). More recently, Vano *et al.* (2015) describe a method that takes into consideration streamflow metrics linked to impacts (e.g., high/low flow thresholds, high/low flow duration) of interest in the selection, as opposed to changes in temperature and precipitation alone. Selections based on temperature and precipitation alone may not adequately represent the changes relevant to potential impacts of the system being evaluated. While hydroclimatology applications of projected future conditions, including this one, often select GCMs on past performance by matching modeled and measured historical values in the application domain, this is not a complete means for ensuring coverage of the uncertainty space around the ensemble of GCMs. A more complete assessment of that uncertainty space would include measures of and selection on model sensitivity to GHG increases, physical processes present in the world but not in the

model, and an index of model diversity; these help ensure that a single GCM or GCM family type is not over-represented in the final subset of all GCMs (Clark *et al.*, 2016).

Following these general ideas, further downselection was pursued for this project by finding a representative subset to be used for hydropower-specific decision making. As part of this analysis all 80 projections will be used for reservoir modeling centered on water supply (MODSIM, USBR) and Flood Risk Management (FRM) system operations. However, hydropower-specific modeling and resulting impact analyses have higher resource demands, which make it unfeasible to model all 80 projections.

Subset selection for this study benefited from having a large number of projections taken through the entire modeling chain, including full hydrological simulations. Thus, the most important variables for water resources system impact assessment, such as temperatures for energy demand modeling, and streamflow volume and timing, were directly available to analyze. Several methods of subset selection based on the streamflow projections were explored during preliminary phases of RMJOC-II (*e.g.*, hydrology model performance weighting, k-means cluster classification). These efforts led to the development of an objective selection technique described in the following sections.

8.2.1 Impact-Relevant Streamflow Metrics

To define a representative subset of climate-changed hydrology projections to carry forward for hydropower analysis, an objective method for selecting individual projections based on stakeholder-relevant streamflow metrics was developed by USACE. The first step was to identify streamflow metrics that are indicators of system vulnerabilities that are most important for stakeholder interests. To identify these metrics, stakeholder outreach meetings were coordinated through technical workshops described in Section 2.3. The Columbia River Forecast Group (CRFG) played a particularly important role in defining the criteria used to further down select from the 80 climate-changed hydrology scenarios used for flood risk management and water supply analysis.

The general categories of system vulnerabilities identified in the stakeholder outreach discussions included vulnerabilities to hydroelectricity generation, temperature-driven energy demand, flood risk management, water supply, ecosystem/habitat, recreation, biological reservoir operations (*e.g.*, operations targeting reservoir storage and releases favorable to fish), and fixed timing-based reservoir operations (*e.g.*, refill operations derived from historical flow seasonality). Six streamflow-based metrics were then selected to reflect potential changes in streamflow that would indicate an impact on each of these key components of the coupled natural and regulated system (**Table 10**). These metrics include four streamflow volume metrics and two streamflow timing-based metrics. Streamflow metrics were evaluated by comparing their median values for a future, 30-year epoch of time to their values for a historical base period. Extremes were not specifically targeted with the selection metrics for hydropower planning.

Table 10: Streamflow metrics and vulnerabilities identified in stakeholder outreach discussions.

Streamflow Metric	System Vulnerabilities
Annual Volume	<ul style="list-style-type: none"> • Hydro-electricity generation • Flood risk management • Water supply • Ecosystem • Recreation • Biological operations • Fixed timing based operations
Winter Volume	
Spring Volume	
Summer Volume	
Winter-to-Spring Volume Ratio	
Annual Half Volume Timing	

These metrics were then evaluated at 14 locations throughout the Columbia River Basin associated with existing FCRPS projects (**Figure 76**). These locations were selected to represent the natural underlying spatial variability in hydroclimatology, potential spatial variability in changes in climate due to anthropogenic climate change, and locations that are important for ongoing operational studies (Columbia River Treaty, Columbia River System Operations NEPA EIS).



Figure 76: Locations (circled, labeled with boxes) in the Columbia River Basin used to define subset selection criteria.

8.2.2 Objective Subset Selection Method

Downselection from the ensemble of 80 projections centered on the concept of having a selected number of projections that capture key elements of the distribution of projected changes in natural streamflow at each of the fourteen locations. The change in a streamflow metric is defined by the difference between its median value for a future period and a historical base period. The distribution of changes in a metric for each location, based on all 80 projections, can then be described using percentiles. The objective in selecting a subset of projections is to capture areas of the distribution that represent low, high, and median amounts of change relative to the historical period (**Figure 77**). Low, high, and median amounts of change are defined as follows:

Low – 10th Percentile: To represent the lower end of the distribution (low amounts of change or largest amounts of change in the negative direction), the 10th percentile was chosen. A buffer of 5% was used around this target to allow some flexibility in selection.

Median – 50th Percentile: The 50th percentile was used to represent the median amount of change in the metric. This range of the distribution often indicates the highest frequency of agreement between projections. A buffer of 5% was used around this target to allow some flexibility in selection.

High – 90th Percentile: To represent the higher end of the distribution (largest amounts of change in positive direction, least amount of change in the negative direction) the 90th percentile was chosen. A buffer of 5% was used around this target to allow some flexibility in selection.

The high and low percentile targets were limited to 5 to 15% and 85 to 95% portions of the distribution to prevent targeting outliers in the tails of the distributions explicitly. If these target ranges extended to the edges of the distributions, the selection would then be largely dominated by projections that consistently fall at the edges of the ensemble of projections because these outlying results are generally generated by the same constructions of the hydrologic modeling chain. This would greatly decrease the diversity of GCMs, downscaling methods, and hydrology models/parameter sets associated with the selected subset of projections. Use of the 10/50/90th percentile of changes for projection selection is consistent with the ensemble-informed approach developed for GCM selection based on precipitation and temperature fields applied as part of RMJOC-I (RMJOC, 2010).

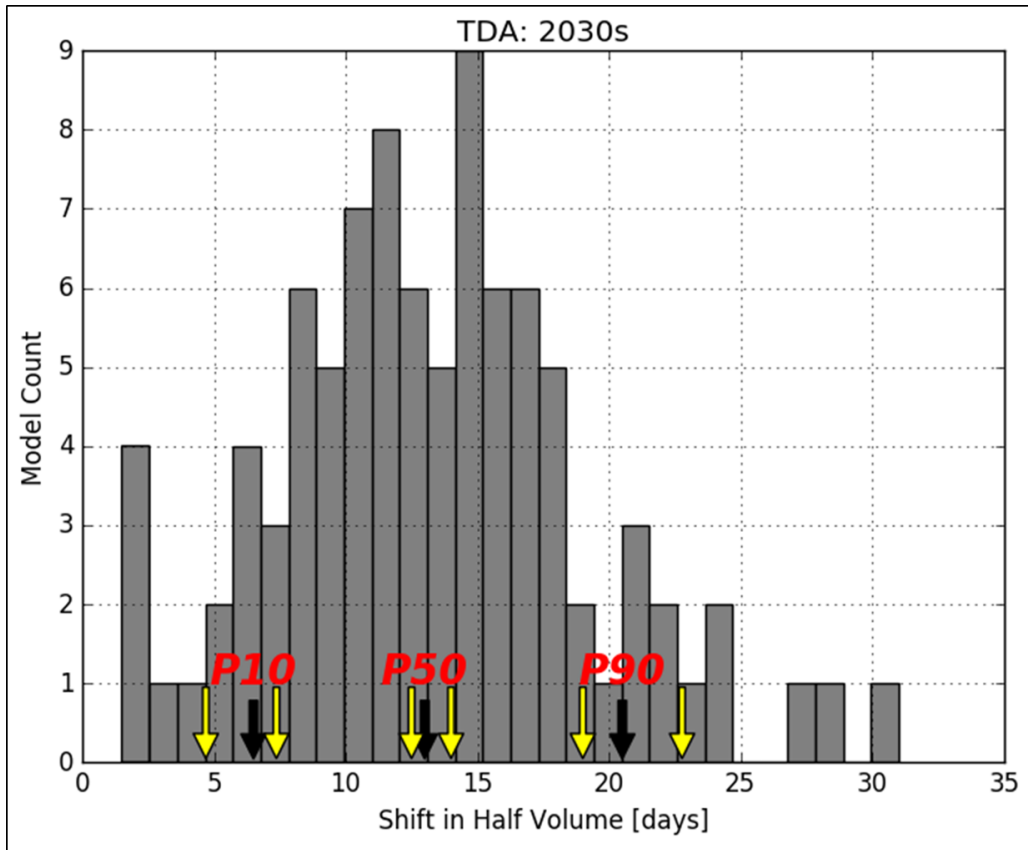


Figure 77: Example distribution of changes in streamflow metric (Half Volume Day) for the 2030 epoch (2030s) at The Dalles, OR (TDA). Model count indicates the number of the 80 projections that fall within in each range of changes in the metric. The yellow arrows indicate the ranges included to define each 10, 50, and 90 percentile targets.

The combinations of the locations, metrics, and percentile targets define the set of constraints deemed to best represent the spread in streamflow changes most relevant to the metrics the regional stakeholders defined in Section 8.2.1. In total, this results in 252 constraints (14 locations x 6 metrics x 3 targets). Given these constraints, the selection method follows an iterative ranking routine to build the subset of projections (**Figure 78**). First, each of the members of the full ensemble is ranked by the number of distribution targets it captured. The top-ranked ensemble member is then added to the subset, and the targets it fulfilled are removed from the ranking criteria. The remaining ensemble members are then ranked again based on the truncated list of targets not yet fulfilled, and the top-ranked member is added to the subset. This iterative ranking procedure is repeated until all targeted constraints are fulfilled.

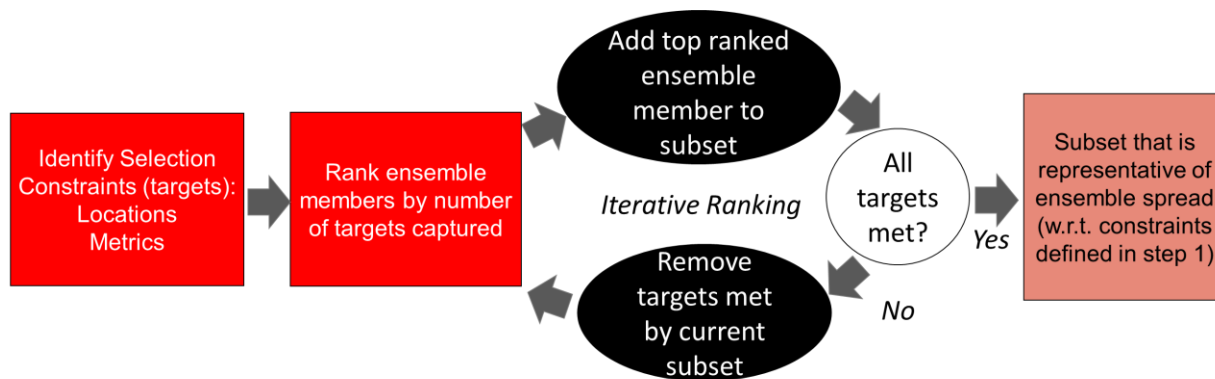


Figure 78: Schematic demonstrating the iterative technique for selecting a representative subset based on constraints derived from distributions of changes in streamflow.

After the automatic selection finds a representative subset, the subset is then further evaluated and validated against criteria that were not explicitly included in the selection constraints but were identified as important to consider. For example, this includes verification of diversity of modeling chain elements: Does the subset include representation of the majority of the GCMs, downscaling techniques, and hydrology models? Does it represent other streamflow vulnerability metrics that were not used in the selection?

8.3 Selected Subset and Characteristics

The procedure was applied to the subset of the 80 projections using the six streamflow metrics at the 14 locations. The changes in metrics were defined by the relative change in median value between the 2030s epoch (2020-2049) and historical base period (1976-2005). The method identified 19 of 80 ensemble members which captured all 252 identified selection constraints. These 19 projections (**Table 11**) include nine out of the 10 GCM temperature and precipitation outputs used in the full distribution, both statistical downscaling methods, and all four hydrological modeling approaches. The one GCM not selected in the subset is the HadGEM2-ES model. This model is similar in structure and process representation to the HadGEM2-CC model. Thus, diversity of model chain elements is still well captured with the subset of 19 model chain combinations for load and hydroregulation modeling.

Table 11: Table of the 19 projections selected as a representative subset of the 80-member ensemble. Each modeling element is listed in the respective column and color-coded for visual comparison.

	GCM	Downscaling	Hydro Model
1	CanESM2	MACA	PRMS_P1
2	CanESM2	BCSD	VIC_P1
3	CCSM4	BCSD	VIC_P1
4	CCSM4	MACA	VIC_P3
5	CNRM-CM5	MACA	VIC_P1
6	CNRM-CM5	BCSD	VIC_P2
7	CNRM-CM5	MACA	VIC_P3
8	CSIRO-Mk3-6-0	BCSD	PRMS_P1
9	GFDL-ESM2M	MACA	VIC_P1
10	GFDL-ESM2M	BCSD	VIC_P2
11	GFDL-ESM2M	MACA	VIC_P2
12	HadGEM2-CC	BCSD	VIC_P1
13	HadGEM2-CC	MACA	VIC_P1
14	inmcm4	BCSD	PRMS_P1
15	inmcm4	BCSD	VIC_P2
16	inmcm4	MACA	VIC_P3
17	IPSL-CM5A-MR	MACA	VIC_P2
18	MIROC5	BCSD	PRMS_P1
19	MIROC5	BCSD	VIC_P3

The projected climate-changed hydrology based on the subset of 19 projections was then compared against the full ensemble of projections using streamflow statistics and locations not directly used in ensemble downselection criteria (**Figure 79**). This analysis is carried out to validate that the subset of 19 projections fully captures the spread in future climate-changed hydrology in the Columbia River Basin. For the 2030s epoch, 5th, 50th, and 95th percentiles of averaged daily streamflow were calculated for each day of the year, for each of the 80 ensemble members. The ensemble downselection method used changes in annual and seasonal metrics represented as medians over a 30-year period, whereas this validation step examines changes in medians and extremes computed at daily intervals. This serves as a test for robustness of the ensemble downselection approach for conditions that were not directly considered in selection. However, it does not indicate an intent to have future analyses focused on extremes at daily intervals for the RMJOC-II study.

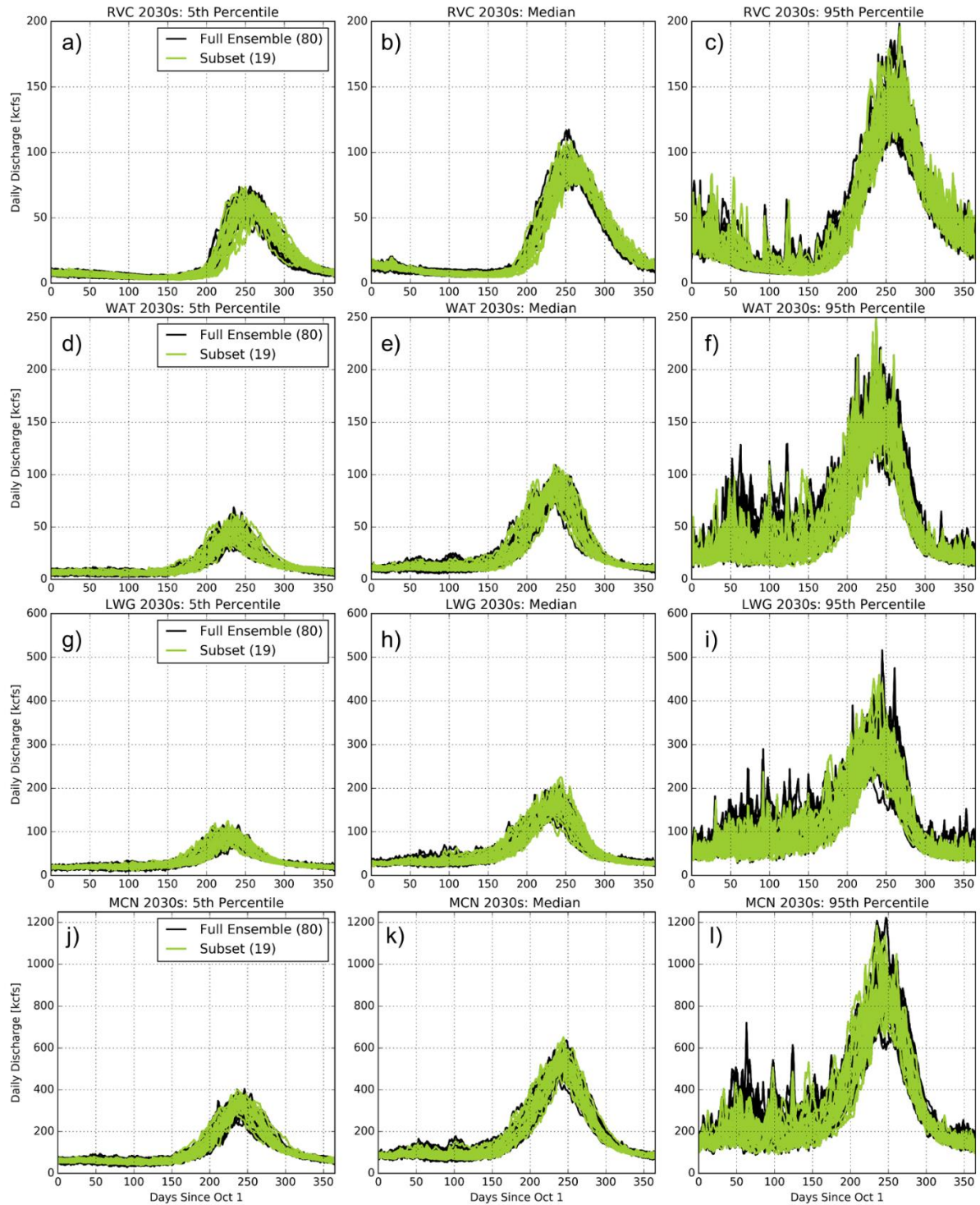


Figure 79: Comparisons of the spread of the 80-member ensemble and the spread of the 19-member subset using daily summary statistics (5%, 50%, and 95%) for locations not included in the selection method (Revelstoke, RVC; Waneta, WAT; Lower Granite, LWG; McNary, MCN).

The 19-member subset was also compared against the 80-member ensemble to validate coverage of annual volumes. For example, **Figures 80 to 85** show the selected scenarios relative to the 80 ensemble scenarios using RCP8.5 and statistical downscaling at three key projects in the Columbia Basin. For the 2030s epoch, annual volumes for the downselected scenarios cover most of the range of the larger set of 80 projections at all three projects. In a few locations, the objectively selected scenarios cluster within the 80-set distribution (e.g., The Dalles 155-160 million acre feet range, **Figure 80**). However, as was emphasized during the downselection process, some of the warmest or wettest GCM outputs in some parts of the basin were not the warmest or wettest in other locations. Fortunately, even though the downselection procedure was focused on the 2030s, the selected scenarios also reasonably cover the range of projected annual volumes by the 2070s. Thus, rather than select a whole different set of scenarios focused on a different time horizon, as was done for RMJOC-I, the same scenarios selected for the 2030s appear adequate for much longer-range analyses focused on the 2070s.

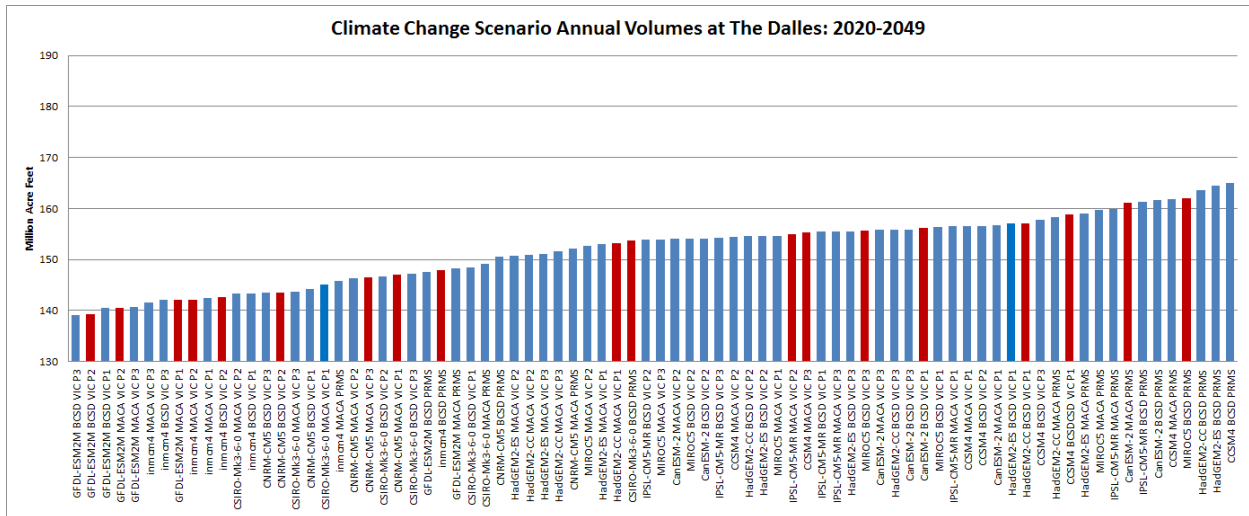


Figure 80: Average annual volumes at The Dalles, OR, for the 2030s (WY 2020-2049) for each of the 80 scenarios using RCP8.5, the 10 GCMs used for this study, and statistical downscaling (BCSD and MACA). Red scenarios are the nineteen selected using the iterative technique described in Section 9.2.2.

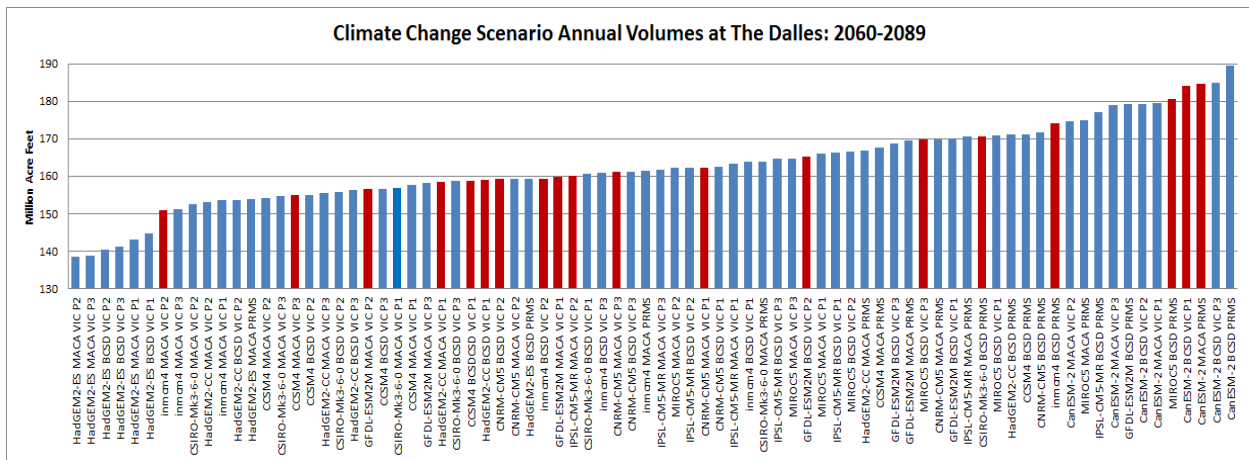


Figure 81: Same as Figure 80, except for the 2070s (WY 2060-2089).

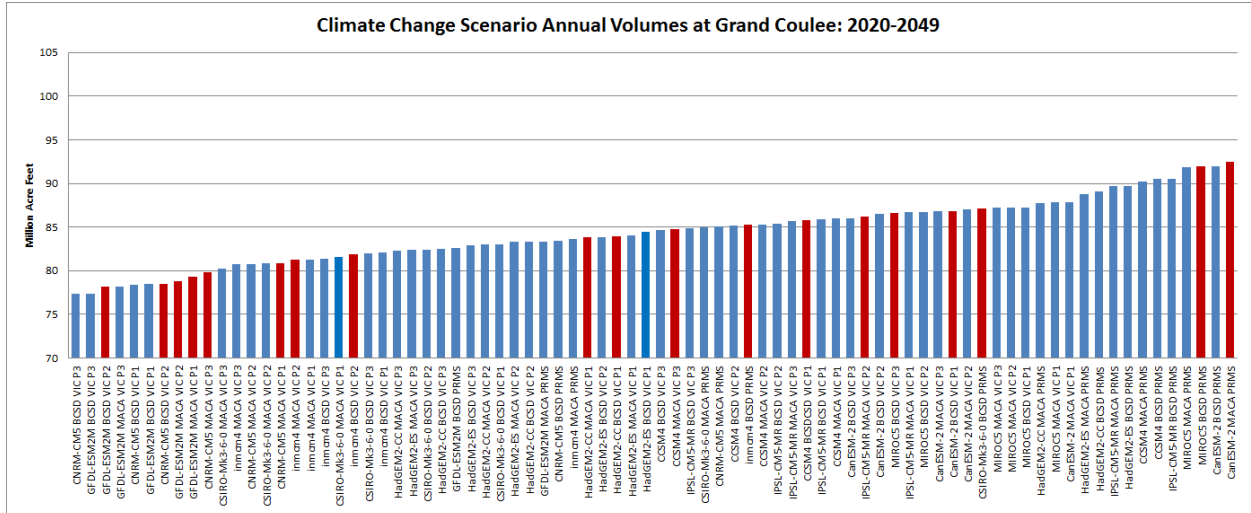


Figure 82: Same as Figure 80, except for Grand Coulee, WA, for the 2030s (WY 2020-2049).

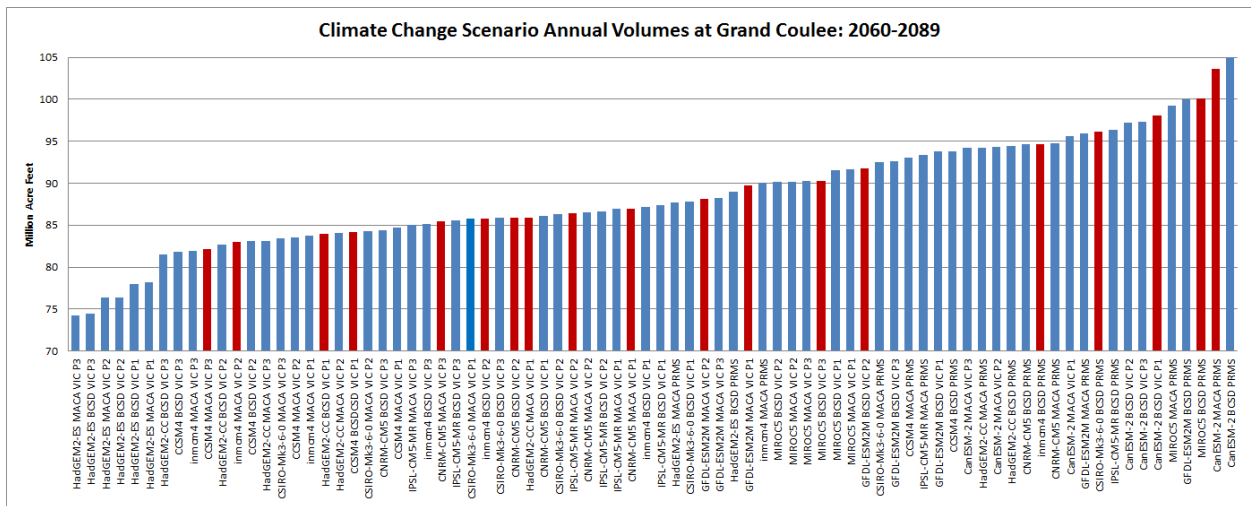


Figure 83: Same as Figure 82, except for the 2070s (WY 2060-2089).

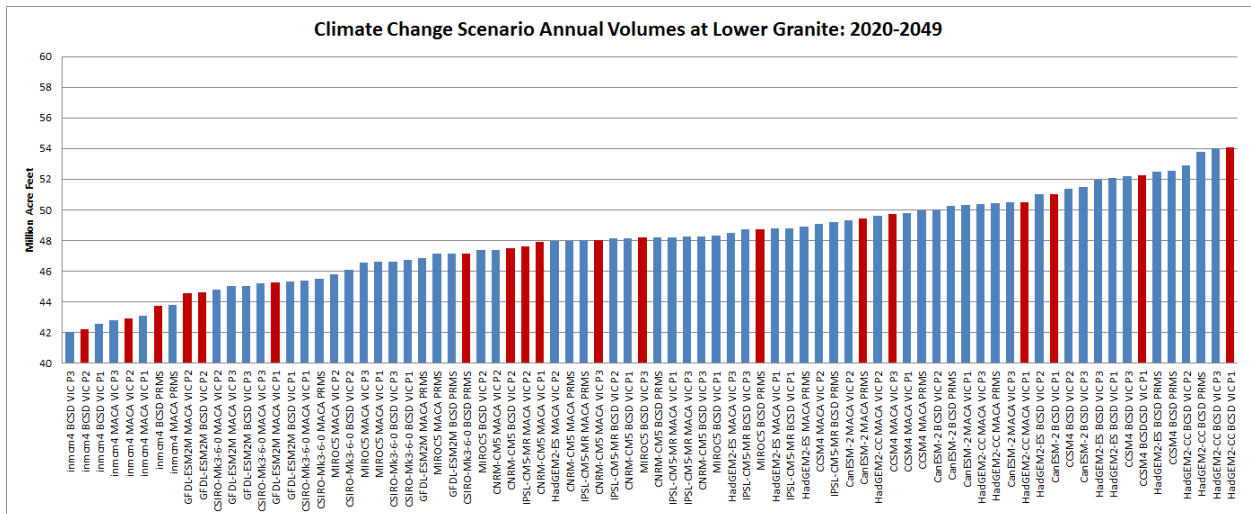


Figure 84: Same as Figure 80, except for Lower Granite for the 2030s (WY 2020-2049).

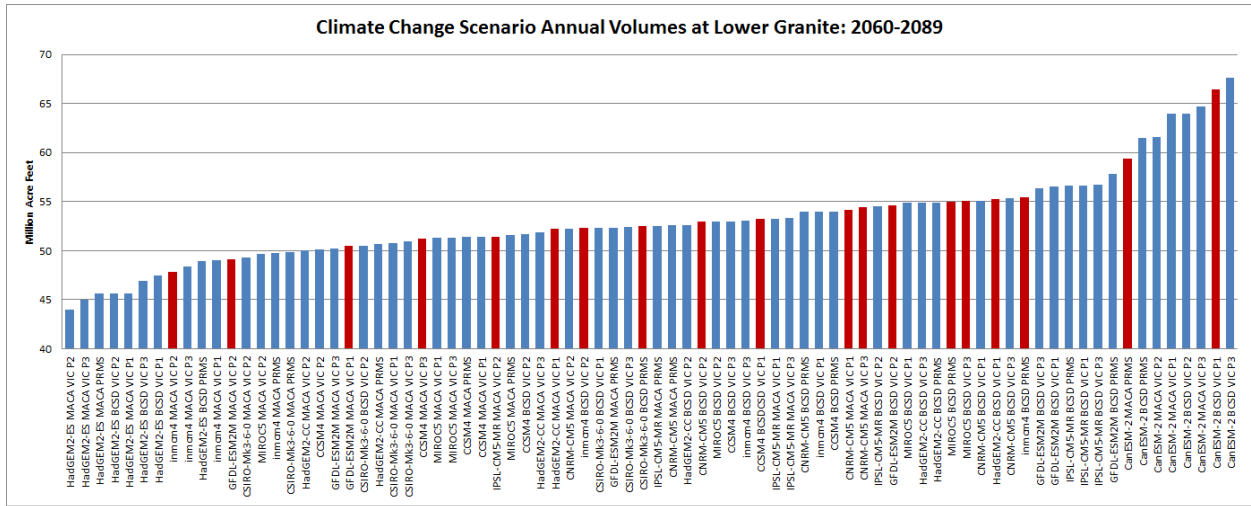


Figure 85: Same as Figure 84, except for the 2070s (WY 2060-2089).

9.0 Summary and Conclusions

Based on the results detailed in the temperature, precipitation, snowpack, and streamflow scenarios prepared for this study:

- Temperatures have already warmed about 1.5°F in the region since the 1970s. They are expected to warm another 1 to 4°F by the 2030s.
- Temperatures are likely to warm 3 to 6°F over what is currently observed in the basin by the 2070s if RCP4.5 emissions pathways are attained. If current trajectory RCP8.5 emissions pathways are realized, though, 4 to 10°F of warming above what is currently observed will be likely by the 2070s.
- Warming is likely to be greatest in the interior, with a greater range of possible outcomes, with less pronounced warming near the coast.
- Future precipitation trends are more uncertain, but a general upward trend is likely for the rest of the 21st century, particularly in the winter months. Already dry summer months could become drier.
- Average winter snowpacks are very likely to decline over time as more winter precipitation falls as rain instead of snow, especially in the US side of the Columbia Basin.
- By the 2030s, higher average fall and winter flows, earlier peak spring runoff, and longer periods of low summer flows are very likely. The earliest and greatest streamflow changes are likely to occur in the Snake River Basin, although that is also the basin with the greatest modeling and forecast uncertainty.
- In the Willamette Basin, fall and winter flows are likely to increase. A slight decrease in spring flows is possible, with a longer period of low summer flows more likely than not.
- To support subsequent RMJOC-II efforts, an objective method of selecting subsets of scenarios was developed. This method found a 19-member subset of 80 statistically downscaled RCP8.5 projections to be representative of projected changes in stakeholder-identified natural streamflow metrics for the 2030s.

The key research objective of this project was to determine, if possible, to what degree each methodological choice made in the hydroclimate modeling chain introduces additional spread into future projections. For the Columbia Basin as a whole, future climate scenarios depicted by the GCMs, as forced by the RCPs and downscaled by different methods, are the largest source of variability in future streamflows. However, the choice of hydrologic model itself, the hydrologic model's particular calibration parameters, the choice of bias correction technique, and the historical dataset used for model calibration, are all important drivers for increasing the spread of the hydrologic projections.

It is important to note that this study does not make a determination on which climate model, downscaling method, or hydrologic models will perform “better” or “worse” in the future. More correctly, because considerable scientific rigor was applied to each step in the process, the diversity of the methods used should be respected and maintained for possible downselection for subsequent scenario-based studies. One important finding from this project is that uncertainties introduced in each step of the modeling chain must be included if planners seek to represent a fuller range of potential hydroclimate change impacts.

One of the more important challenges and findings uncovered in this project involved commonly used post-processing techniques for correcting raw streamflows to what had been observed in the historical period. The scientific issues involved are multifaceted and complex. What was “observed” in the past, even in more recent decades when more numerous and higher-quality observations became available, has uncertainty associated with it. This is particularly noted in sub-basins with more complex surface water-groundwater exchange, irrigation withdrawals and poorly measured return flows, and large reservoirs with day-to-day measurement fluctuations caused by non-hydrologic factors such as changes in instrumentation and gauge locations. Also, traditional monthly quantile mapping techniques are effective in correcting modest biases arising in the hydroclimate modeling process when the desired outputs are in monthly time steps. However, these methods can lead to unrealistic flow changes at monthly boundaries (*i.e.*, unrealistic day-to-day flow drops or spikes) due to abrupt changes in the mapping used from one month to the next. Perhaps more importantly, conducting bias-correction on a fixed monthly basis assumes stationarity for the seasonal cycle. Given that the results project large shifts in the seasonal cycle, with some months of the year (*i.e.*, winter) likely to receive significantly higher flows than previously seen, it is important to incorporate bias-correction that is not month-specific. The novel bias-correction method developed by the University of Washington team used for this study mitigates these issues, and has made the dataset usable for rules-based hydraulic/hydroregulation analyses.

However, the tradeoff is that the streamflows from this study do not fully match streamflow behavior in the historical period. For some planning purposes, this may be an undesirable side effect of bias-correction. For other data users, particularly in smaller sub-basins, unregulated or headwater locations, or specific streams where historical data was not available on daily time steps, it may be more useful to use the raw streamflow outputs from this study for follow-on research and applications.

Another key component of this hydroclimate study was the availability of daily temperature and precipitation forcings from the CMIP-5 GCM outputs. This allowed the project to directly produce daily downscaled temperature and precipitation sequences to drive daily streamflows. This, in turn, has allowed more specific evaluation of streamflow timing shifts as the regional climate evolves. However, generating realistic daily temperature, precipitation, and streamflows is challenging, even in short-term applications, let alone for future climate. In the RMJOC-II study, considerable effort was dedicated to calibrating the UW-VIC and UW-PRMS, and ensuring that daily time series are realistic relative to the large-scale hydrology of the Columbia Basin. There are tradeoffs in this process. By concentrating on reproducing realistic hydrologic behavior at the basinwide scale for these two parameter sets, daily streamflow sequences in very small sub-basins, and basins with particularly complex surface-groundwater hydrology, are in some cases less hydrologically realistic at fine time scales. It is important for individual users to evaluate the streamflow time series at any given site to assess whether they meet the criteria for their specific use. Also, because different historical data was used to calibrate ORNL-VIC and NCAR-VIC, more attention was focused on ensuring that month-averaged streamflows from these models are realistic relative to the historical period, and useful for hydroregulation studies.

References

- Abatzoglou, J.T. and T.J. Brown, 2012: Development of gridded surface meteorological data for ecological applications and modelling. *Int. J. Climatol.*, **32**, 772-780. doi: 10.1002/joc.3413.
- Acharya, A. and J.H. Ryu, 2013: A simple method for streamflow disaggregation. *Journal of Hydrologic Engineering*, **10.1061**/(ASCE)HE.1943-5584.0000818. Available online at: [https://doi.org/10.1061/\(ASCE\)HE.1943-5584.0000818](https://doi.org/10.1061/(ASCE)HE.1943-5584.0000818)
- Ashfaq, M., L.C. Bowling, K. Cherkauer, J.S. Pal, and N.S. Diffenbaugh, 2010: Influence of climate model biases and daily-scale temperature and precipitation events on hydrological impacts assessment: A case study of the United States. *J. Geophys. Res.*, **115**, D14116. doi:10.1029/2009JD012965.
- Ashfaq, M., D. Rastogi, R. Mei, S.-C. Kao, S. Gangrade, B. S. Naz, and D. Touma, 2016: High-resolution Ensemble Projections of Near-term Regional Climate over the Continental United States. *J. Geophys. Res.-Atmos.*, **121**, 9943-9963. doi:10.1002/2016JD025285.
- Bahr, D.B., M.F. Meier, and S.D. Peckham, 1997: The physical basis of glacier volume-area scaling. *Journal of Geophysical Research*, **102**(B9), 20355-20362. Available online at: <https://doi.org/doi:10.1029/97JB01696>
- Bonneville Power Administration, 2004: 2000 Level Modified Streamflow (1928-1998). Bonneville Power Administration, Portland, OR, unnumbered DOE/BP publication.
- Bonneville Power Administration (BPA), 2011a: 2010 Level Modified Streamflow (1928-2008). Bonneville Power Administration, DOE/BP-4352. Available online at: <https://www.bpa.gov/p/Power-Products/Historical-Streamflow-Data/Pages/Historical-Streamflow-Data.aspx>.
- Bonneville Power Administration (BPA), 2011b: Fact Sheet: Northwest federal agencies prepare for a changing climate. DOE/BP-4360. Available on line at: https://www.bpa.gov/p/Generation/Hydro/hydro/cc/Climate_Change_Sept_2011_post.pdf.
- Bonneville Power Administration (BPA), 2013a: FY2014 Opportunity Announcement: Technology Innovation Funding Opportunity Announcement FOA#:BPA-0002617. 37pp.
- Bonneville Power Administration (BPA), 2013b: FY2014 Opportunity Announcement: Proposal Guidance for Technology Innovation Focus Areas. 18pp.
- Brakebill, J.W., D.M. Wolock, and S.E. Terziotti, 2011: Digital hydrologic networks supporting applications related to spatially referenced regression modeling. *J. Am. Water Resour. Assoc.*, **47**(5), 916-932. doi: 10.1111/j.1752-1688.2011.00578.x
- Bureau of Reclamation, 2016a: SECURE Water Act Section 9503(c) – Reclamation Climate Change and Water 2016. 307pp. Available online at: <https://www.usbr.gov/climate/secure/index.html> .
- Bureau of Reclamation, 2016b: West-wide Climate Risk Assessments: Hydroclimate Projections. Technical Memorandum 86-68210-2016-01. 154pp. Available online at: <https://www.usbr.gov/climate/secure/docs/2016secure/wwcra-hydroclimateprojections.pdf>.
- Bureau of Reclamation, 2017: Unregulated Flows in the Upper Deschutes Basin, Oregon. Internal technical documentation, Pacific Northwest Regional Office, Boise, ID. 22pp.
- Bürger, G., T.Q. Murdock, A.T. Werner, and S. R. Sobie, 2012: Downscaling extremes—an intercomparison of multiple statistical methods for present climate. *J. Climate*, **25**, 4366-4387.
- Cannon, A.J., S.R. Sobie, and T.Q. Murdock, 2015: Bias correction of GCM precipitation by quantile mapping: How well do methods preserve changes in quantiles and extremes? *J. Climate*, **28**, 6938-6959.

- Chegwidden, O., D.E. Rupp, B. Nijssen, E. Pytlak and K. Knight, 2016: Collaboration as a means toward a better dataset for both stakeholders and scientist. *Preprints*, American Geophysical Union Annual Meeting, San Francisco, CA, PA33D-01.
- Clark, M.P., R.L. Wilby, E.D. Gutman, J.A. Vano, S. Gangopadhyay, A. W. Wood, H. J. Fowler, C. Prudhomme, J. R. Arnold, and L.D. Brekke, 2016: Characterizing uncertainty of the hydrologic impacts of climate change. *Climate Change Reports*, **2**, 54-64.
- Daly, C., Taylor, W. Gibson, 1997: The PRISM approach to mapping precipitation and temperature. *Preprints*, 10th Conf. on Applied Climatology, American Meteorological Society, Reno, NV, 10-12.
- Daly, C., W.P. Gibson, G.H. Taylor, G. L. Johnson, and P. Pasteris, 2002: A knowledge-based approach to the statistical mapping of climate. *Climate Res.*, **22**, 99-113, doi: 10.3354/cr022099
- Daly, C., W.P. Gibson, G.H. Taylor, M.K. Doggett and J.I. Smith, 2007: Observer bias in daily precipitation measurements at United States Cooperative Network Stations. *Bull Amer. Meteor. Soc.*, **7**, 899-912. DOI:10.1175/BAMS-88-6-899.
- Daly, C., J.W. Smith, J.I. Smith, and R.B. McKane, R. B., 2007: High-resolution spatial modeling of daily weather elements for a catchment in the Oregon Cascade Mountains, United States. *J. Appl. Meteor. Climatol.*, **46**(10), 1565-1586.
- Daly, C., D.R. Conklin, and M.H. Unsworth, 2010: Local atmospheric decoupling in complex topography alters climate change impacts. *International Journal of Climatology*, **30**(12), 1857-1864.
- Department of Energy, 2017: Effects of Climate change of Federal Hydropower, The Second Report to Congress, January, 2017. 33pp. Available online at: <https://energy.gov/eere/water/downloads/effects-climate-change-federal-hydropower-report-congress>.
- Elsner, M.M., L. Cuo, N. Voisin, J.S. Deems, A.F. Hamlet, J.A. Vano, K.E.B. Mickelson, S.Y. Lee, and D.P. Lettenmaier, 2010. Implications of 21st century climate change for the hydrology of Washington State. *Climatic Change*. DOI:10.1007/s10584-010-9855-0.
- Eum, H.-I., Y. Dibike, T. Prowse, and B. Bonsal, 2014: Inter-comparison of high-resolution gridded climate data sets and their implication on hydrological model simulation over the Athabasca Watershed, Canada. *Hydrol. Process.*, **28**, 4250-4271. doi: 10.1002/hyp.10236.
- Fuss, S., J.G. Canadell, G.P. Peters, M. Tavoni, R.M. Andrew, P. Ciais, R.B. Jackson, C.D. Jones, F. Kraxner, N. Nakicenovic, C. Le Quéré, M.R. Raupach, A. Sharifi, P. Smith, and Y. Yamagata, 2014: Betting on negative emissions. *Nature Climate Change*, **4**, 850-853. doi:10.1038/nclimate2392.
- Gao, H., Q. Tang, X. Shi, C. Zhu, T. J. Bohn, F. Su, J. Sheffield, M. Pan, D. P. Lettenmaier, and E. F. Wood, 2010: Water Budget Record from Variable Infiltration Capacity (VIC) Model. Algorithm Theoretical Basis Document Version 1.2. Dept. of Civil and Environmental Engineering, University of Washington, Seattle, WA. Available online at: <http://www.hydro.washington.edu/Lettenmaier/Models/VIC/Overview/ModelOverview.shtml>.
- Giorgi, F., E. Coppola, F. Solmon, L. Mariotti, M. B. Sylla, X. Bi, N. Elguindi, G. T. Diro, V. Nair, and G. Giuliani, 2012: RegCM4: model description and preliminary tests over multiple CORDEX domains. *Climate Res.*, **2**(7). doi:10.3354/cr01018.
- Gutmann, E., T. Pruitt, M.P. Clark, L. Brekke, J.R. Arnold, D.A. Raff, and R.M. Rasmussen, 2014: An intercomparison of statistical downscaling methods used for water resource assessments in the United States, *Water Resour. Res.*, **50**, 7167-7186. doi: 10.1002/2014WR015559.
- Hamlet, A.F. and D.P. Lettenmaier, 1999: Effects of climate change on hydrology and water resources in the Columbia River Basin. *J. Am. Water Res. Assoc.*, **35**, 1597-1623.

- Hamlet, A.F., P. Carrasco, J. Deems, M.M. Elsner, T. Kamstra, C. Lee, S. Lee, G. Mauger, E.P. Salathé, I. Tohver, and L. Whitely Binder, 2008: Final Report for the Columbia Basin Climate Change Scenarios Project. Center for Science of the Earth System, Climate Impacts Group, University of Washington. Available on line at: <http://warm.atmos.washington.edu/2860/report>.
- Hamlet, A.F., M.M. Elsner, G.S. Mauger, S.-Y. Lee, I. Tohver, and R.A. Norheim, 2013: An overview of the Columbia Basin Climate Change Scenarios Project: Approach, methods, and summary of key results. *Atmos. Ocean*, **51**, 392-415. doi:10.1080/07055900.2013.819555.
- Hay, L.E., S.L. Markstrom, and C. Ward-Garrison, 2011: Watershed scale response to climate change through the twenty-first century for selected basins across the United States. *Earth Interact.*, **15**. doi:10.1175/2010EI370.1.
- Hildago, H.G., T. Das, M.D. Dettinger, D.R. Cayan, D.W. Pierce, T.P. Barnett, G. Bala, A. Mirin, A.W. Wood, C. Bonfils, B.D. Santer, and T. Nozawa, 2009: Detection and attribution of streamflow timing changes to climate change in the western United States. *J. Climate*, **22**, 3838-3854.
- Intergovernmental Panel on Climate Change (IPCC), 2007: Climate Change 2007, The Physical Science Basis. Contribution of Working Group I to the Fourth Assessment Report of the Intergovernmental Panel on Climate Change.
- Intergovernmental Panel on Climate Change (IPCC), 2013: Climate Change 2013, The Physical Science Basis. Contribution of Working Group I to the Fifth Assessment Report of the Intergovernmental Panel on Climate Change. 1552pp.
- Intergovernmental Panel on Climate Change (IPCC), 2014: Synthesis Report. Contribution of Working Groups I, II and III to the Fifth Assessment Report of the Intergovernmental Panel on Climate Change [Core Writing Team, R.K. Pachauri and L.A. Meyer (eds.)]. IPCC, Geneva, Switzerland. 151 pp.
- Jiang, Y., J.B. Kim, C.J. Still, B.K. Kearns, J.D. Kline, and P.G. Cunningham, 2018: Inter-comparison of multiple statistically downscaled climate datasets for the Pacific Northwest, USA. *Scientific Data*, **5**, 180016. DOI: 10.1038/sdata.2018.16.
- Jost, G. and F. Weber, 2012: The Potential Impacts of Climate Change on BC Hydro's Water Resources. BC Hydro, Burnaby, BC. GDS12-314. 27pp.
- Jung, I.W. and H. Chang, 2011: Assessment of future runoff trends under multiple climate change scenarios in the Willamette River Basin, Oregon. *Hydrological Processes*, **25**(2), 258-277.
- Kao, S., M. Ashfaq, B. S. Naz, R. Uría Martínez, D. Rastogi, R. Mei, Y. Jager, N. M. Samu, and M. J. Sale, 2016: The Second Assessment of the Effects of Climate Change on Federal Hydropower-- Technical Assessment. Oak Ridge National Laboratory, Oak Ridge, TN. 308pp. Available online at: <https://nhaap.ornl.gov/9505-2>.
- Kendall, M.G., 1975: *Rank Correlation Methods, 4th edition*. Charles Griffin, London, UK. 202pp.
- Kotlarski, S., Szabó, P., Herrera, S., Rätty, O., Keuler, K., Soares, P. M., Cardoso, R. M., Bosshard, T., Pagé, C., Boberg, F., Gutiérrez, J. M., Isotta, F. A., Jaczewski, A., Kreienkamp, F., Liniger, M. A., Lussana, C., and Pianko-Kluczyńska, K., 2017: Observational uncertainty and regional climate model evaluation: a pan-European perspective. *Int. J. Climatol.* doi:10.1002/joc.5249
- Leavesley, G.H., Lichty, R.W., Troutman, B.M., and Saindon, L.G., 1983: Precipitation-Runoff Modeling System: User's Manual: U.S. Geological Survey Water-Resources Investigations Report 83-4238. 207pp.
- Liang X., D.P. Lettenmaier, E.F. Wood, and S.J. Burges, 1994: A simple hydrologically based model of land surface water and energy fluxes for GSMs. *J. Geophys. Res.*, **99** (D7): 14,415-14,428.

- Liang X., E.F. Wood, and D.P. Lettenmaier, 1996: Surface soil moisture parameterization of the VIC-2L model: Evaluation and modifications. *Glob. Planet Change*, **13**: 195-206.
- Livneh, B., E.A. Rosenberg, C. Lin, V. Mishra, K. Andreadis, E.P. Maurer, and D.P. Lettenmaier, 2013: A long-term hydrologically based dataset of land surface fluxes and states for the conterminous United States: update and extensions. *J. Climate*, **26**, 9384-9392.
- Luce, C.H. and Z.A. Holden, 2009: Declining annual streamflow distributions in the Pacific Northwest United States, 1948-2006. *Geophysical Research Letters*, **36**(16).
- Mann, H.B., 1945: Non-parametric tests against trend, *Econometrica*, **13**, 163-171.
- Mantua, N.J., I. Tohver, and A.F. Hamlet, 2009: Impacts of climate change on key aspects of freshwater salmon habitat in Washington State. *The Washington Climate Change Impacts Assessment: Evaluating Washington's Future in a Changing Climate* (Chapter 6). Climate Impacts Group, University of Washington, Seattle, Washington.
- Markstrom, S.L., R.S. Regan, L.E. Hay, R.J. Viger, R.M.T. Webb, R.A. Payn, and J.H. LaFontaine, 2015: PRMS-IV, the precipitation-runoff modeling system, version 4. *U.S. Geological Survey Techniques and Methods*, Book 6, Chapter B7. 158pp. Available online at: <http://dx.doi.org/10.3133/tm6B7>.
- Mauger, G.M, S-E. Lee, C. Bandaragoda, Y. Serra, and J. Won, 2016: Effect of Climate Change on the Hydrology of the Chehalis Basin. Climate Impacts Group, University of Washington, Seattle, WA. 53pp. Available online at: <http://chehalisbasinstrategy.com/wp-content/uploads/2016/09/Mauger-et-al-2016-Effects-of-Climate-Change.pdf>.
- Maurer, E.P., A.W. Wood, J.C. Adam, D.P. Lettenmaier, and B. Nijssen, 2002: A Long-Term Hydrologically-Based Data Set of Land Surface Fluxes and States for the Conterminous United States. *J. Climate*, **15**, 3237-3251.
- Maurer, E.P. and H.G. Hidalgo, 2008: Utility of daily vs. monthly large-scale climate data: an intercomparison of two statistical downscaling methods. *Hydrol. Earth Syst. Sci.*, **12**, 551-563.
- McGinnis, S.A., J.A. Thompson, D.W. Nychka, and L.O. Mearns, 2011: Elevation correction and interpolation bias in regional climate data analysis. Poster Elevation Correction and Interpolation Bias in Regional Climate Data Analysis. Poster GC21A-0866, American Geophysical Union Annual Meeting, San Francisco, CA. Available on line at: <http://www.narccap.ucar.edu/doc/pubs/mcginnis-agu-poster-2011.pdf>
- Mendoza, P.A., M.P. Clark, N. Mizukami, A.J. Newman, M. Barlage, E.D. Gutmann, R.M. Rasmussen, B. Rajagopalan, L.D. Brekke, and J.R. Arnold, 2015: Effects of hydrologic model choice and calibration on the portrayal of climate change impacts. *J. Hydrometeor.*, **16**(2), 762-780.
- Milly, P.C., J. Betancourt, M. Falkenmark, R.M. Hirsch, Z.W. Kundzewicz, D.P. Lettenmaier, and R.J. Stouffer, 2008: Stationarity is dead: Whither water management. *Science*, **319** (5863), 573-574.
- Mizukami, N., M.P. Clark, E.D. Gutmann, P.A. Mendoza, A.J. Newman, B. Njissen, B. Livneh, L.E. Hay, J.R. Arnold, and L.D. Brekke, 2016: Implications of the methodological choices for hydrologic portrayals of climate change over the contiguous United States: Statistically downscaled forcing data and hydrologic models. *J. Hydrometeor.*, **74**, 73-98. Available online at: <https://doi.org/10.1175/JHM-D-14-0187.1>
- Mizukami, N., M.P. Clark, A.J. Newman, A.W. Wood, E.D. Gutmann, B. Njissen, O. Rakovec, L. Samaniego, 2017: Towards seamless large-domain parameter estimation for hydrologic models. *Water Resour. Res.*, **53**, 8020-8040. Available online at: <https://doi.org/10.1002/2017WR020401>.
- Minder, J.R., P.W. Mote, and J.D. Lundquist, 2010: Surface temperature lapse rates over complex terrain: Lessons from the Cascade Mountains. *J. Geophys. Res.*, **115**, D14122. doi:10.1029/2009JD013493.

- Mote, P.W. and E.P. Salathé, 2010: Future climate in the Pacific Northwest. *Climatic Change*, **102**, 29-50. doi: 10.1007/s10584-010-9848-z.
- Naz, B.S., S.-C. Kao, M. Ashfaq, D. Rastogi, R. Mei, and L. C. Bowling, 2016: Regional Hydrologic Response to Climate Change in the Conterminous United States Using High-resolution Hydroclimate Simulations. *Glob. Planet Change*, **143**, 100-117. doi:10.1016/j.gloplacha.2016.06.003.
- Neiman, P. J., F. M. Ralph, G. A. Wick, J. D. Lundquist, and M. D. Dettinger, 2008: Meteorological characteristics and overland precipitation impacts of atmospheric rivers affecting the west coast of North America based on eight years of SSM/I satellite observations. *J. Hydrometeor.*, **9**, 22-47.
- Nijssen, B., D. P. Lettenmaier, X. Liang, S. W. Wetzel, and E. F. Wood, 1997: Streamflow simulation for continental-scale river basins. *Water Resour. Res.*, **33**, 711-724.
- NOAA National Marine Fisheries Service, 2016: Policy Memo , Revised Guidance for Treatment of Climate Change in NMFS Endangered Species Act. Issued June, 2016. 8pp.
- NOAA National Centers for Environmental Information, 2018: State of the Climate: Global Climate Report for Annual 2017, published online January 2018. <https://www.ncdc.noaa.gov/sotc/global/201713>
- Nolin, A.W. and C. Daly, 2006: Mapping "at risk" snow in the Pacific Northwest. *J. Hydrometeor.*, **7**, 1164-1171.
- Oubeidillah, A. A., S.-C. Kao, M. Ashfaq, B. S. Naz, and G. Tootle, 2014: A Large-Scale, High-Resolution Hydrological Model Parameter Data Set for Climate Change Impact Assessment for the Conterminous US. *Hydrol. Earth Syst. Sci.*, **18**, 67-84. doi: 10.5194/hess-18-67-2014.
- Oyler, J.W., S.Z. Dobrowski, A.P. Ballantyne, A.E. Klene, and S.W. Running, 2015: Temperature trend biases in gridded climate products and the SNOTEL network. *Preprints*, 83rd Western Snow Conference, Grass Valley, CA. pp. 15-22.
- Pacific Northwest Climate Impacts Consortium (PCIC), 2014: High resolution PRISM climatology for British Columbia. Pacific Climate Impacts Consortium, University of Victoria, BC. Available on line at: <https://www.pacificclimate.org/data/high-resolution-prism-climatology>.
- Pal, J.S., F. Giorgi, X. Bi, N. Elguindi, F. Solmon, X.J. Gao, R. Francisco, A. Zakey, J. Winter, M. Ashfaq, F. Syed, J. Bell, N. Duffenbaugh, J. Karmacharya, A. Konare, D. Martinez-Castro, R. Porfirio da Rocha, L. Sloan, and A. Steiner, 2007: Regional climate modeling for the developing world: The ICTP RegCM3 and RegCNET. *Bull. Amer. Meteor. Soc.*, **88**, 1395-1409. doi:10.1175/BAMS-88-9-1395
- Pan, M. and E.F. Wood, 2013: Inverse streamflow routing. *Hydrol. Earth Syst. Sci.*, **17**, 4577-4588. doi:10.5194/hess-17-4577-2013.
- Pierce, D.W., D.R. Cayan, and B.L. Thrasher, 2014: Statistical Downscaling Using Localized Constructed Analogs (LOCA). *J. Hydrometeorol.*, **15**, 2558-2585.
- Pierce, D.W., D.R. Cayan, E.P. Maurer, J.T. Abotzoglou, and K.C. Hegewisch, 2015: Improved bias correction techniques for hydrological simulations of climate change. *J. Hydrometeorol.*, **16**, 2021-2442.
- Poulin, A., F. Brissette, R. Leconte, R. Arseanault, and J-S. Malo, 2011: Uncertainty of hydrological modelling in climate change impact studies in a Canadian, snow-dominated river basin. *J. Hydrology*, **409**, 626-636.
- River Management Joint Operating Committee (RMJOC), 2010: Climate and Hydrology Datasets for use in the RMJOC Agencies' Longer-Term Planning Studies: Part I - Future Climate and Hydrology Datasets. 183pp. Available on line at: <https://www.bpa.gov/p/Generation/Hydro/Pages/Climate-Change-FCRPS-Hydro.aspx>

- River Management Joint Operating Committee (RMJOC), 2011a: Climate and Hydrology Datasets for Use in the RMJOC Agencies' Longer-Term Planning Studies: Part II - Reservoir Operations Assessment for Reclamation Tributary Basins. 201pp. Available on line at:
<https://www.bpa.gov/p/Generation/Hydro/Pages/Climate-Change-FCRPS-Hydro.aspx>
- River Management Joint Operating Committee (RMJOC), 2011b: Climate and Hydrology Datasets for use in the RMJOC Agencies' Longer-Term Planning Studies: Part III – Reservoir Operations Assessment: Columbia Basin Flood Control and Hydropower. 223pp. Available on line at:
<https://www.bpa.gov/p/Generation/Hydro/Pages/Climate-Change-FCRPS-Hydro.aspx>
- River Management Joint Operating Committee (RMJOC), 2011c: Climate and Hydrology Datasets for Use in the River Management Joint Operating Committee (RMJOC) Agencies' Longer-Term Planning Studies: Part IV – Summary. 73pp. Available on line at:
<https://www.bpa.gov/p/Generation/Hydro/Pages/Climate-Change-FCRPS-Hydro.aspx>
- River Management Joint Operating Committee (RMJOC), 2014: Memorandum of Understanding: Relating to the 2014-2017 River Management Joint Operating Committee (RMJOC) climate change study. 5pp.
- Rupp, D.E., J.T. Abatzoglou, K.C. Hegewisch, and P.W. Mote, 2013: Evaluation of CMIP5 20th century climate simulations for the Pacific Northwest USA. *Journal of Geophysical Research: Atmospheres*, **118**, 10,884-10906. doi:10.1002/jgrd.50843.
- Rupp, D.E., J.T. Abatzoglou, and P.W. Mote, 2017: Projections of 21st century climate of the Columbia River Basin. *Climate Dynamics*, **49**, 1783-1799. doi: 10.1007/s00382-016-3418-7.
- Safeeq, M., G.S. Mauger, G.E. Grant, I. Arismendi, A.F. Hamlet, and S-E. Lee, 2014: Comparing large-scale hydrological model predictions with observed streamflow in the Pacific Northwest: Effects of climate and groundwater. *J. Hydrometeorol.*, **15**, 2501-2521. doi:10.1175/JHM-D-13-0198.1.
- Salathé, E P., Jr., A. F. Hamlet, C. F. Mass, S. Lee, M. Stumbaugh, and R. Steed, 2014: Estimates of twenty-first-century flood risk in the Pacific Northwest based on regional climate model simulations. *J. Hydrometeorol.*, **15**, 1881-1899. doi:10.1175/JHM-D-13-0137.1.
- Sanford, T., P.C. Frumhoff, A. Luers, and J. Gullede, 2014: The climate policy narrative for a dangerously warming world. *Nature Climate Change*, **4**(3), 164.
- Schnorbus, M. and D. Rodenhuis, 2010: Assessing Hydrologic Impacts on Water Resources in BC: Summary Report Joint Workshop, BC Hydro, 20 August 2010. University of Victoria, BC. 49 pp. Available on line at:
<https://pacificclimate.org/sites/default/files/publications/Schnorbus.BCHWorkshopReport.Aug2010.pdf>.
- Sen, P.K., 1968: Estimates of the regression coefficient based on Kendall's Tau. *American Statistics Journal*, **63**, 324.
- Snover, A.K., A.F. Hamlet, and D.P. Lettenmaier, 2003: Climate change scenarios for water planning studies. *Bull. Amer. Meteor. Soc.*, **84**, 1513-151.
- Teng, J., J. Vaze, F.H.S. Chiew, B. Wang and J-M. Perraud, 2011: Estimating the relative uncertainties sourced from GCMs and hydrological models in modeling climate change impact on runoff. *J. Hydrometeorol.*, **13**, 122-139.
- Thornton, P.E., S.W. Running, and M.A. White, 1997: Generating surfaces of daily meteorology variables over large regions of complex terrain. *J. Hydrology*, **190**, 214-251. doi: 10.1016/S0022-1694(96)03128-9.

- Tohver, I., A. F. Hamlet, and S.-Y. Lee, 2014: Impacts of 21st century climate change on hydrologic extremes in the Pacific Northwest region of North America. *J. Amer. Water Res. Assoc.*, **50**, 1461-1476. doi: 10.1111/jawr.12199
- Tripathi, S., and R.S. Govindaraju, 2008: Propagating Uncertainty in Climate Data for Hydrologic Prediction. World Environmental and Water Resources Congress 2008, Honolulu, HI. American Society of Civil Engineers. doi: 10.1061/40976(316)400.
- United States Global Change Research Program (USGCRP), 2017: Climate Science Special Report: Fourth National Climate Assessment, Volume I [Wuebbles, D.J., D.W. Fahey, K.A. Hibbard, D.J. Dokken, B.C. Stewart, and T.K. Maycock (eds.)]. U.S. Global Change Research Program, Washington, DC, USA. 470 pp. doi: 10.7930/J0J964J6.
- U.S. Army Corps of Engineers (USACE), 2015: Recent US Climate Change and Hydrology Literature Applicable to US Army Corps of Engineers Missions – Water Resources Region 17, Pacific Northwest. Civil Works Technical Report, CWTS 2015-23, USACE, Washington, DC.
- U.S. Army Corps of Engineers (USACE), 2016: Guidance for Incorporating Climate Change Impacts to Inland Hydrology in Civil Works Studies, Designs, and Projects. USACE Engineering and Construction Bulletin (ECB) 2016-25.
- U.S. Army Corps of Engineers (USACE), 2017: Guidance for Detection of Nonstationarities in Annual Maximum Discharges, to detect nonstationarities in maximum annual flow time series. USACE Engineering Technical Letter (ETL) 1100-2-3.
- UW-CIG, 2010: Hydrologic Climate Change Scenarios for the Pacific Northwest Columbia River Basin and Coastal drainages, University of Washington Climate Impacts Group, Seattle, WA. Available on line at: <http://www.hydro.washington.edu/2860/>.
- Vano, J.A., M. Scott, N. Voisin, C.O. Stöckle, A.F. Hamlet, K.E.B. Mickelson, M.M. Elsner, D.P. Lettenmaier, 2010: Climate change impacts on water management and irrigated agriculture in the Yakima River basin, Washington, USA. *Washington State Climatic Change*. doi: 10.1007/s10584-010-9856-z.
- Vano, J.A., J.B. Kim, D.E. Rupp, and P.W. Mote, 2015: Selecting climate change scenarios using impact-relevant sensitivities. *Geophysical Research Letters*, **42**(13), 5516-5525.
- Warner, M.D., C. F. Mass, and E. P. Salathé, 2012: Wintertime extreme precipitation events along the Pacific Northwest coast: Climatology and synoptic evolution. *Mon. Wea. Rev.*, **140**, 2021-2043. doi: 10.1175/MWR-D-11-00197.1.
- Warner, M.D. and C.F. Mass, 2017: Changes in climatology, structure and seasonality of Northeast Pacific Atmospheric Rivers in CMIP5 climate simulations. *J. Hydrometeor.*, **18**, 2131-2141
- Wilby, R.L. and T.M.L. Wigley, 1997: Downscaling general circulation model output: a review of methods and limitations. *Progress in Physical Geography*, **21**(4), 530-548.
- Wilby, R. L., 2005: Uncertainty in water resource model parameters used for climate change impact assessment. *Hydrol. Processes*, **19**, 3201-3219. doi:10.1002/hyp.5819.
- Wilby, R.L., and I. Harris, 2006: A framework for assessing uncertainties in climate change impacts: Low-flow scenarios for the River Thames, UK. *Water Resour. Res.*, **42**, W02419. doi: 10.1029/2005wr004065.
- Wood, A.W., E.P. Maurer, A. Kumar, and D.P. Lettenmaier, 2002: Long range experimental hydrologic forecasting for the eastern U.S. *J. Geophys. Res.*, **107** (D20), 4429.
- Wood, A.W., L.R. Leung, V. Sridhar, and D.P. Lettenmaier, 2004: Hydrologic implications of dynamical and statistical approaches to downscaling climate model outputs. *Climatic Change*, **15**, 189-216.